Organophosphate Triesters in the Chattahoochee River and Chattahoochee Water Treatment Plant

Drugstore Cowboys

Matt Andrews, Sam Haffey, Joe Lin, and Alexandros Machairas

Master of Engineering Group Project

May 2004

Table of Contents

1   Executive Summary

The Drugstore Cowboys Inc. explored the fate and transport tributyl phosphate (TBP), tri(2-chloroethyl) phosphate (TCEP), and tri(2-butoxyethyl) phosphate (TBEP) in the Chattahoochee River and Chattahoochee Water Treatment Plant in Atlanta, GA. These three organophosphate triesters are commonly used as flame retardants and plasticizers. Through disposal to the sewage system, these xenobiotic chemicals enter the environment, posing health risks to humans and biota.

Mr. Andrews explored natural attenuation within the Chattahoochee River. Samples were collected at four different locations along the river and analyzed for TBP, TCEP, and TBEP concentration. These values were implemented in the construction of several mass balances seeking to identify the presence of a natural sink. A separate study was completed specifically targeting biodegradation within the Chattahoochee. Two additional sets of samples were analyzed at various times over a 24-hour period, leading to the calculation of a biodegradation rate for each compound. The results indicate that for the conditions present along the particular reach of the Chattahoochee River no removal mechanism exists.

Mr. Haffey developed a numerical model of the reach of the Chattahoochee River extending downstream from Buford Dam to the GA 280 highway crossing in North West Atlanta. The aim of the model was to evaluate the magnitude of potential sinks within the modeled reach and to make predictions of the concentration distribution of all three organophosphoric acid triesters. The model was developed using WASP5 and supporting software packages. Model predictions showed considerable agreement with concentration observations made by Mr. Andrews and Mr. Lin in the January sampling survey. The model predicted the phosphate ester concentration patterns in time and space and showed how they varied with the diurnal flow variations imposed by hydroelectric dams located within the reach. These predictions were then used to predict the weekly cycle of concentration levels at the Atlanta Water Works intake. The model also predicted that TBEP is the most susceptible to natural attenuation processes and that

sorption to settling solids and biodegradation are the most likely processes to reduce TBEP concentrations. TCEP was shown to be the most resistant to natural attenuation.

Mr. Lin focused on drinking water treatment processes, and whether or not these processes were effective in removing the phosphate triesters. Specifically, he took samples after major processes at the Chattahoochee Water Treatment Plant in Atlanta, GA. His findings suggested that removal of the phosphate triesters might occur after the pre-treatment chemical addition of sodium hypochlorite. In addition, large amounts of TCEP were detected after the filtration and post-treatment chemical addition stage. Contamination from the plant itself was the chief potential reason for the addition of TCEP.

Mr. Machairas focused on the issue of how to remove phosphate esters from drinking water. From the various treatment processes available, the oxidation of phosphate esters through hydroxyl radical generated by the UV/H2O2 process applied at a UV disinfection unit was selected for evaluation.

The second-order rate constants of the reactions of two phosphate esters, Tri(2-butoxyethyl) phosphate (TBEP) and Tri-2-chloroethyl phosphate (TCEP) , with hydroxyl radical were estimated from our experimental data to be $2 \cdot 10^{10}$ $M^{-1}s^{-1}$ and $2 \cdot 10^{9}$ $M^{-1}s^{-1}$ respectively A comprehensive kinetic model of the oxidation process was derived. Finally computer simulations were used to exhibit the potential of this treatment process and to examine the effects of pH, total carbonate species concentration, initial hydrogen peroxide dose, and light intensity on its efficiency.

The results are not very encouraging when a UV unit designed for disinfection is used. For typical values of pH and total carbonate species (pH=8 and $C_T=5 \cdot 10^{-4}$ M) the 1st order rate coefficients for removal of the phosphate esters are $6.3 \cdot 10^{-4}$ (s^{-1}) for TBEP and $6.3 \cdot 10^{-5}$ (s^{-1}) for TCEP.

If higher light intensity is applied in the reactor (50 times higher), and initial hydrogen peroxide dose of 10^{-3} M and C_T remains $5 \cdot 10^{-4}$ M, the 1st order reaction rate coefficients become $2.9 \cdot 10^{-2}$ (s^{-1}) and $2.9 \cdot 10^{-3}$ (s^{-1}) for TBEP and TCEP respectively.

Drugstore Cowboys, Inc. is pleased to submit the final report for the occurrence and fate of the selected organophosphoric acid triesters in the Chattahoochee River Basin.

Further details available at:

http://web.mit.edu/andrewsm/www/DrugstoreCowboys.htm

2 Background Information

2.1 September 2003 Presentation

In September 2003, Peter Shanahan made a presentation concerning PPCPs in the environment. This presentation focused on two specific studies conducted by the USGS.
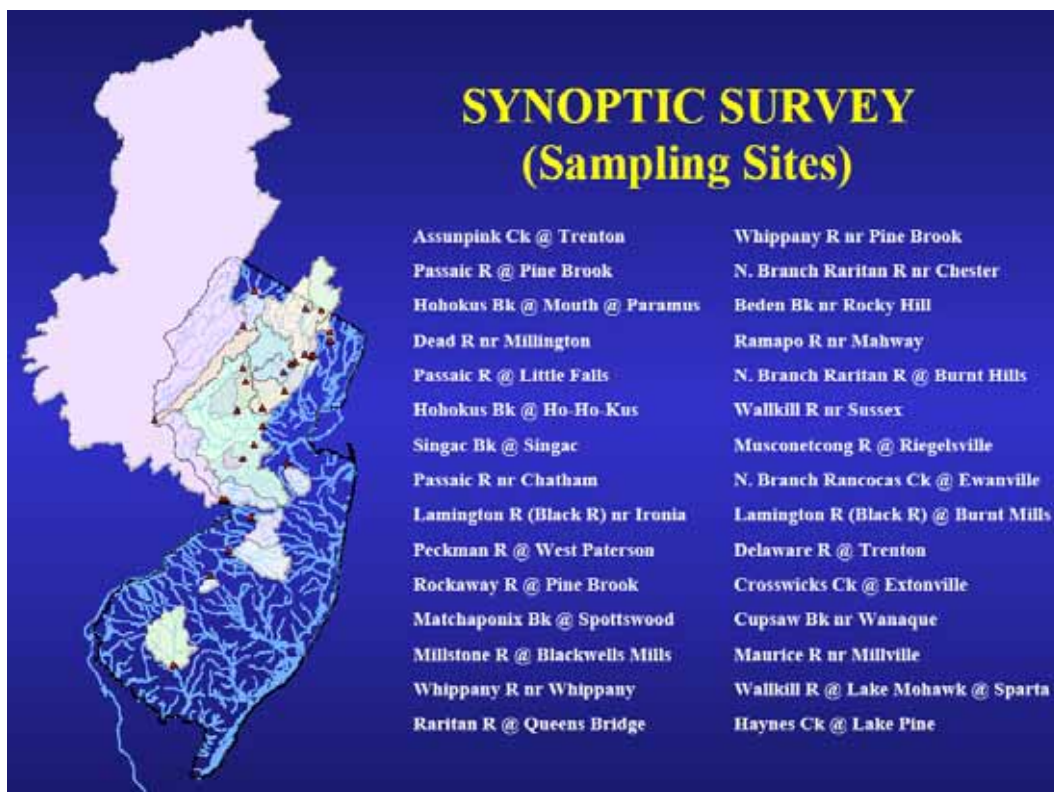
2.1.1 New Jersey Study

SYNOPTIC SURVEY (Sampling Sites)

Assunpink Ck @ Trenton	Whippany R nr Pine Brook
Passaic R @ Pine Brook	N. Branch Raritan R nr Chester
Hohokus Bk @ Mouth @ Paramus	Beden Bk nr Rocky Hill
Dead R nr Millington	Ramapo R nr Mahway
Passaic R @ Little Falls	N. Branch Raritan R @ Burnt Hills
Hohokus Bk @ Ho-Ho-Kus	Wallkill R nr Sussex
Singac Bk @ Singac	Musconetcong R @ Riegelsville
Passaic R nr Chatham	N. Branch Rancocas Ck @ Ewanville
Lamington R (Black R) nr Ironia	Lamington R (Black R) @ Burnt Mills
Peckman R @ West Paterson	Delaware R @ Trenton
Rockaway R @ Pine Brook	Crosswicks Ck @ Extonville
Matchaponix Bk @ Spottswood	Cupsaw Bk nr Wanaque
Millstone R @ Blackwells Mills	Maurice R nr Millville
Whippany R nr Whippany	Wallkill R @ Lake Mohawk @ Sparta
Raritan R @ Queens Bridge	Haynes Ck @ Lake Pine

Figure 2-1 Sampling sites investigated in Stackelberg and Lippincott (undated).

The first of two studies examined was a joint study conducted by the USGS and the New Jersey Department of Environmental Protection (Stackelberg and Lippincott, undated). It focused on the state of New Jersey where samples were taken from treated municipal sewage discharging to river systems.. Error! Reference source not found. shows the sampling locations. Ninety percent of samples tested positive for at least one of the

OWCs being screened for. In addition, all types of PPCPs were present, with varying concentrations (Figure 2-2**Error! Reference source not found.**).
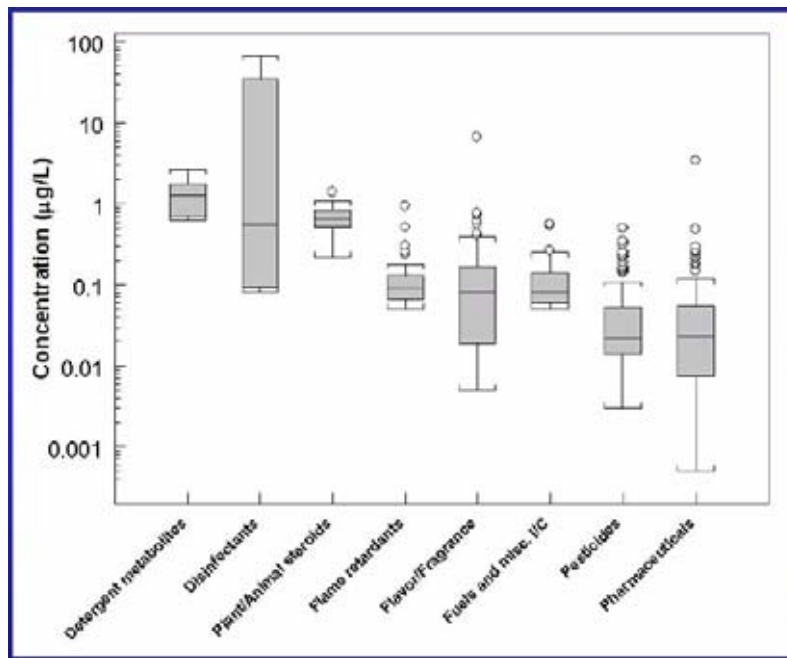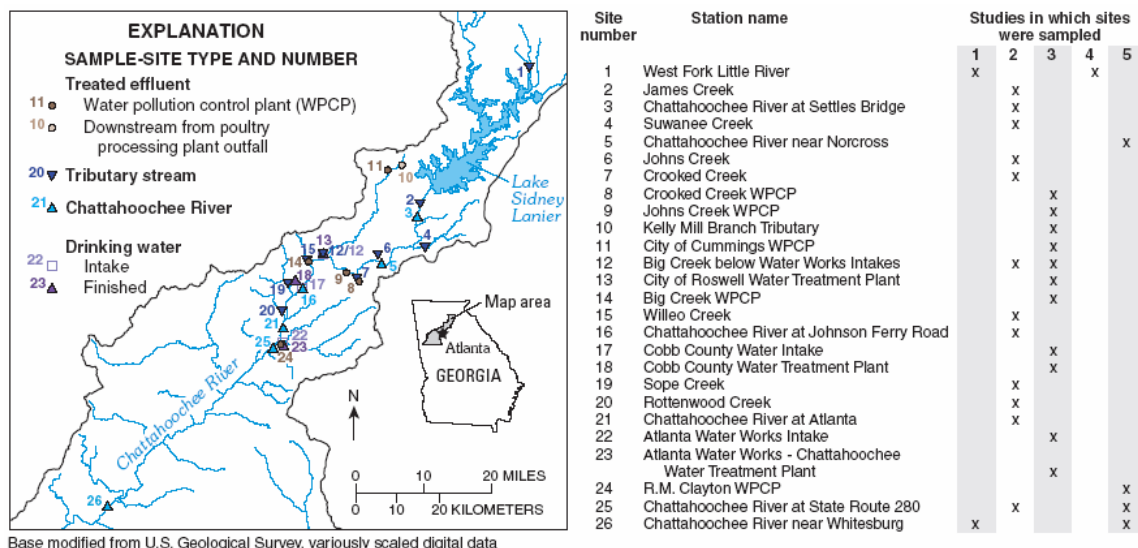

Figure 2-2 Average, minimum, maximum, 25th percentile and 75 percentile concentrations found in Stackelberg and Lippincott (undated).

2.1.2   Summary of Previous USGS Studies Done on the Chattahoochee River Basin

Second, Frick and Zaugg (2003) compiled data of OWCs measured in Kolpin et al. (2002), Frick et al. (2001), and Henderson et al. (2001), and Gregory and Frick (2001). All data focused on the Chattahoochee River basin (Error! Reference source not found.).

Site number	Station name	1	2	3	4	5
		Studies in which sites were sampled				
1	West Fork Little River	x			x	
2	James Creek		x			
3	Chattahoochee River at Settles Bridge		x			
4	Suwanee Creek		x			
5	Chattahoochee River near Norcross					x
6	Johns Creek		x			
7	Crooked Creek		x			
8	Crooked Creek WPCP			x		
9	Johns Creek WPCP			x		
10	Kelly Mill Branch Tributary			x		
11	City of Cummings WPCP			x		
12	Big Creek below Water Works Intakes		x	x		
13	City of Roswell Water Treatment Plant			x		
14	Big Creek WPCP			x		
15	Willeo Creek		x			
16	Chattahoochee River at Johnson Ferry Road		x			
17	Cobb County Water Intake			x		
18	Cobb County Water Treatment Plant			x		
19	Sope Creek		x			
20	Rottenwood Creek		x			
21	Chattahoochee River at Atlanta		x			
22	Atlanta Water Works Intake			x		
23	Atlanta Water Works - Chattahoochee Water Treatment Plant			x		
24	R.M. Clayton WPCP					x
25	Chattahoochee River at State Route 280		x			x
26	Chattahoochee River near Whitesburg	x				x

Base modified from U.S. Geological Survey, variously scaled digital data

Figure 2-3 Sampling sites from Frick and Zaugg (2003). 25 of 26 sampling sites were in the upper Chattahoochee River basin.

All of the sampling was conducted between 1999 and 2002. Sampling was done along the river, in tributaries of the river, at WWTP intakes and effluents, and at DWTP intakes and effluents.

2.1.2.1 Description of Frick et al. (2001) and Henderson et al. (2001)

Study 3 from Figure 2 comprises the sampling sites taken in Frick et al. (2001) and Henderson et al. (2001). These studies were done simultaneously, and were jointly sponsored by the Centers for Disease Control (CDC) and the USGS. Sampling methods were the same as Kolpin et al. (2002), and all sampling was completed in the summer of 1999. The findings were quite similar to Stackelberg and Lippincott (undated) and Kolpin et al., where detectable concentrations of many OWCs were found in most sampling sites. Every type of OWC (e.g. detergents, plasticizers, pharmaceuticals, etc.) had similar detection frequencies, and were found at levels ranging from 10 to 2000 parts per trillion. Numbers of some of the detections are in the next sections. In addition, the specific sampling times, sampling points, and concentrations measured at each site were also available from the authors.

2.1.3   The Formation of the Drugstore Cowboys

The proposal presented by Dr. Shanahan was to get an engineer's view of the survey done in Atlanta, as described in the previous section. Through Alden Henderson, who was one of the people in charge of the Chattahoochee River study, Dr. Shanahan obtained the full data of the samples and its subsequent concentrations of PPCPs. Four Masters of Engineering students at MIT, Matthew Andrews, Samuel Haffey, Alexandros Machairas, and Joseph C. Lin, made a request for proposal on this project. Advising them in the proposal was Peter Shanahan, Prof. Phil Gschwend, Prof. Tina Voelker, and Dr. John Macfarlane, who are all current faculty at MIT. The four group members also picked the name Drugstore Cowboys, Inc., for their project name.

The resumes of the four primary engineers are attached in the Appendix.

2.2   Focusing on a Location to Do Field Work

After determining that more work must be done than just interpreting the USGS/CDC data, the group decided that they needed a location to focus their work on. Some location ideas presented were the Assabet River in Massachusetts, the Chattahoochee River, and surface waters in Switzerland. The group chose to focus on the Chattahoochee River for the following reasons:

- All the work would be a good supplement to already-collected data.
- Because of time constraints, choosing multiple areas to conduct field research would not be possible.
- Peter Shanahan had connections in Atlanta that would be useful in obtaining more information about the area, such as Alden Henderson and Daniele Lantagne, a former MIT Masters of Engineering student who now works at the CDC.

2.3   The Selected Family of Chemical Compounds – Organophosphate Triesters

The three chemicals picked for the study reported in this thesis were tributyl phosphate (TBP), tri(2-chloroethyl) phosphate (TCEP), and tri(2-butoxyethyl) phosphate (TBEP). These chemicals were chosen because:

- Due to time constraints of this group project, multiple families could not be chosen.
- These three organophosphates were frequently detected in previous USGS studies. From Stackelberg and Lippincott (undated), TCEP was detected in 50% of all samples, and TBEP was in 38%. Within the WWTP intake water, TCEP were detected in 12 of 12 samples, and TBP and TBEP was detected in 10 of 12 samples. From Kolpin et al. (2002), TCEP was detected in 57.6% of 85 samples, and TBEP was detected in 45.9% of 85 samples. From Frick and Zaugg (2003), TCEP and TBP were detected in 100% of 13 WWTP effluent samples and TBEP was detected in 38% of the 13 samples.. In addition, for the DWTP samples taken in Frick and Zaugg, the percentage of detections for all three phosphate triesters actually increased from raw water to finished water! (Table 1)
- The three chemicals have similar structure. This study focuses only on phosphate triesters. A phosphate triester is comprised of a phosphorus atom, with four oxygen atoms bonded to the atom: one doubly-bonded, and the other three singly-bonded. Each of the three singly-bonded oxygen atoms has an organic group attached to it. Specifically, the phosphate triesters studied in this paper are phosphotriesters, where the functional group is identical for each three oxygen atoms.
- The chemicals are widely used as flame-retardants, plasticizers, in floor polishes, and for many other purposes. Thus, there was good reason to believe that these compounds will be in the Chattahoochee River when the sampling was done in January 2004.

Table 2-1 Percent Detections at Specific Sites. Note that the numbers in parentheses are the number of samples taken for each type. Source: Frick and Zaugg (2003)

Chemical	Reporting Limit (ug/L)	Treated Effluent WWTP % (13)	Tributary Stream Baseflow % (9)	Wet Weather % (17)	Chattahoochee River Baseflow % (8)	Wet Weather % (7)	DWTP Intake % (9)
TBP	0.04	100	0	7/9	43	0/4	0
TCEP	0.04	100	33	82	50	57	56

2.3.1 The Phosphate Triesters' Main Use – Flame Retardants

Organophosphate flame-retardants represent 20% of worldwide production of flame-retardants (World Health Organization, 1997). When the flame-retardants are put into a fire, they break down into phosphoric acid and other components upon heating. The resulting phosphoric acid forms a char on the burning surface, resulting in less surface area available as fuel; this acid also reduces the release of volatiles. Both of these phenomena reduce the intensity of the flame.

The problem with these flame-retardants is not when they are used, but when they are not used. For example, the organophosphates may be in very small concentrations in a person's clothing. Through washing of the clothes, the organophosphates go into a waste stream, thus starting the possible chemical transport into the environment. Other uses, as described in the following sections, also cause the phosphate triesters to get into the environment.

2.3.2 Tributyl Phosphate

TBP has an n-butyl group attached to each of the single-bonded oxygen atoms.
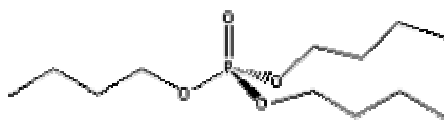
Figure 2-4 Chemical Structure of TBP.

Some of the important chemical properties are (Syracuse Research Corporation (2003), Risk Assessment Information System (2004), and World Health Organization (2001):

- Liquid at room temperature, miscible with water and chloroform.
- Boiling point: 289 °C. Melting point: -79 °C.
- Log K_{ow} = 4.
- K_{oc} = 1900 L/kg.
- Solubility in water at 20 °C: 280 mg/L
- Henry's Law constant: 6.13 x 10^{-6} (dimensionless)
- Density: 0.973 – 0.983 mg/L at 25 °C
- Vapor pressure: 0.00349 mm Hg 20 °C

TBP is made through the reaction of phosphorus oxychloride ($POCl_3$) and butyl alcohol (World Health Organization, 1991). There is little information on the production of TBP. The Environmental Protection Agency requires any company producing at least 10,000 pounds of a chemical to report to them through the Inventory Update Rule (IUR). From the 2002 IUR, the production of TBP in the United States was between 1 and 10 million pounds. Three companies (Akzo Nobel Functional Chemicals, LLC; Ferro Corporation; Great Lakes Chemical Corp.) produced at least 10,000 pounds of TBP that year (US EPA, 2002). Chemical Sources International, Inc. (2004) lists 21 companies in the United States that produce TBP, but only Akzo Nobel was listed in this website among the three

companies that produced more than 10,000 pounds in 2002. Thus, the production volume within the United States may be significantly more than the reported volume.

The major use (forty to sixty percent) of TBP is in fire resistant hydraulic fluid for aircraft. (World Health Organization, 1991)

The second most prevalent use of TBP is as a plasticizer for plastics and vinyl resins. It is a preferred plasticizer due to its dual capability as a plasticizer and flame retardant in plastics.

An interesting, emerging use of TBP is in the recovery of uranium ores from reactor products. This use of TBP has become increasingly significant in recent years (Thomas et al., 1998; World Health Organization, 1991).

The estimated oral lethal dose of TBP is between one ounce and one pint for a 150 pound person. Most direct encounters with significant quantities of TBP occur through dermal contact by airline mechanics or workers in TBP production plants. Skin irritation is reported in most cases and headaches and dizziness have been reported due to exposure to TBP vapor (National Library of Medicine, 2004).

Although there have been no fatal effects to humans, animals with TBP in their system have displayed neurological effects such as weakness and dyspnea (difficulty in breathing). TBP's most dramatic effects are to plant life. TBP has been shown to increase the drying rate of leaves and plants exposed to TBP stopped respiring (World Health Organization, 1991).

2.3.3 Tri(2-butoxyethyl) Phosphate

TBEP has a 2-butoxyethyl group attached to the single-bonded oxygen atoms (**Error! Reference source not found.**).
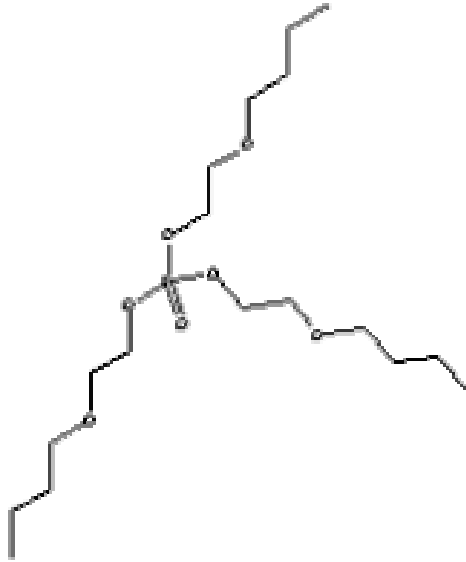
Figure 2-5 Chemical Structure of TBEP.

Major chemical properties:

- Liquid at room temperature, miscible with water and chloroform.
- Boiling point: 200-230 °C. Melting point: -70 °C.
- Log K_{ow} = 4.38.
- K_{oc} = 24000.
- Solubility in water at 20 °C: 1100-1300 mg/L.
- Henry's law constant: 1.20 x 10^{-6} (dimensionless).
- Density: 1.02 mg/L at 20 °C.
- Vapor pressure: 2.8 x 10^{-8} mm Hg at 20 °C

TBEP is made through the reaction of phosphorus oxychloride with butoxyethanol (World Health Organization, 2000). The World Health Organization estimated production to be between 11-13 million pounds, but no year was cited. In the 2002 IUR, the production volume was 10-50 million pounds, reported by two companies (Akzo Nobel and Great Lakes Chemical). The 1994 and 1998 IUR also report a 10-50 million pound range (US EPA, 2002). This range is larger than the 1-10 million pound range for

TBP and TCEP; therefore, the loading into the surface water environment may be much larger than the loadings for TBP and TCEP

The most likely pathway TBEP takes into the wastewater system is through its use in floor polishes (NIH, 2003). TBEP adds elasticity and gloss to floor polishes. The increased elasticity increases the leveling and spreading properties of the polish. It is a component of several household floor polishes, including such familiar names as Mop & Glo and Brilliance, in concentrations as high as eight percent. Disposal of wastewater after floor polishing is an obvious pathway to municipal wastewater systems.

TBEP is also used as an antifoam agent and solvent for complex organic compounds such as resins, waxes, poly acrylites, and acrylic co-polymers. (World Health Organization, 2000)

TBEP was found to be a mild skin irritant (National Library of Medicine, 2004). Significant testing has been done to determine its non-human toxicity. Among other effects it has been found to reduce the production of red blood cells in rats and chickens. (World Health Organization, 2000)

2.3.4 Tri-(2-chloroethyl) Phosphate

TCEP has a 2-chloroethyl group attached to each of the single-bonded oxygen atoms. TCEP has different chemical properties because of the chlorine atom end group, as shown in Error! Reference source not found..
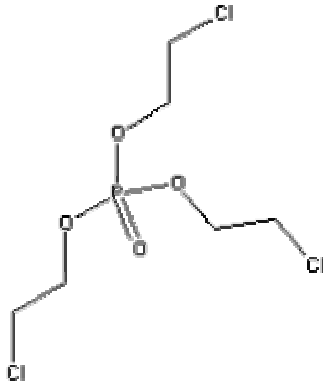
Figure 2-6 Chemical Structure of TCEP.

Major chemical properties:

- Liquid at room temperature, miscible with water and chloroform.

- Boiling point: 330 °C. Melting point: -35 °C.

- Log K_{ow} = 1.44.

- K_{oc} = 300 L/kg.

- Solubility in water at 20 °C: 7000 mg/L.

- Henry's Law constant: 1.04×10^{-6} (dimensionless)

- Density: 1.425 mg/L at 20 °C

- Vapor pressure: 0.000391 mm Hg at 20 °C

TCEP is made through the reaction of phosphorus oxychloride and ethylene oxide, followed by subsequent purification (World Health Organization, 1998). Brown et al. (1975) indicated that the United States produced 29.4 million pounds and consumed 25.5 million pounds of TCEP. Twelve million of the 25.5 million consumed was used as a flame retardant, and the other 13.5 million was used in synthetic lubricants and hydraulic fluids. In 1997, the estimated demand was 9 million pounds, a significant decline in use compared to Brown et al. In the 2002 IUR, TCEP production in the United States was 1-10 million pounds. This production volume is based on the reports of two companies, Akzo Nobel and Great Lakes Chemical (US EPA, 2002). TCEP is also used as a plasticizer in PVC and resins.

TCEP is known to be a carcinogen (recognized in 1992 by California through Proposition 65 (2004)), and is suspected to be a reproductive, kidney, and liver toxicant. The current chronic dermal RfD is 0.15 mg/kg-day.

TCEP has several uses that provide ready pathways into the municipal wastewater stream. TCEP is used as fire retardant in liquid unsaturated polyester resins (World Health Organization, 1998). The normal concentration is five to two percent in these resins. (Jiangdu Dajian Chemical Factory web site) The resins are used in the casting of bathtubs, spas, and pipes. It is possible that leaching from these surfaces could provide a pathway into the environment.

An even more likely pathway into the environment is the use of TCEP as a back coating for textiles used in furniture and protective clothing. Maintenance and cleaning of these products and subsequent disposal of the wastewater used in the process could provide a pathway to the WWTP (World Health Organization, 1998)

In tests regarding bioconcentration, TCEP was found to accumulate in the brains of rats, and with repeated exposure was found to have adverse effects on the brain, liver, and kidneys. It is also known to adversely affect the reproduction rates of rats and mice (National Library of Medicine, 2004)

3   Natural Attenuation

An exploration into the fate and transport of these three phosphate triesters is an important component of an overall assessment of the Chattahoochee River. Few studies have explored the natural removal of organophosphate triesters in surface waters (Fries and Puttman, 2001, Kawagoshi et al., 2002). The goal of this study was to determine if natural attenuation of these compounds exists within the Chattahoochee River. Samples were collected at four sites along the Chattahoochee and analyzed for the presence of each phosphate triester. Coupling these concentrations with flow rate along the river and source inputs from several sewage treatment plants (STPs) on the Chattahoochee, several mass balances were completed. The intent was to reveal a) whether significant sinks exist and b) which portions of the river are likely to contain a phosphate triester sink.

Upon consideration of the physical and chemical properties of these compounds, the Drugstore Cowboys reasoned that biodegradation was a likely removal mechanism over the time period of flow down the Chattahoochee (Drugstore Cowboys, 2003). To test for the presence of biodegradation, a second set of samples was collected and incubated prior to analysis at various times over a 24-hr period. These results were then analyzed in order to obtain a decay rate for each compound.

In this chapter a brief explanation of the sampling and analysis methods will be presented (refer to Andrews (2004) for a detailed description). Results will be then be reported and discussed, drawing conclusions regarding natural attenuation in the Chattahoochee as well as identifying potential follow-up studies.

3.1   Experiment Summary

In order to facilitate a comparison of results, the same 50-mile stretch of the Chattahoochee used during the USGS surveys was implemented in determining sampling sites for this study. Four locations along this stretch were chosen for sampling, beginning at Buford Dam and ending downstream of the Atlanta Water Treatment Plant
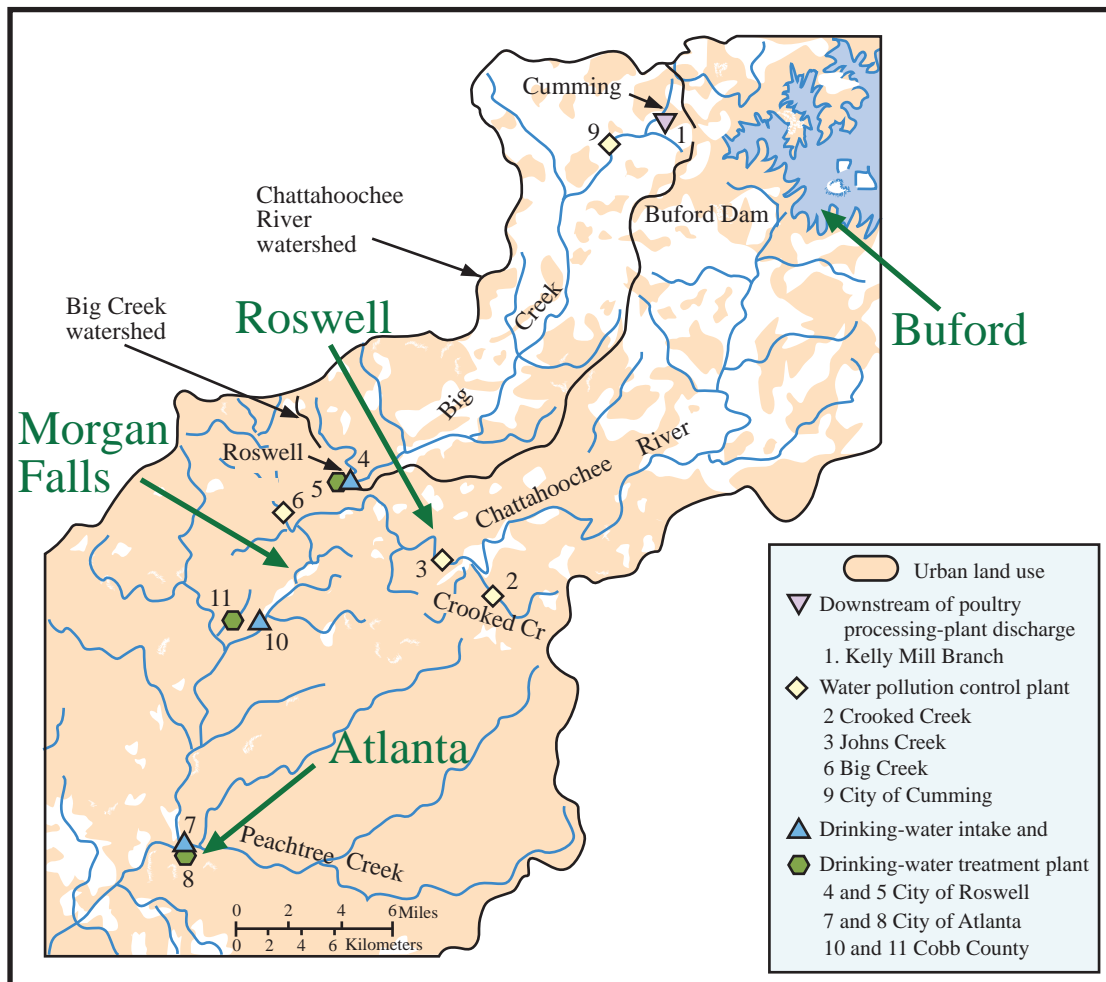
Figure 3-1: Chattahoochee River Sampling Sites

in northwest Atlanta. Two intermediate sampling sites were chosen, one behind the Morgan Falls Dam in Bull Sluice Lake and another located further upstream near the town of Roswell (Figure 3-1). The specific sampling locations were chosen based on accessibility to the river and a desire to sample downstream of STP outfalls. The goal was to be far enough downstream of the outfalls that it can be reasonably assumed that the phosphate triesters were well mixed within the river and no attention need be paid to transverse concentration variations.

The sampling sites divide the 50-mile stretch into three sections, Buford Dam to Roswell, Roswell to Morgan Falls, and Morgan Falls to Atlanta, each containing two STP sources. The sites serve as end points for three separate mass balances on the river. Combining the concentrations measured at each site with flow rate data for the Chattahoochee River yields input and output mass rates for each mass balance. By combining concentrations from the STPs discharges (Frick and Zaugg, 2003) with their typical effluent flow rates (Haffey, 2004), the source term for each mass balance can be constructed. Although other sources of phosphate triesters exist (e.g. atmospheric deposition, groundwater infiltration, land runoff) it is assumed that these inputs are negligible compared to STP effluent. The only remaining variable is the sink term, which is a simple mathematical exercise to evaluate. A positive sink term indicates the likely presence of removal mechanism within the river.

During the second experiment, two separate sets of samples were collected at each site in order to specifically target biodegradation as a removal process. These samples were stored in a water bath full of river water for either 5 or 24 hours, allowing biodegradation to proceed. At the allotted time following collection from the river, the samples were removed from the bath and analyzed for phosphate triester content. Coupling these results with the samples collected for the mass balance (0-hour), phosphate triester concentration was analyzed with respect to time, yielding a biodegradation removal rate. Triplicates of each sample were collected for a total of nine at each site. The reason for additional samples was to increase the likelihood of reliable results and allow for the prospect of ruined samples.

Every river sample was tested for phosphate triester content through a combination of liquid-liquid extraction and gas chromatography/mass spectrometry (GC/MS). A total of 400 mL of chloroform was introduced to each 3.8-L river sample, extracting the phosphate triesters from the water. The chloroform was allowed to settle, then pipetted out of the river sample. The volume of chloroform was then reduced through roto-evaporation and N_2 blow-down processes. Once the samples had been sufficiently

condensed, an injection standard was supplied just before analysis on a JEOL GC/MS. A short calculation, utilizing this injection standard, converted the GC/MS signal to the original river concentration. For a more detailed description of the sampling procedure and lab analysis, refer to Andrews (2004).

Data Analysis / Results

3.1.1   Data Validation

The preliminary component of the data analysis was to validate the results utilizing several mechanisms. The analytical methods used to derive the data were validated through a comparison with blank solutions, standards containing a known quantity of each phosphate triester, and a comparison to other data extracted from the same equipment. The lowest concentration standard tested was 500 µg/L of chloroform. Given that each river sample was condensed by a factor of approximately 40,000 (3.8 L reduced to 0.1 mL) the concentration of 500 µg/L of chloroform in the GC vial corresponds to a river water sample of approximately 0.01 µg/L. Therefore, the best that can be stated with assurance is that the detection limit of the GC/MS is 0.01 µg/L, or lower.

Blank solutions, containing only chloroform from the same source as each sample, were interwoven into sample runs in order to check for interference from the GC/MS. At no time did blank solutions yield discernable peaks at any of the four output times, an indication that the chloroform contributed less than 0.01 µg/L of phosphate triesters (Figure 3-2). This is relative assurance that neither the chloroform used nor the GC/MS supplied more than 0.01 µg/L to the results.
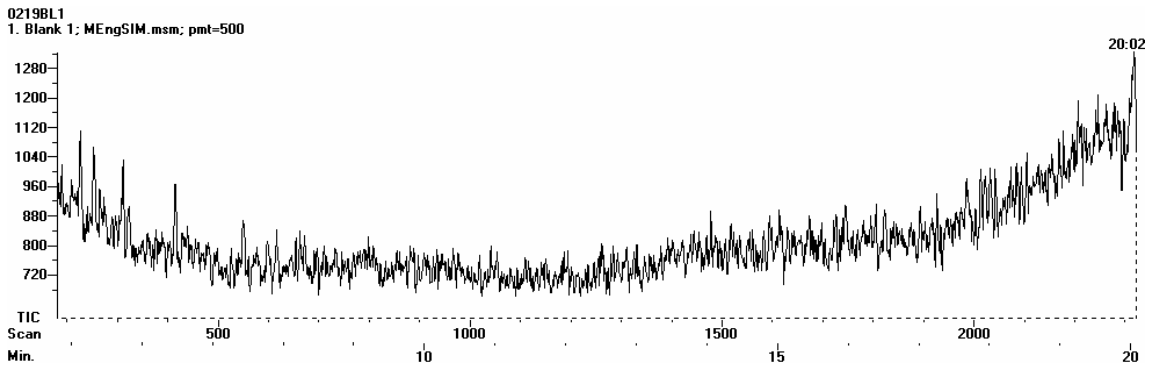
Figure 3-2: Blank chloroform GC/MS output

An inspection of previous work performed on the same GC/MS equipment revealed that a similar count per mass ratio of injection standard was observed, indicating that the equipment had remained relatively consistent.

Data published from the USGS/CDC study was used to give a sense of the expected concentration and a degree of confirmation. The flow in the Chattahoochee is extremely variable, fluctuating by as much as a factor of ten on a particular day. Therefore, depending on the precise time that samples were taken by the USGS, results may vary from the results of this study due to dilution [Haffey, 2004, USGS Real-Time, 2004). Differences in sampling and analysis procedure could also lead to variations in results. An order of magnitude difference, therefore, is deemed sufficient for an agreeable comparison of the two studies.

As mentioned previously, the USGS/CDC study detected these three phosphate triesters at concentrations typically observed throughout the world (Fries and Puttman, 2001, Frick and Zaugg, 2003). The only samples representative of the Chattahoochee River by the USGS/CDC were the three drinking water intakes. Fortunately, these sites align reasonably well with the Roswell, Morgan Falls, and Atlanta sampling sites, allowing a comparison to be made (Figure 3-3). However, no detections were observed for TBP at the any of the drinking water intakes. Because the USGS/CDC's detection limit was 0.06 μg/L, concentrations were at least below this threshold. For general comparison purposes

it is assumed that since there is a constant source of TBP from STPs, the non-detects do not constitute a zero concentration. As a result, the only conclusion that can be made for TBP is that both sets of data determined concentrations below 0.06 µg/L.
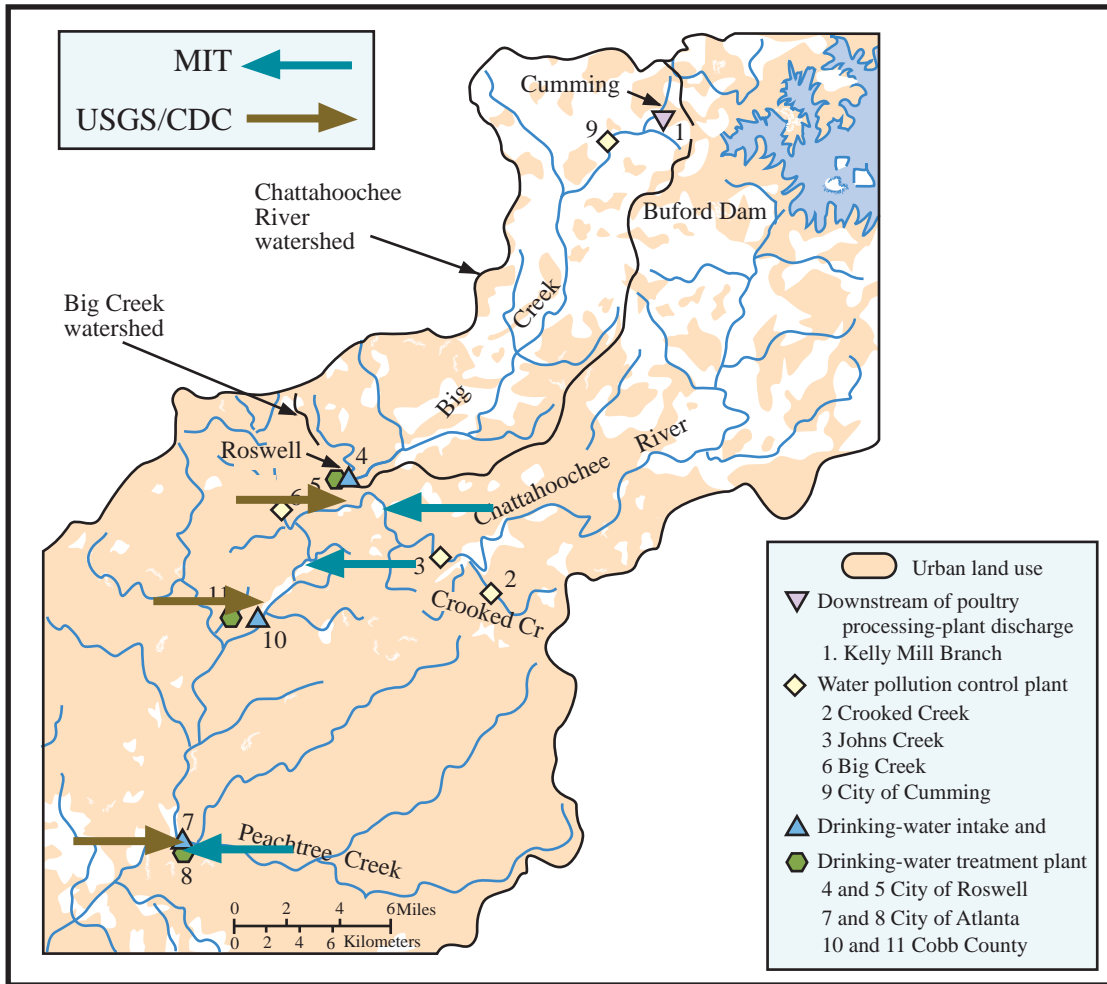
Figure 3-3: Map of USGS/CDC and MIT sampling sites.

A more direct comparison can be made for TCEP and TBEP. Both studies detected these two compounds at concentrations of the same order of magnitude (Figure 3-4). Realizing that the data collected in this study matches not only the USGS/CDC, but several other surveys throughout Europe and Japan substantially raises confidence in the results.
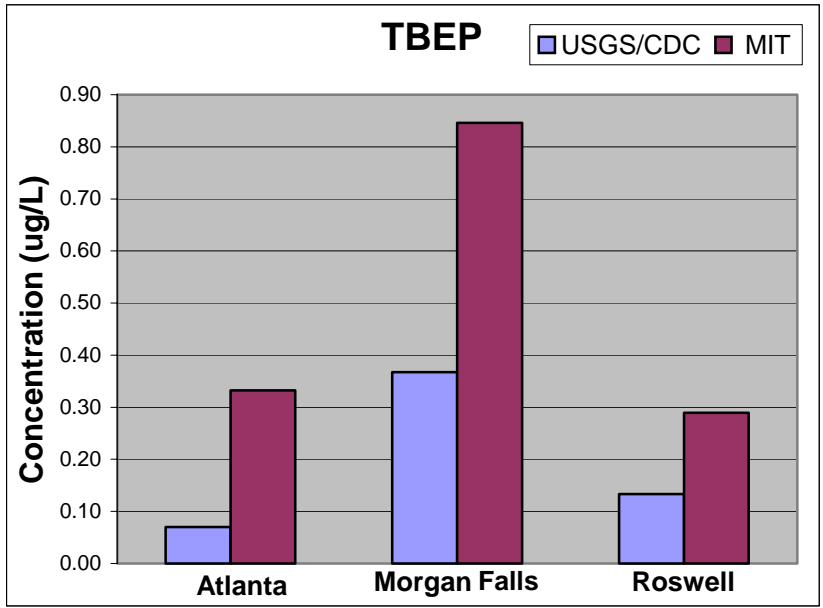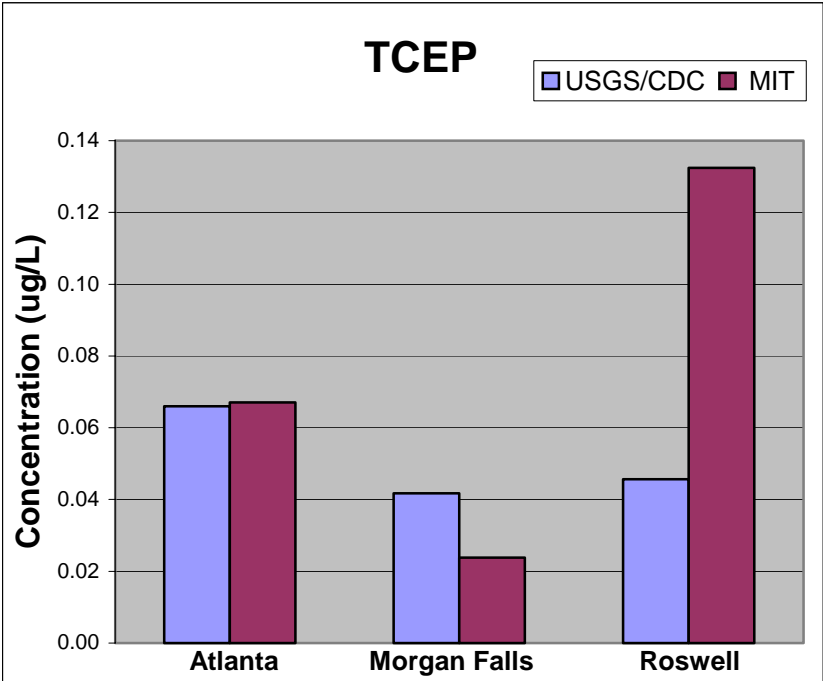
Figure 3-4: USGS/CDC and MIT data comparison.

3.1.2   River Mass Balance

The objective for collecting samples at various sites was to divide the river into smaller segments that can act as control volumes for phosphate triester mass balance calculations. Each river control volume contains an advective input determined at one of the sampling sites, an advective output at the next sampling site, and sources at STP discharges (Figure 3-5). It was assumed that no other major sources exit. This is a sound assumption given the various uses of each phosphate triester.   An analysis of each control volume, comparing inflows to outflows, yields a quantity of unaccounted mass. If a sink is active within the particular stretch of river, there will be less mass exiting each control volume than being added. Additional mass exiting the control volume suggests the presence of sources other than the major STPs.
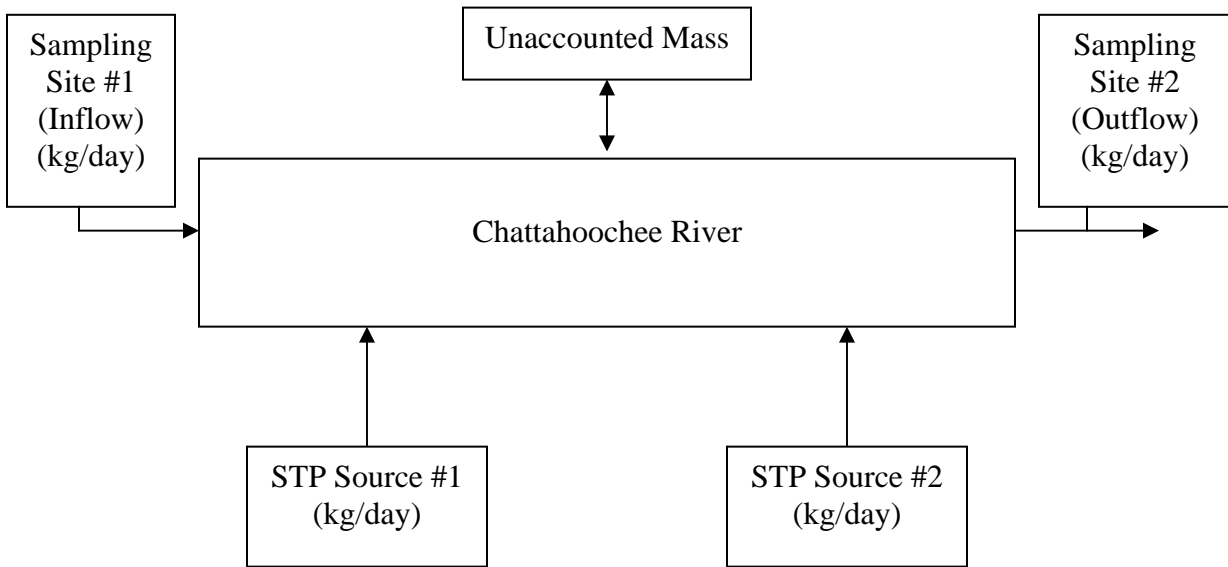
Figure 3-5: Mass Balance Schematic

Mass balances were constructed by first multiplying the average concentration at each sampling site by the average flow rate at that point to yield a mass rate entering and exiting the control volume via river flow (Haffey, 2004).   Average STP discharge concentrations were then taken from the USGS/CDC study and multiplied by average

plant discharge rates obtained from plant records to yield a mass rate entering the control volume. There were two STPs located between Morgan Falls and Atlanta whose discharges were not measured during the USGS/CDC survey. In order to account for their presumed contribution of phosphate triesters, the concentration of these discharges were assumed to equal the average of the four plants that were tested. Since each STP is handling similar domestic waste, an average concentration was deemed most appropriate. Multiplying the average concentration by each plant's average flow rate, obtained from plant records, yields the necessary mass-loading rate. The missing mass rate term is then determined by adding the input loading to each STP source loading and subtracting the output loading. There is a range of values for each concentration and flow rate. As a result, mass loadings were also calculated using plus and minus one standard deviation on all factors (Andrews, 2004). Hence, within one standard deviation, an assessment was made as to the presence of a sink within the Chattahoochee.

Based on the results of the three different mass balances, no sink was observed within the river for any of the phosphate triesters with at least one standard deviation confidence. In fact, unaccounted sources are a possibility, as the calculations often resulted in more mass exiting the control volume than entering. The conclusion of no sink in the Chattahoochee River is specific to the 50-mile stretch tested and the river conditions present at the time of sampling.

3.1.3   Biodegradation Data

Analysis of phosphate triester removal by biodegradation begins with an inspection of the 0, 5, and 24-hr sample concentrations. If microorganisms were degrading these phosphate triesters, the expected result would be for the 0-hr samples to contain the highest concentration, followed by smaller concentrations for the 5-hr and 24-hr samples, thus depicting clear decay over time. The data do not exhibit a clear decrease in concentration or any consistency in the triplicate measurements at the three times (Figure 3-6). This lack of clear removal in the batch studies was generally seen for all cases (Andrews, 2004).
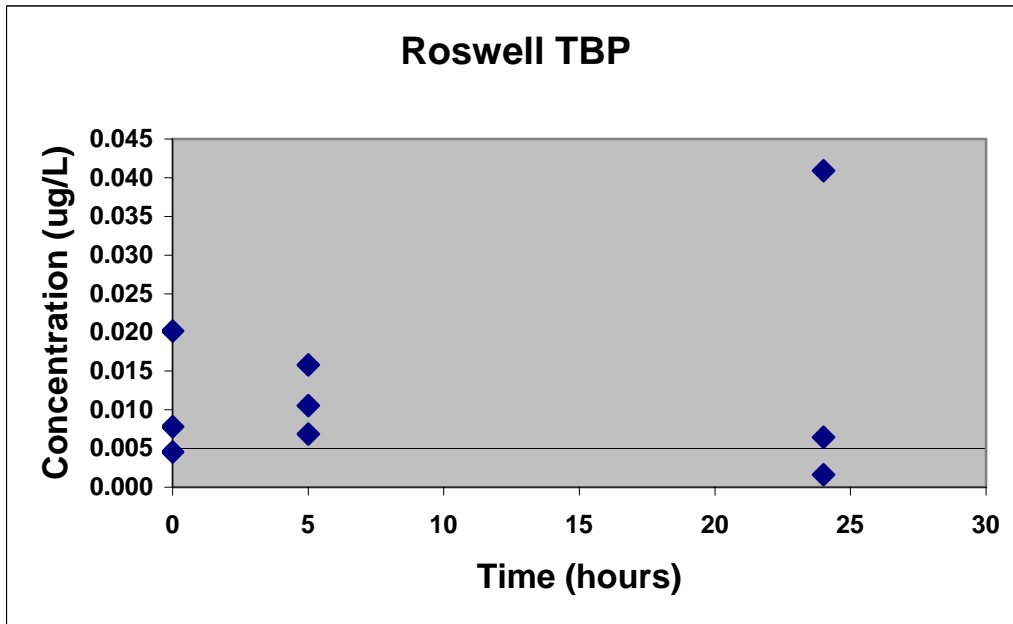
Figure 3-6: Plot of typical data, depicting the typical scatter resulting from biodegradation studies

The triplicate samples are independent, meaning there is no difference between any of the three 0-hr samples, which have no direct connection to any specific 5-hr or 24-hr sample. Each site therefore has nine independent points with which to perform a statistical analysis. By compiling all the factors that impact biodegradation, a mass balance, with the control volume equal to the river water sample in the amber glass bottle, can be solved to yield a linear equation (Figure 3-7). Linear regression analysis can then be incorporated to obtain a 1st order rate constant, k.

$$\textbf{Mass Balance:}$$

$$\frac{dC}{dt} = -kC$$

$$\int_{Co}^{C} dC/C = \int_{0}^{t} -kdt$$

$$\ln C = -kt + \ln Co$$

$$y = ax + b$$

Figure 3-7: Derivation of biodegradation equation

A number of different parameters were calculated to assess the statistical significance of a least squares fit to a set of data. Each phosphate triester at all three sites tested for biodegradation was analyzed, yielding a 1st order decay constant and a wide array of statistical parameters, the *p-value* included (Andrews, 2004).

Each *k* and *p-value* was compiled into a new spreadsheet (Table 3-1). Based on the high *p-values* for TBP and TCEP at each site, biodegradation was clearly not demonstrated during the experiment. TBEP had some locations, Roswell in particular, where the rate constant might have some legitimacy. But overall, the results demonstrated that biodegradation of organophosphoric acid esters does not occur along this particular stretch of the Chattahoochee River.

Table 3-1: Results of linear regression analysis on biodegradation data

Chemical	Site	k (hr^{-1})	P-value %
TBP	Roswell	-0.010	76
	Morgan Falls	-0.030	60
	Atlanta	0.022	54
TCEP	Roswell	-0.014	83
	Morgan Falls	0.064	24
	Atlanta	-0.001	99
TBEP	Roswell	-0.040	19
	Morgan Falls	-0.053	36
	Atlanta	-0.018	78

In light of the field results perhaps it is not surprising that the batch biodegradation study revealed little evidence of biodegradation over the 24-hour timescale. Biodegradation is controlled by a number of factors, several of which are likely to be extremely limiting in the river ecosystem. One is the abundance and distribution of bacteria capable of degrading phosphate triesters. These microorganisms may not be indigenous to the Chattahoochee River, or may be present but only in sediment and not in the water column where the grab samples were collected. It is unclear whether the bacteria are capable of acclimating to the degradation of phosphate triesters when the concentrations are so low; perhaps there is a threshold concentration before degradation can begin. Also, these bacteria require a sufficient nutrient supply, which the Chattahoochee might not provide. January may be a stagnant time period for these bacteria, which are likely very sensitive to water temperature, pH, and other water quality characteristics (Thomas and Macaskie, 1998). Of course the error associated with the experiment itself cannot be overlooked as a contributor to the inconclusive results.

The grab sample is also not completely indicative of the conditions in the river, which are constantly changing downstream. A grab sample is a snapshot of the conditions at the sampling site, but this technique fails to account for many variations downstream that could alter the conditions for biodegradation. Unfortunately, results of this study could

not be discerned from zero, making an analysis of the observed differences in rate constants at the various sampling sites impractical.

3.2   Conclusion

The goal of this project was to determine if a natural sink existed which degraded phosphate triesters over the time scale of a day. The results establish that no natural attenuation of these three phosphate triesters is present on the time scale of one day. These findings are specific to the conditions under which sampling occurred. Perhaps given a longer stretch of river or a different time of year, a removal mechanism would manifest itself.

The other objective of this work was to look closely at biodegradation, which was determined through a review of available data to be the most likely removal mechanism. Field sampling and lab analysis led to the determination that biodegradation was not present over a 24-hour period. Results could certainly vary, depending on the time of year and location of sampling within the Chattahoochee. Despite results in the negative, this grab sample experiment should be used as a building block for future studies.

This project is just a small aspect of the much bigger issue of low-level organic contaminants in natural surface water. Through studies such as this a wealth of knowledge can be compiled to assess the ultimate risks to human and environmental health as well as the treatment options available. Armed with this invaluable information, policy makers can make well-educated decisions regarding a future course of action.

4 Numerical Modeling

A numerical modeling approach was used to make predictions of phosphate ester concentrations and to identify potential sinks within the environment. To this end a water quality model was constructed using the Waster Quality Analysis Simulation Program (Ambrose et al., 1993) and supported by two additional software packages. Hydrologic Engineering Center – River Analysis System (Brunner, 2002) was used to estimate the characteristics of the river flow in the modeled reach. ArcGIS (ArcGIS, 2003) was used to identify the locations of point sources, tributary inflows, drinking water intakes and other important features of the river reach. ArcGIS also aided in the estimation of ungauged tributary in-flow.
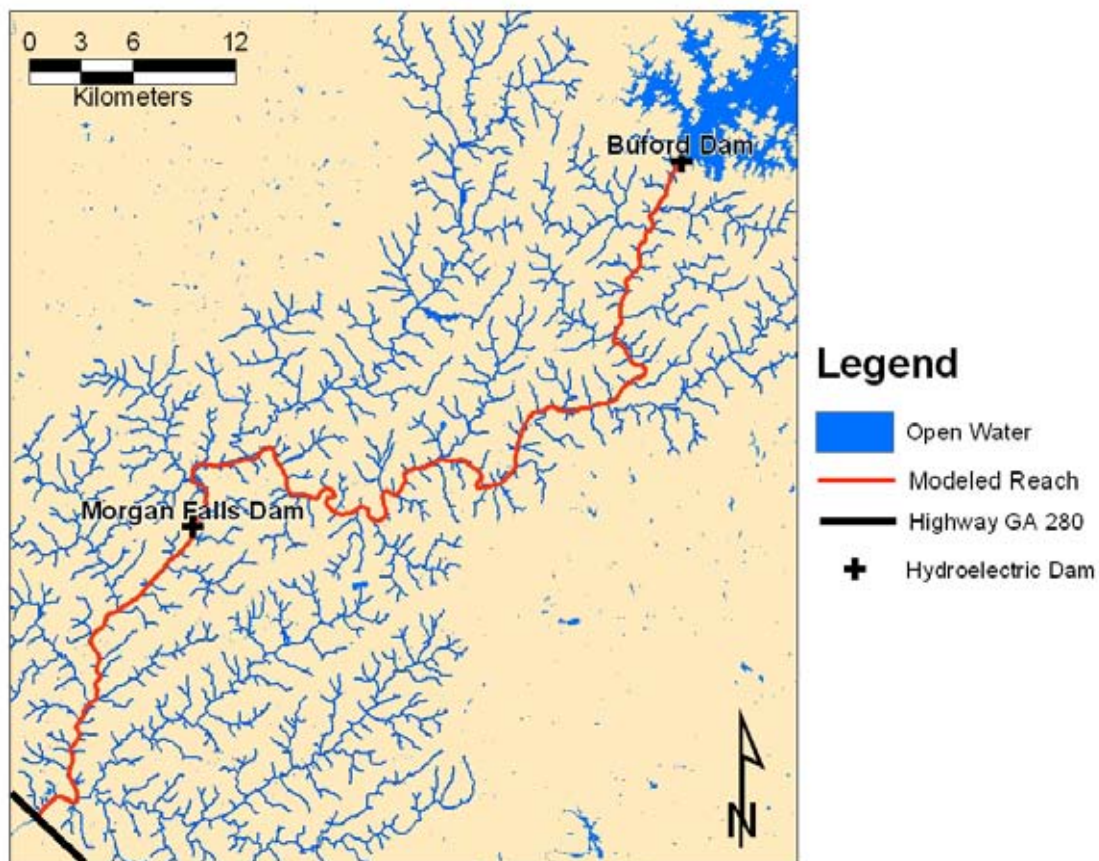
Figure 4-1 Map Showing Location of Hydroelectric dams within the modeled reach

The time frame of the model was selected so as to simulate the five days from January 12, 2004 to January 16, 2004. This encompasses the time during which the Drugstore Cowboys, Inc. sampling was conducted and enabled the comparison of the model predictions with the observations of TBP, TBEP, and TCEP concentration.

Flow data collected at fifteen-minute intervals at the hydroelectric Dams in the modeled reach (Figure 4-1) for the modeled period was acquired from the USGS (Stamey, 2004). Flow rates from WWTPs discharging to the modeled reach were obtained and estimates of the loads were estimated using the WWTP flow rates and the average concentrations found by Henderson et al. (2003).

Flow was a major consideration in constructing the water quality model. The hydroelectric dams, Buford Dam and Morgan Falls Dam, within the reach are major factors in altering the flow of the reach between Buford and North West Atlanta and the results of the model show that pattern in flow is a considerable factor in the concentration patterns observed for the three phosphate esters. The model resolves the daily fluctuations in flow that occur as a result of the operation of the hydroelectric dams.

Models were constructed to route the flood waves released at Buford Dam through the model reach, to approximate suspended solids distribution in the modeled reach and to simulate chemical and physical reactions that the organophosphoric acid triesters undergo in the water column. For a detailed description of the flow, sediment, and reaction models see Haffey (2004).

4.1 Phosphate Ester Reactions Modeled

Four reactions were evaluated as potential sinks of the phosphate esters in the water column. These were sorption to settling solids, biodegradation, volatilization, and oxidation by free radicals. Hydrolysis and direct photolysis were neglected.

4.1.1 Sorption

4.1.1.1 Overview of Sorption

Sorption is a process in which chemicals dissolved in water bind onto solid surfaces. DA chemical specific partition coefficient, K_p, is a constant describes the ratio at equilibrium of sorbed phase to dissolved phase. Using the specific parition coefficients the model approximates the different sorption behavior of the three modeled phosphate esters.

A reliable method exists for approximating K_p values for neutral organic chemicals (Hemond and Fechner-Levy, 1994). The method assumes that absorption into organic matter is the primary method of sorption for these compounds. The parameter K_{oc} is the partition coefficient for a particular chemical with organic carbon and is used to determine sorbed concentration. Where a K_{oc} has not been measured one is often approximated using the K_{ow}, the octanol-water partition coefficient. The K_{ow} describes how hydrophobic a particular compound is and methods are available for converting a K_{ow} into a K_{oc} value.

For TCEP and TBP no K_{oc} value was available and the value had to be calculated using K_{ow}. The correlation in Equation 4-1 has been shown to hold provided values of a_0 and a_1 are available for the particular compounds.

$$LogK_{oc} = a_0 + a_1 LogK_{ow}$$

Equation 4-1

Setting a_1 equal to 0.544 and a_0 equal to 1.377 has been shown to hold for a wide variety of chemicals (Hemond and Fechner-Levy, 2002), and these values were used to calculate the K_{oc} for TBP and TCEP.

In the case of the Chattahoochee River, sorption may act as a sink for phosphate esters. Phosphate esters dissolved in the water column may sorb to organic matter in the

suspended solids being transported downstream. Once sorbed to the organic carbon the phosphate ester may be removed from the water column through settling.

4.1.1.2 Sorption Constants Used For Phosphate Esters

Only for TBEP was a calculated K_{oc} value available. This was a $LogK_{oc}$ of 4.38 (van Esch, 2000)

K_{ow}. values were available for TCEP and TBP. These along with the correlation in Equation 4-1 were used to determine K_{oc}. The K_{ow} values used were

- $LogK_{ow} = 3.99$ for TBP (Nakamura, 1991)

- $LogK_{ow} = 1.7$ for TCEP (WHO, 1998)

4.1.2 Biodegradation

4.1.2.1 Overview of Biodegradation

Biodegradation is the process by which organic chemicals are broken down by bacterial enzymes. Bacteria in the water column can utilize the energy stored in the bonds of organic compounds and break them down for sustenance. Biodegradation is a complicated process and may depend strongly on both the concentration of the chemical and the size of the bacterial population.

4.1.2.2 Biodegradation First Order Rates

The study conducted in January of 2004 had as one of its aims the estimation of first-order biodegradation rates for the phosphate esters within the modeled reach (Andrews, 2004). The first-order biodegradation rate constants used by the model for each of the phosphate esters are listed in Table 4-1. These were based on statistically supported averages taken from Andrews (2004).

Table 4-1 First Order Biodegradation Rate Constants
(Andrews, 2004)

Compound	Biodegradation Rate (day^{-1})
TBP	1.99E-02
TBEP	3.72E-02
TCEP	7.60E-03

4.1.3 Volatilization

4.1.3.1 Overview of Volatilization

Volatilization is the process by which chemicals dissolved in water partition across the air-water interface. As in sorption a partition coefficient, the Henry's Law constant, is defined which describes the equilibrium ratio between the dissolved phase of a chemical and the gas phase. However chemical concentrations in the atmosphere above the water surface are assumed to be zero and therefore equilibrium is never reached. It is assumed that the rate of transfer across the air-water interface is proportional to the Henry's Law constant as well as the concentration gradient across the interface. Furthermore it is assumed that only the water at the surface is involved in this transfer. Therefore the rate at which water is renewed to the surface is also taken into account when calculating the transfer rate.

A transfer coefficient, K_v, is a constant that describes the rate at which a chemical can transfer across the air-water interface. K_v is in the form of a velocity and this velocity divided by the depth of the river segment can be used as a decay rate.

4.1.3.2 Volatilization Constants Used

WASP calculates the volatilization rate using the water body depth and velocity and only a chemical specific Henry's Law Constant and a molecular weight are required for each phosphate ester. The velocity and depth at each model tank were calculated from information contained in the flow model (Haffey, 2004).

Molecular weights were calculated from the molecular formula. The Henry's Law Constants used are listed below.

- $H_{TBP} = 1.41$E-6 atm-m^3/mole (SRC, 2004)

- $H_{TBEP} = 1.2\text{E-}11$ atm-m^3/mole (SRC, 2004)

- $H_{TCEP} = 3.29\text{E-}6$ atm-m^3/mole (WHO, 1998)

4.1.4 Oxidation by Free Radicals

4.1.4.1 Overview of Oxidation

Oxidation occurs when free radicals such a hydroxyl radical, $OH\cdot$, encounter organic chemicals and attack the C-H bonds. Radicals are formed in the water column through photochemical reactions.

4.1.4.2 Oxidation Model

The second-order oxidation rate constants used in this model are listed in Table 4-2.

Table 4-2 Second-Order Oxidation Rate Constants
(Machairas, 2004)

Compound	Oxidation Rate (L/mole*day)
TBP	8.64E+14
TBEP	1.73E+15
TCEP	1.73E+14

No data was available regarding the concentration of oxidation radicals in the modeled reach of the Chattahoochee. Illuminated surface waters contain hydroxyl radical at concentrations of about 10^{-17} moles/L (Hemond and Fechner-Levy, 1994) and this value was used as the concentration of oxidation radicals in each tank in the model. This is a simplifying assumption and it is recognized that radicals other than hydroxyl may be present and that deeper and more turbid waters will have lower concentration of oxidation radicals. It is assumed that 10^{-17} moles/L is the average concentration of oxidation radicals in the modeled reach.

4.1.5 Neglected Reactions

4.1.5.1.1 Hydrolysis

Hydrolysis is a reaction in which both a chemical molecule and a molecule of water are split and recombined to form two new compounds. Depending on the compound hydrolysis may be catalyzed by basic, acidic or neutral environment. For the three

phosphate esters hydrolysis is a base-catalyzed reaction and will only occur significantly in waters with pH of 12 or higher (Schwarzenbach et al., 2003). The pH in the Chattahoochee rarely is less than 6.9 or greater than 7.5 (USGS, 2004) and therefore it is assumed that hydrolysis is not an important reaction for phosphate esters in the Chattahoochee River.

4.1.5.2 Photolysis

Photolysis is the process by which chemical molecules are broken up by sunlight. Every chemical absorbs light within a spectrum specific to that chemical. If the ambient light waves fall with the absorption spectrum of the chemical then enough light energy may be absorbed by the molecule to break it apart. No absorption spectra for the phosphate esters were available for this study. In addition the phosphate esters are either clear or very lightly colored. A clear compound allows light to pass directly through it and therefore does not absorb light energy. TBEP being lightly colored has some possible potential for photolysis but since this is simply conjecture it will be assumed that photolysis is not an important reaction for any of the phosphate esters being studied.

4.2 Load Estimates

Point source loadings were estimated for each of the three phosphate esters. It is necessary to understand the manner in which the loadings were estimated to adequately evaluate the results.

4.2.1 Estimate of Loads

Seven municipal wastewater treatment plants (WWTPs) discharge, either directly or through tributaries, into the Chattahoochee River in the reach between Buford Dam and the GA 280 highway crossing in Atlanta. The CDC study conducted in 1999 tested at four of these WWTPs and consistently detected TBP, TBEP, and TCEP in the treated wastewater entering the Chattahoochee. The four WWTPs, their permitted daily discharge and the average concentration of the three compounds detected in their effluent are listed in Table 4-3, (for the purposes of averaging concentrations that were reported below the detection limit were taken to be half the detection limit). The locations of the plants can be found by consulting Figure 4-2.
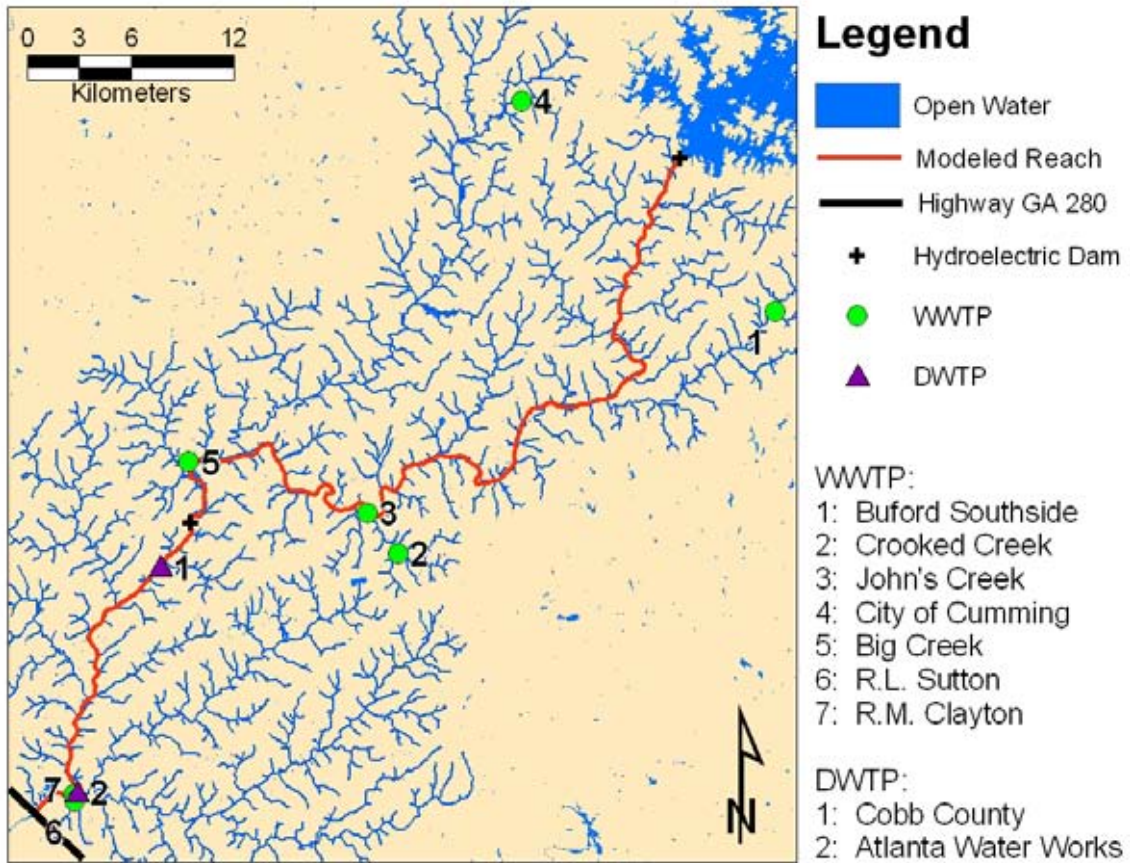
Figure 4-2 Location of Municipal DWTPs and WWTPs in Modeled Reach
(EPA, 2003 & Frick and Zaugg, 2003)

Table 4-3 Phosphate Ester Concentrations Found at WWTPs
(GNR, 1997 & Frick and Zaugg, 2003)

WWTP	Permitted Discharge (MGD)	Concentration (μg/L)		
		TBP	TBEP	TCEP
Crooked Creek	36	0.19	0.35	0.07
Johns Creek	7	0.26	9.57	0.35
City of Cumming	2	0.17	0.12	0.40
Big Creek	24	0.79	0.45	0.34

The three plants that were not tested are listed in Table 4-4. The locations of the plants can be found in Figure 4-2. In addition to these point source loads, in-stream concentrations were detected at the headwaters of the Big Creek and in Lake Sydney Lanier, the reservoir impounded by Buford Dam. The method of compiling this

information and estimating the phosphate ester loads on the system are discussed in the following sub sections.

Table 4-4 WWTPs That Were Not Screened for Phosphate Esters
(GNR, 1997)

WWTP	Permitted Discharge (MGD)
Buford Southside	2
R. M. Clayton	100
R. L. Sutton	40

4.2.1.1 Point Source Loads

The WWTPs discharging directly into the Chattahoochee in the modeled reach are all considered point source loads. Out of the seven discussed above Crooked Creek, John's Creek, Big Creek, R.M. Clayton, and R.L. Sutton discharge directly into the Chattahoochee. The method for determining the loads over the modeled period (January 12, 2004 – January 16, 2004) was to determine the discharge on the particular day and then multiply that by an estimated average concentration at the plant.

4.2.1.1.1 Estimation of Daily Discharge

The daily discharges for the entire modeled period were available for the Big Creek, Crooked Creek, and Johns Creek plants. The records for January 14, 2004 – January 16, 2004 were available for the R. L. Sutton plant. No records were available for the R. M. Clayton plant. The plants and the known discharges for the modeled period are listed in Table 4-5.

Table 4-5 Known Daily Point Source Discharges
(Harburn, 2004 & Chastain, 2004)

WWTP	Daily Discharge (MGD)					Percent of Permit Limit
	1/12/2004	1/13/2004	1/14/2004	1/15/2004	01/162004	
Crooked Creek	25.3	26.3	26.3	26.7	25.8	72%
Johns Creek	4.66	4.95	4.84	4.49	4.89	68%
Big Creek	19.62	18.72	19.83	18.55	18.64	79%
R. M. Clayton						
R. L. Sutton			28.17	26.89	27.25	69%

For the case of the R.L. Sutton Plant, the average discharge over the known days was used as the discharge for the January 12, 2004 and January 13, 2004. The discharge of the R. M. Clayton plant was estimated by first observing that the known discharges were on average 72% of their permitted discharge. The assumption was made that the R. M. Clayton facility was also operating at 72% of its permitted discharge. It has a permitted discharge of 378,500 m^3/day and therefore was assigned a daily discharge of 273,100 m^3/day for this simulation.

4.2.1.1.2 Determination of Time Variable Discharge

The base case model assumes that the plant discharge is constant through out the day and only varies from day to day as expressed in Table 4-5. The treated wastewater is not discharged from the plants at a constant rate but varies throughout the day. Hourly discharge patterns were available for only one plant, R. L. Sutton. A sensitivity test was conducted by normalizing the discharge curve for a single day at R. L. Sutton by the daily discharge for that day. This normalized curve was applied to the discharges of all five point source loads. The effects of this change were insignificant, altering the concentrations by a maximum of 10% and therefore the assumption that the rates are constant on a given day does not dramatically alter the results (Haffey, 2004).

### 4.2.1.1.3 Determination of Point Source Discharge Concentration

The average concentrations listed in Table 4-3 were applied to the discharges of the corresponding three point source plants (City of Cumming WWTP is not considered a point source since it does not discharge directly to the Chattahoochee, its treatment is discussed below). Effluent concentrations for the two plants not sampled by the 1999 study had to be estimated. Since the R. L. Sutton plant is comparable in size to the

Crooked Creek plant the average concentration of the Crooked Creek plant was applied to the effluent of the R. L. Sutton Plant. There were no plants of comparable size to the R. M. Clayton plant and therefore a combined average concentration for each compound over all three plants was determined and was applied to the R. M. Clayton effluent.

Loads were determined by multiplying the average concentrations detected by the CDC/USGS survey at a particular WWTP by the daily discharge from that WWTP. For those WWTPs that discharge to tributaries rather than directly into the Chattahoochee, a boundary concentration for the inflow to the Chattahoochee from the tributary receiving the effluent was calculated. The calculation involved dividing the daily load of each phosphate by the daily flow of the tributary to the Chattahoochee.

In the case of the Big Creek, the boundary concentration also took into account the concentrations reported by Frick and Zaugg (2003) in the Kelly Mill Branch, a tributary to the headwaters of the Big Creek. A constant upstream boundary concentration was determined by calculating the average concentration in Lake Sydney Lanier as reported by Andrews (2004). Figure 4-3 shows the location of all the sources of phosphate esters to the model. For a more detailed discussion of the calculation of these boundary conditions see Haffey (2004).
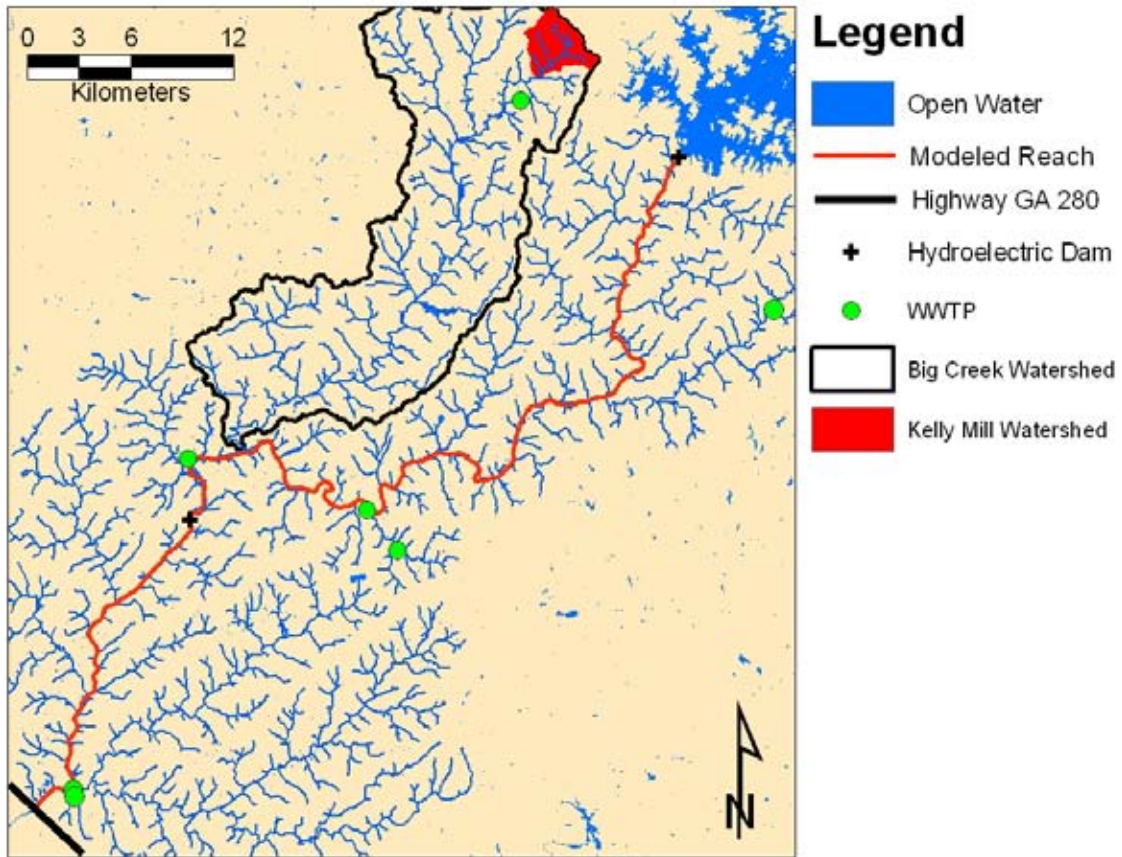
**Figure 4-3 Location of Phosphate Ester Sources in the Model
(Location of Kelly Mill Frick and Zaugg, 2003)**

4.2.1.2 Comparisons of Load Magnitude

Table 4-6 contains the names of the loads cross referenced with the tanks in which they enter the model. This is accompanied by the histogram in Figure 4-4 that shows the comparative orders of magnitudes of each of the phosphate ester loads.

Table 4-6 Point Sources and Corresponding Tanks

Load Name	Tank
Suwanee Creek	11
Crooked Creek WWTP	26
John's Creek WWTP	27
Big Creek	44
Big Creek WWTP	51
R.L. Sutton WWTP	101
R.M. Clayton WWTP	102

From Figure 4-4 it can be easily seen where in the model to expect jumps in concentration. For example TBEP will not show significant increases in concentration between tank 27 and tank 102 because the source at John's Creek is orders –of magnitude larger than any subsequent source before R. M. Clayton. This information will be used in Chapter 4 where we analyze the results of the model.
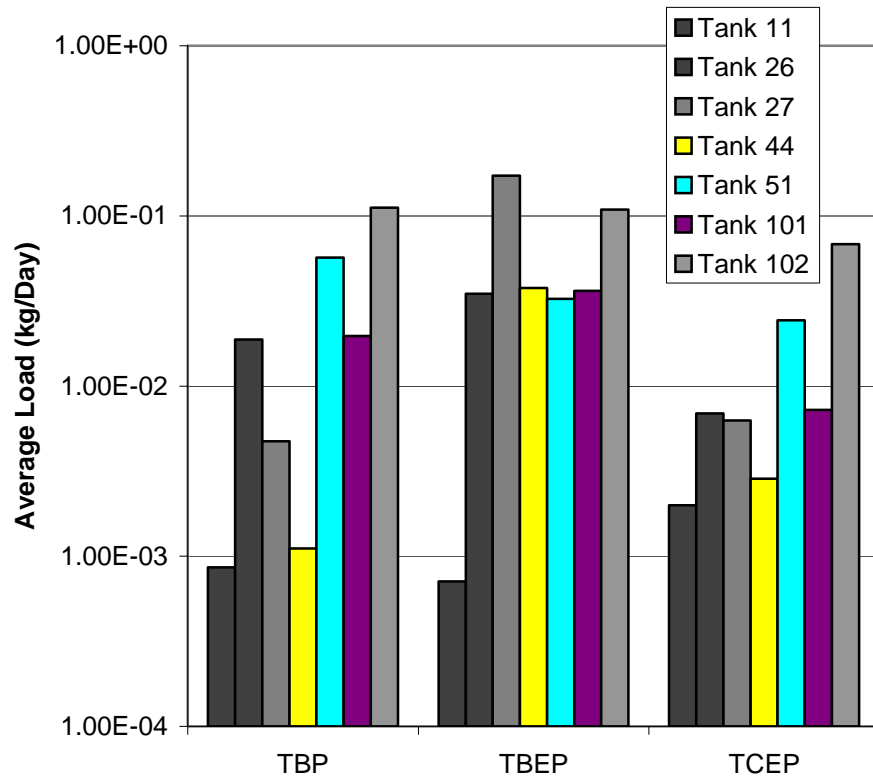

Figure 4-4 Average Daily Phosphate Ester Loads

4.2.2 Generation of Initial Conditions

In order to accurately model conditions in the river during the five days being simulated (January 12, 2004 – January 16, 2004) an initial concentration distribution had to be determined for each phosphate ester. The model begins simulating at midnight January 12. Because midnight January 12 was a Sunday night, the river had been at low flow since the previous day. Therefore in order to achieve a reasonable concentration distribution for the start of the model, conditions in the river at the end of a weekend should be calculated.

To produce this initial concentration distribution the model was run with a simplified flow regime for a forty-two-day cycle. For the first five days of the cycle flows leaving Buford Dam were set to a steady 77.6 m^3/s, the average flow during the simulated five days. This is followed by two days of a steady low flow of 19.9 m^3/s. All other parameters were kept the same as the base five-day case. The purpose was to simulate four typical weeks in an effort to achieve the initial concentration distribution described above.

4.3   Results

In this section the results of the model will be discussed. We will first discuss the spatial and temporal concentration distribution, then examine the effect of each of the modeled reactions, and finally we will compare the results of this model with the observations made between January 14, 2004 and January 16, 2004.

4.3.1   Flow Pattern vs. Concentration

The model predicts that diurnal flow variations imposed by Buford Dam and the regulation of flow at Morgan Falls Dam have an effect on the daily and weekly concentration patterns of the phosphate esters. Due to the position of phosphate ester point sources and depending on the position relative to Morgan Falls Dam these patterns are manifested differently at different locations on the river.

4.3.1.1   Initial Conditions Model Results

The model was run for a forty-two day cycle in order to generate an initial concentration distribution. The results of this model make some predictions as to what the pattern of concentration variance is within the Chattahoochee over a two-month period. This model averages out the flow variation occurring during the five-day workweek when power is generated at the hydroelectric dams. The model uses an average weekly flow and average weekend flow and alternates between them.
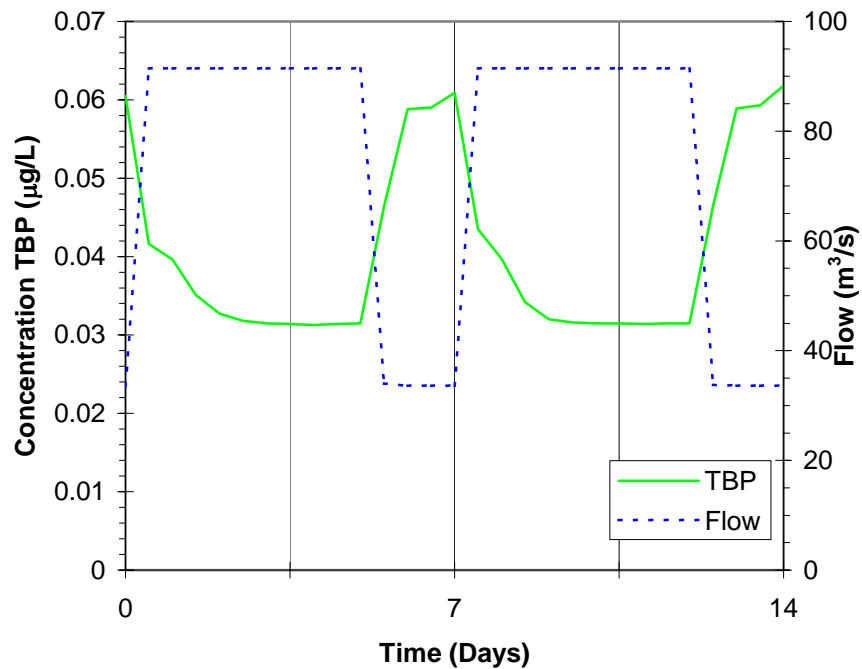
Figure 4-5 Flow and TBP Concentration at Highway GA 280 Crossing (Tank 103) Forty-Two Day Model

Figure 4-5 shows the concentration of TBP in water at the downstream end of the initial conditions model for a two-week period. Flow is also shown on the plot and it is easy to see that TBP concentration varies inversely with flow. During the week when flow is high TBP concentration at tank 103 is approximately 0.032 μg/L. When the weekly low flow period arrives concentration increases by almost a factor of two and then drops back down at the start of the week. Note that the five-day model begins at the end of day 14 shown above. The cycle of concentrations is similar for TBEP and TCEP with TBEP fluctuating between 0.15 μg/L and 0.17 μg/L and TCEP between 0.04 μg/L and 0.025 μg/L.

4.3.1.2 Five Day Simulation and Initial Conditions Model

While the initial conditions model assumes a steady average weekly flow, the five-day simulation resolves the individual flow fluctuations caused by the operation of the hydroelectric dams during the weekdays January 12, 2004 – January 16, 2004. While the initial conditions model reveals something about the way concentrations may vary from

week to weekend the five-day simulation zooms in on the fluctuations of flow and concentration that are experienced during the week. Figure 4-6 displays the fluctuations predicted at the Highway GA 280 crossing for a typical week and can be thought of as the details of what happens in between low flow periods in Figure 4-6. The remainder of Section 4.3 will investigate the patterns predicted by the five-day simulation.
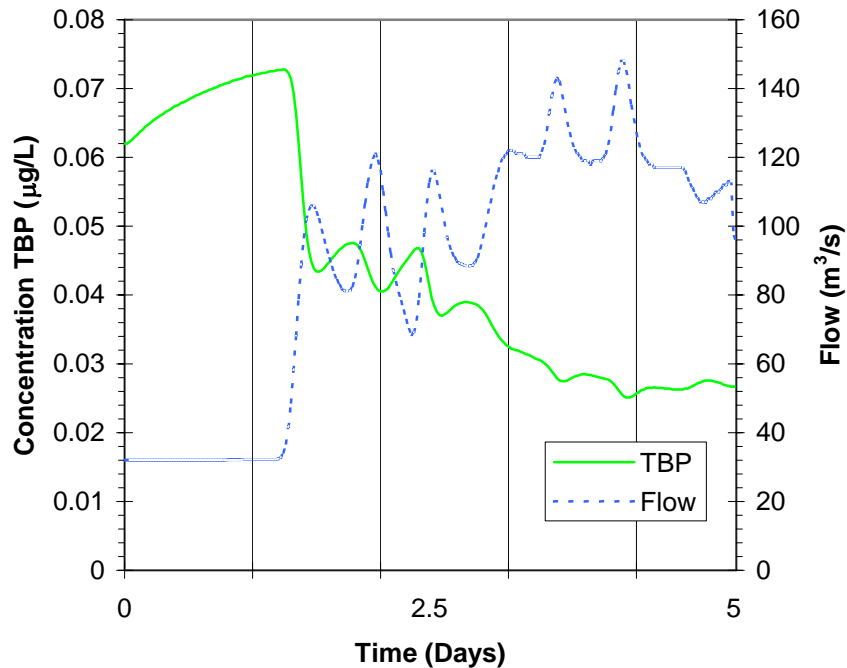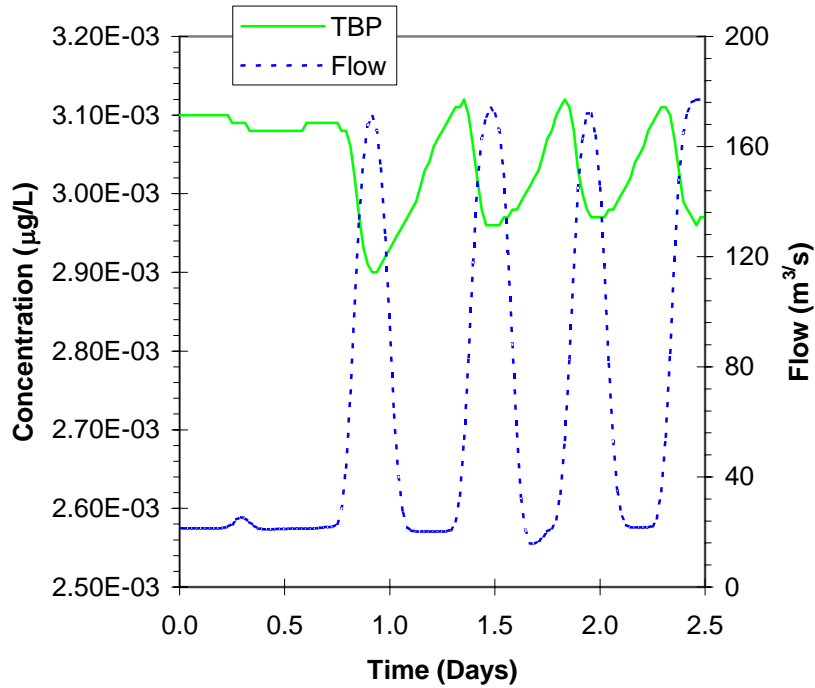

Figure 4-6 Flow and TBP Concentration at Highway GA 280 Crossing
(Tank 103) Five-Day Model

4.3.2   Concentration Patterns above Morgan Falls

4.3.2.1   Suwanee Creek to Crooked Creek

The inflow at Suwanee Creek is less than 2 m^3/s and has a concentration comparable to that leaving Buford Dam except in the case of TBEP where the inflow at Suwanee Creek actually serves to slightly dilute concentrations. Directly below the mouth of Suwanee Creek concentrations are higher during low flow periods due to the greater effect of the Suwanee Creek inflow (Figure 4-7). Concentrations of TBP entering at Suwanee Creek are two times as large as the background in the Chattahoochee before the confluence. During low flow periods the Suwanee Creek flow is 10% of the Chattahoochee and causes the increase in concentration.

**Figure 4-7 Flow and TBP Concentration Directly Below
The Mouth of the Suwanee Creek (Tank 12)**

In comparison, TBP concentrations decrease during low flow periods 21 kilometers down stream at tank 25 (Figure 4-8). Here lateral inflow in the reach between Suwanee Creek and tank 26 dilutes the ambient concentrations at low flow and has less effect at high flow resulting in increasing concentrations during the passage of the flood wave. This pattern is less pronounced for TBEP and TCEP and even for TBP the variation is less than a nanogram but nonetheless is a pattern worth noting.
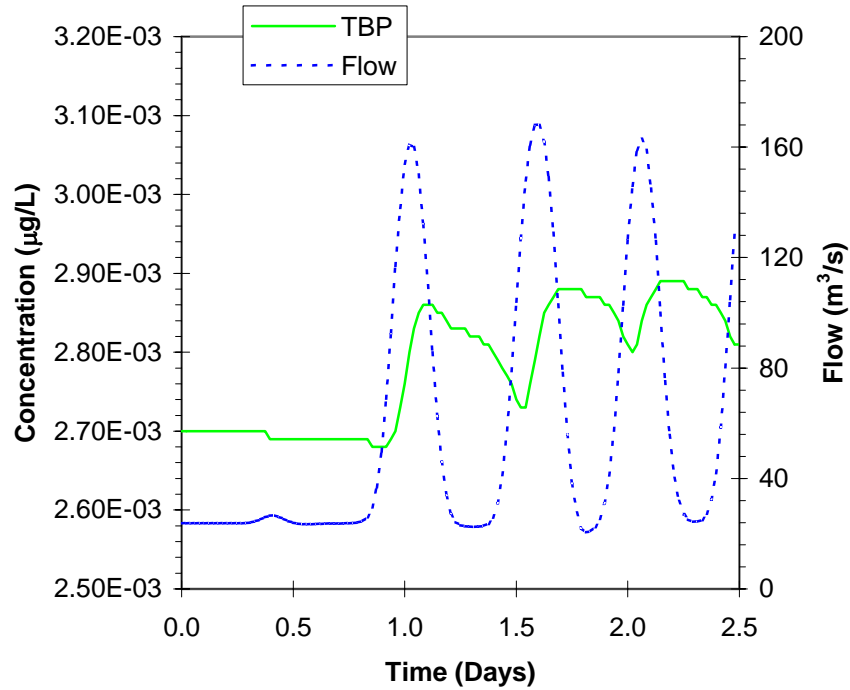
**Figure 4-8 Flow and TBP Concentration Directly above the Crooked Creek WWTP Outfall
(Tank 25)**

4.3.2.2 Crooked Creek to the Mouth of the Big Creek

Two outfalls exist in the beginning of this reach, Crooked Creek WWTP in tank 26 and
John's Creek in tank 27. Crooked Creek is a relatively large source of TBP while John's
Creek is the largest source of TBEP in the modeled reach. Directly downstream of the
outfalls, concentrations of TBP rise by 6 ng/L, TBEP rise by 64 ng/L and TCEP rise by 4
ng/L. The pattern of concentration in this reach is similar for all three compounds and is
illustrated in Figure 4-9, which shows the first half of the simulation for TBEP in tank 36.
Studying Figure 4-9 reveals that concentrations steadily rise during low flow periods and
drop off during the passage of the flood wave. In general concentrations of all three
phosphate esters follow a similar pattern in this reach.
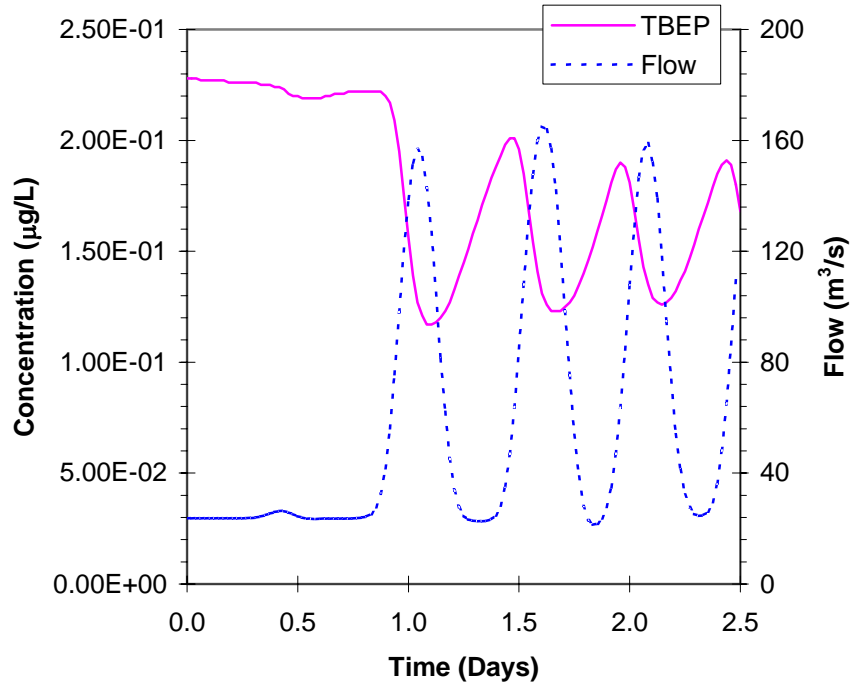
Figure 4-9 Flow and TBEP Concentration in the Center of the Reach between the Crooked Creek Outfall and the Mouth of the Big Creek (Tank 36)

4.3.2.3 Mouth of Big Creek to Bull Sluice Lake

Within this reach the river begins to become wider and slower as it approaches Bull Sluice Lake. Figure 4-10 shows the concentration of TCEP and flow at tank 51 between the confluence of the Big Creek and the Big Creek WWTP outfall. This plot begins at day one of the simulation since before then at this model tank the river is at low flow. One can plainly see that the range of fluctuation in concentration is not as pronounced as upstream. This can be explained by the fact that the tanks in this region have higher volume and therefore do not get fully flushed by the flood waves. It is interesting to note that the concentration does not immediately drop when the first flood wave passes through. This is again a consequence of the tanks in this reach being much larger and therefore do not immediately become diluted by the lower concentration waters arriving on the flood wave.
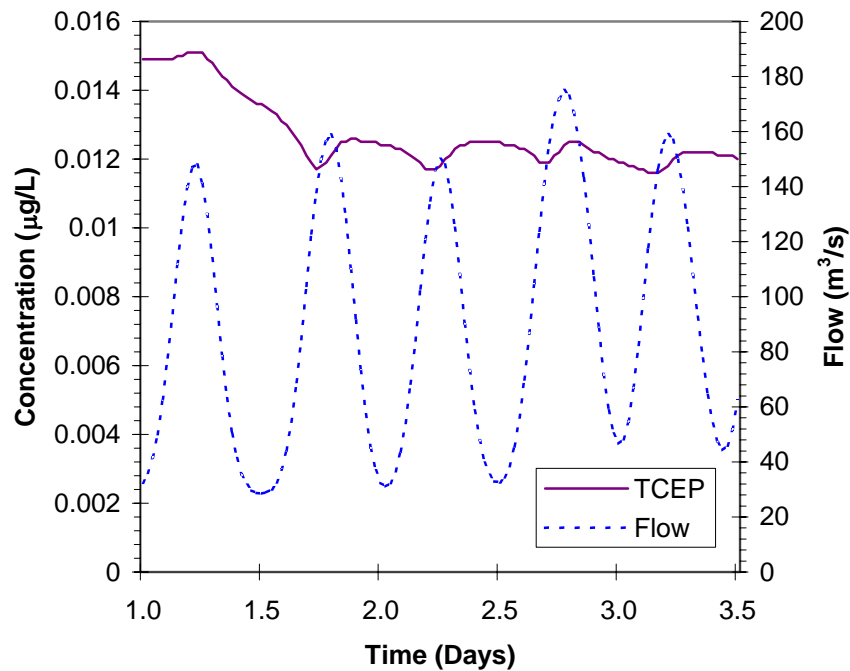
Figure 4-10 Flow and TCEP Concentration between the Mouth of Big Creek and the Big Creek WWTP Outfall (Tank 50)

The behavior of TCEP in the region is representative of the other phosphates as well. Concentrations for the TCEP and TBEP will rise after tank 51 were the Big Creek WWTP outfall discharges. TBEP will not exhibit a marked increase since the TBEP load at Big Creek WWTP and the Big Creek confluence is orders of magnitude lower than the load at John's Creek 15 kilometers upstream (Figure 4-4).

4.3.3   Concentration in Bull Sluice Lake

Concentrations in Bull Sluice Lake are important to address separately since they represent the boundary between two very different concentration patterns. The large volume of Bull Sluice Lake along with the change in flow patterns at Morgan Falls produces these different patterns.

As we have seen in the oscillation between low and high concentrations becomes less pronounced as we move into the slower moving waters near Bull Sluice Lake. The concentration patterns in Bull Sluice Lake are most easily illustrated by looking at TBEP due to it being at a relatively higher concentration, however all three compounds exhibit

much the same pattern in Bull Sluice Lake. Figure 4-11 displays the TBEP concentration and average flow curves for Bull Sluice Lake.
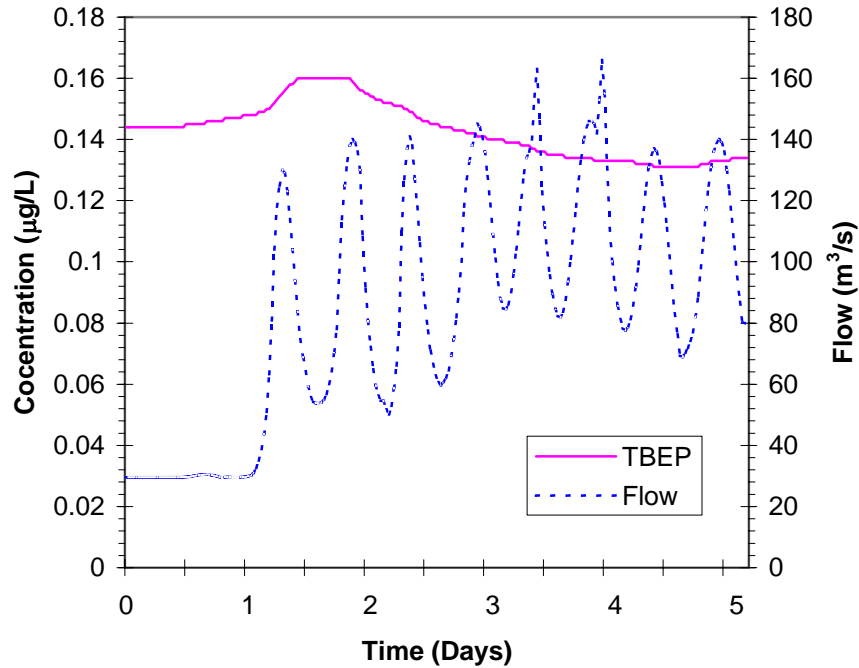
Figure 4-11 Flow and Concentration of TBEP at Bull Sluice Lake (Tank 51)

Studying Figure 4-11 one can see that the concentration of TBEP in Bull Sluice Lake steadily rises coming out of the weekend through Monday (Day 0). At midnight Tuesday (Day 1) the first flood wave arrives at Bull Sluice Lake and for the next half-day concentration rises more sharply as the high concentration waters from upstream are flushed through the system and mix into Bull Sluice Lake. This volume is small though compared to Bull Sluice Lake and after leveling out between noon Tuesday and midnight Wednesday (Day 2) the concentration begins to drop off hitting its minimum in the afternoon Friday (Day 4) when it begins to rise again. It is our conjecture that the concentrations will rise through the weekend repeating a similar pattern again at the start of following week.

4.3.4   Concentration Downstream of Morgan Falls

Concentration downstream of Morgan Falls can be broken down into two different patterns. Patterns in this area are of considerable interest since it is here at tank 99 that

the Atlanta Water Works withdraws water for the city of Atlanta. Immediately after the Atlanta Water Works the outfalls of the R.L. Sutton WWTP and the R. M. Clayton WWTP increase the concentration in the final tanks in the model.

4.3.4.1 Concentration between Morgan Falls Dam and Atlanta

The concentrations upstream of the R. M. Clayton and the R. L. Sutton plant outfalls follow a similar pattern as that in Bull Sluice Lake discussed in the previous Section. Bull Sluice Lake can be thought of as a large mixing tank that averages out the concentration fluctuations caused by the diurnal flow cycle. The mean residence time of a water body can be estimated with

$$t_{res} = \frac{V}{Q}$$

Equation 4-2

Where:

- t_{res} = mean residence time of a parcel of fluid [T]

- V = volume of water body [L^3]

- Q = average flow rate through water body [L^3/T]

The water released over Morgan Falls Dam at time t has the average concentration of the waters that have entered since $t - t_{res}$. Only dilution and degradation processes affect the concentration in this reach. Fluctuations in flow caused by the operation of Morgan Falls Dam have no effect, which can be seen in Figure 4-12.
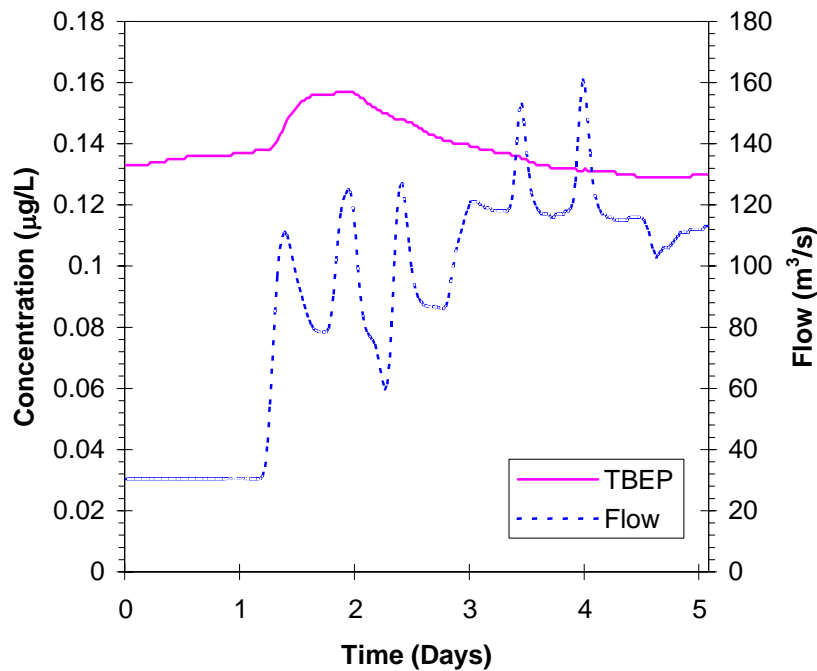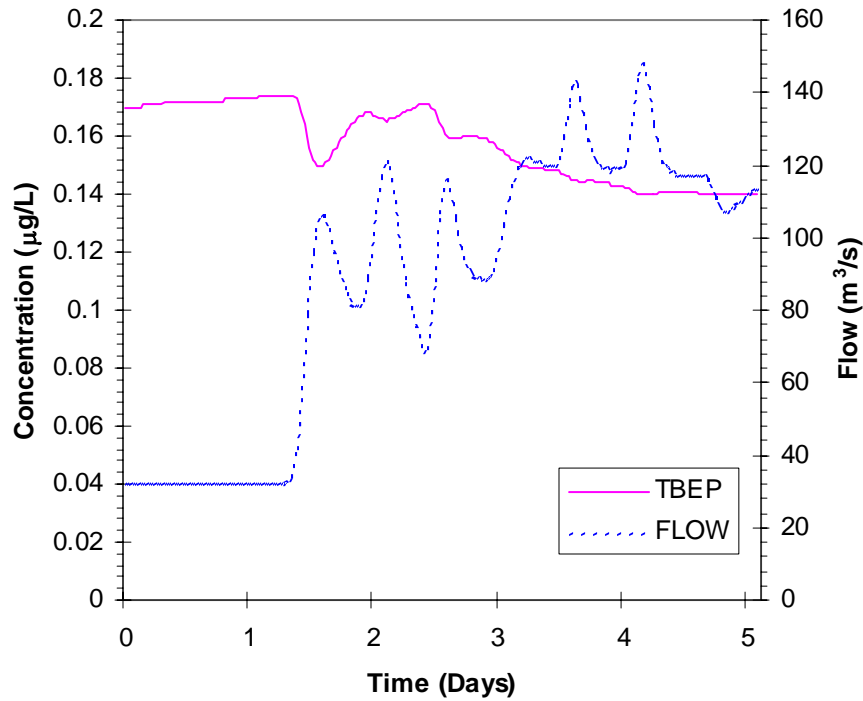
Figure 4-12 Flow and TBEP Concentration in the Reach between Morgan Falls and Atlanta (Tank 79)

It is interesting to note that a slug of relatively high concentration water is flushed from Bull Sluice Lake and travels downstream passing this point between noon on Tuesday (Day 1) and Wednesday (Day 2) morning. This may have implications for drinking water treatment plants drawing water from the Chattahoochee in this reach; this will be discussed further in the conclusions. It should also be noted that the specific shape of the concentration curves for TBP and TCEP are not exactly the same as that displayed here for TBEP and have subtle differences. Still the general patterns are the same and the above analysis applies for all three phosphate esters.

4.3.4.2 Downstream of the Atlanta Treatment Plants

Discharges from R.M. Clayton and R.L. Sutton WWTPs dominate the concentration characteristics of this portion of the model. R. L. Sutton discharges into tank 101 and is estimated to be the second largest source of TCEP, and is an average size source of both TBEP and TBP. The R. M. Clayton facility is the largest in the modeled reach and discharges into tank 102. This is estimated to be the largest load of TCEP and TBP and the second largest of TBEP in the reach. Concentrations of all phosphate esters are

expected to increase in these final tanks. The model predicts that between tank 100 and 103 TBP exhibits an increase of 16%, TBEP increases by 106%, and TCEP increases by 70%. The differences in percentage of increase can be understood by viewing Figure 4-4 where a relative comparison of load magnitude is made.

Figure 4-13 Flow and TBEP Concentration at Highway GA 280 Crossing
(Tank 103)

The pattern that the concentration vs. time curve takes can be seen in Figure 4-13. The concentration is rising slowly coming out of the weekend at the beginning of the simulation. This is due to the rising concentration of the waters released at Morgan Falls Dam (Section 4.3.3) as well as the loads from R.L. Sutton and R.M. Clayton WWTPs being discharged to the weekend low flow. When the first flood wave arrives after midnight on Tuesday (Day 1) a sudden decrease in concentration occurs which rebounds in between the following two flood waves but trails off as the week goes on and high flows flush the high concentrations downstream. Again the pattern of the concentration curves is similar for TBP and TCEP although, as can be seen in Figure 4-6, the rebounds

after the first flood wave are hardly as pronounced and concentration stays relatively low during the week.

4.3.5 Sorption Model Results

The sorption model discussed in Section 4.1.1 did not have a significant effect on the concentrations of any of the phosphate esters. TBEP is the compound most likely to sorb to organic matter suspended in the water column and less than 1% of the TBEP concentration in any model tank is transported as sorbed to the solid phase. In this case settling of suspended solids will not be a significant sink of the phosphate esters.

The fraction of organic carbon (f_{oc}) in the base case suspended solids model is 1% and this was raised to 10% to quickly assess the sensitivity of the model to f_{oc} values. The results of this test showed as much as 4.3% of TBEP being transported as sorbed in the final tank in the model. While this sorbed percentage is still not a substantial fraction of the total TBEP concentration, it represents an increase of a factor of 20 over the previous case. The percentages of each phosphate ester being transported as sorbed to the solid phase for the two cases are displayed in Table 4-7.

Table 4-7 Average Percentage of Phosphate Ester Sorbed to Suspended Solids (Tank 103)

Phosphate	f_{oc}	
	1%	**10%**
TBP	0.0%	0.4%
TBEP	0.3%	2.8%
TCEP	0.0%	0.0%

Figure 4-14 shows the relationship between concentration of suspended solids and of TBEP transported as sorbed to the solid phase. From studying this figure it is apparent that the percentage of total TBEP concentration sorbed to suspended solids is proportional to the concentration of solids. Therefore one can expect that during turbid conditions that sorption could be a much more important process for TBEP and even possibly TBP. Highly turbid conditions were simulated and results show that during these high turbidity events sorption can be a significant sink of TBEP (up to 40%

transported as sorbed) (Haffey, 2004). The reader is directed to Haffey (2004) for detailed description of this sensitivity testing.
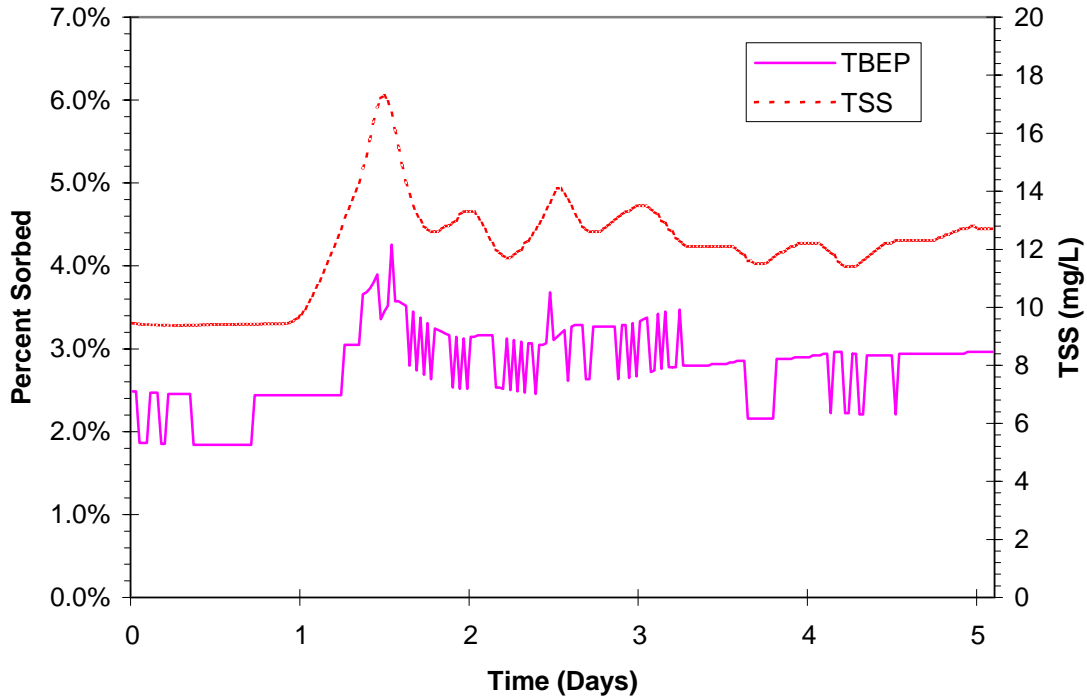
Figure 4-14 TSS and Percentage TBEP Sorbed at Highway GA 280 Crossing (Tank 103) (Note that fluctuations in sorbed percentage are due to numerical imprecision in the output file)

TBEP has been shown to be the most likely to sorb to organic matter and it is interesting to compare the average concentration of TBEP leaving the model at the Highway GA 280 crossing in both cases discussed above. The concentration in tank 103 for the f_{oc} equal to 10% case is 95.5% of the concentration in the f_{oc} equal to 1% case. Although not a significant loss some degradation can be attributed to suspended solid settling.

4.3.6 Biodegradation Model Results

The magnitude of the sink due to biodegradation was evaluated by observing concentrations just upstream of the R. L. Sutton WWTP for both the base case model and a case without biodegradation. Phosphate esters that enter the system at R.L Sutton and

R. M. Clayton WWTPs do not have a long enough residence time for biodegradation to become a large factor and for this reason were left out of this comparison.

TBEP concentrations were the most affected by biodegradation and were an average of 11% lower than in the model without biodegradation at the observation point (tank 100). TBP was an average of 5% lower and TCEP an average of 2% lower.
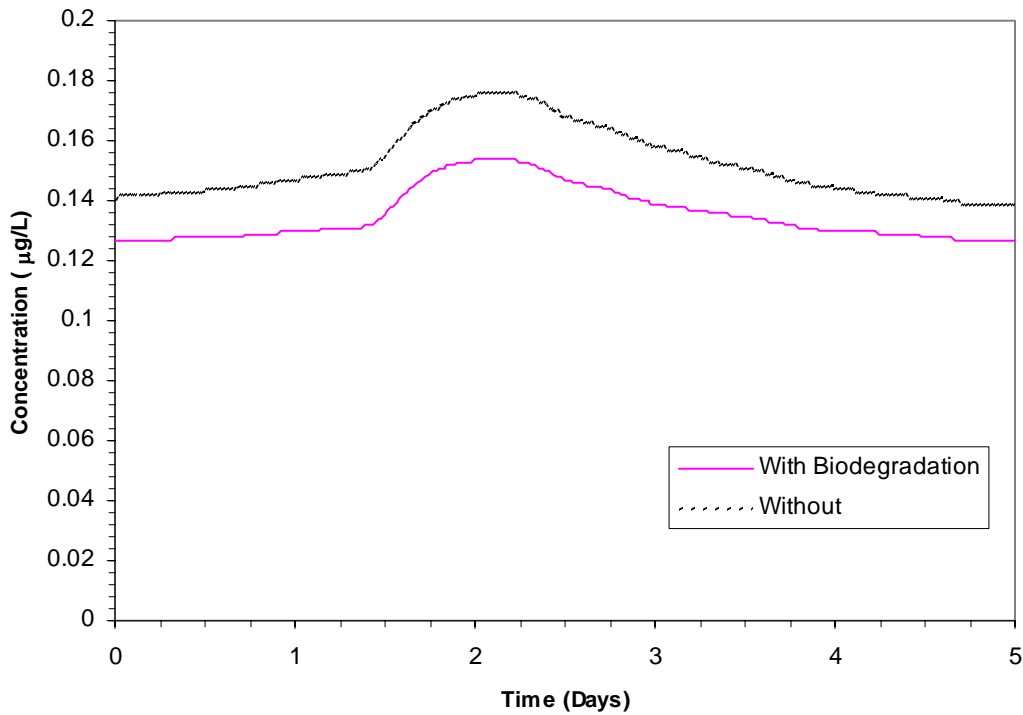
Figure 4-15 Concentration of TBEP Upstream of R.L. Sutton WWTP
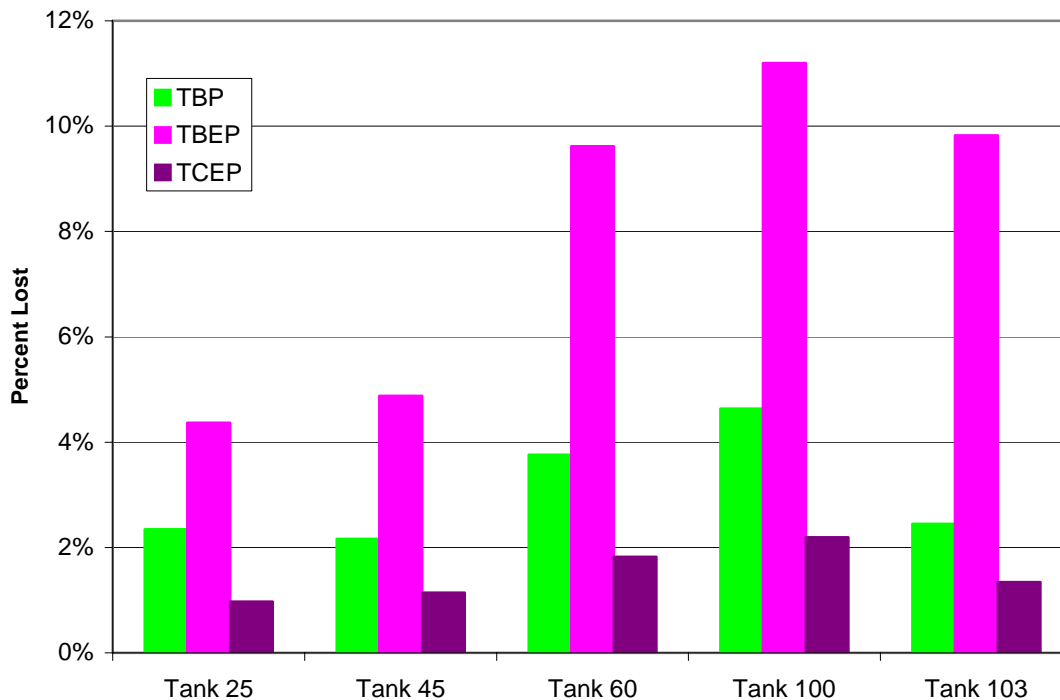**with Biodegradation and without Biodegradation**

Figure 4-15 shows the concentration curves at tank 100 for both the case with biodegradation and the case without biodegradation. It is apparent that the concentration in the simulation with biodegradation is consistently lower. Examination of Figure 4-16 shows how the percentage of loss due to biodegradation changes during the simulation. It reaches a maximum on noon on the second day of the simulation corresponding to the end of the weekend low flow period. This increase in loss to biodegradation is due to the increased travel times during low flow periods between the WWTP outfalls upstream of Morgan Falls Dam and tank 100. As the high flows typical of weekdays begin after noon

on the second day, the travel times decrease and biodegradation does not have as much time to take effect.
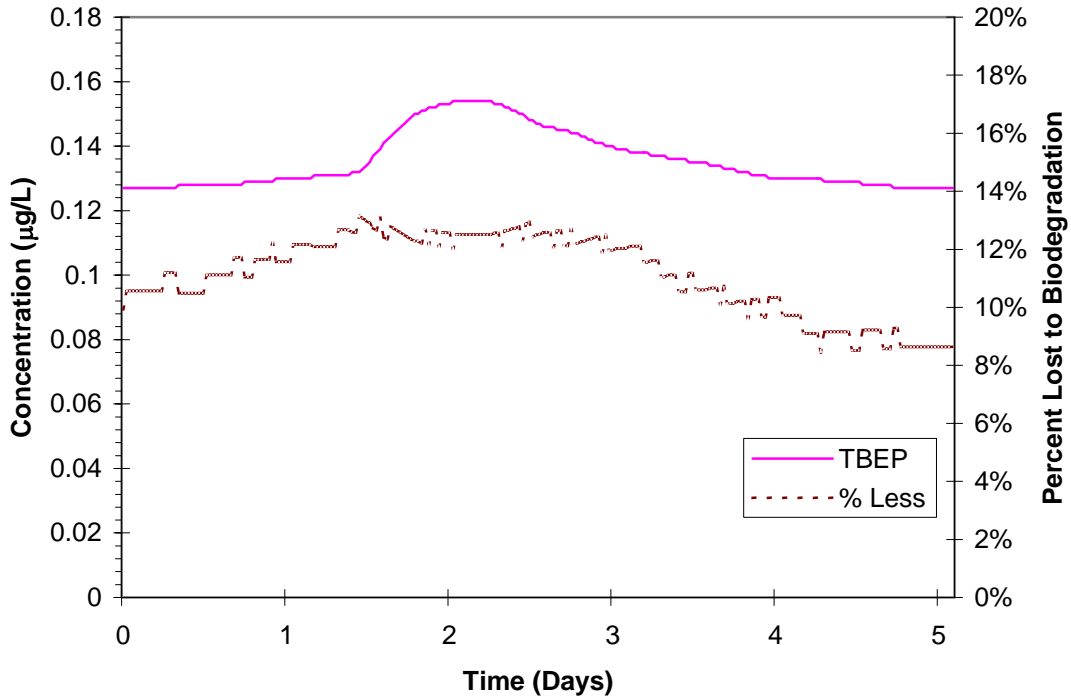
Figure 4-16 TBEP Concentration and Percent Loss Due to Biodegradation Upstream of the R.L. Sutton WWTP

Figure 4-17 shows the average percentage by which the simulation with biodegradation is less than the simulation without biodegradation at five locations along the river. The difference in height of the columns in the graph in Figure 4-17 reveals where in the modeled reach there is the maximum potential for loss to biodegradation. As can be seen from the large increase in the percent lost between tank 45 and tank 60 the biggest potential for loss to biodegradation is in this region. The slower waters in this region, especially in Bull Sluice Lake, result in long travel times through the reach. The percentage lost decreases downstream of the R.L. Sutton and R.M. Clayton outfalls since phosphate esters added by these WWTPs do not remain in the system long enough for an appreciable difference to develop between the two models.

Figure 4-17 Percentage of Cumulative Phosphate Loss to Biodegradation at Locations along the Modeled Reach

The biodegradation constants were varied within the confidence interval reported in Andrews (2004). The results of the sensitivity tests are reported on in detail in Haffey (2004).

4.3.7 Volatilization Model Results

The magnitude of the sink attributed to volatilization was evaluated by comparing the results of the base case model with the results from a simulation run with volatilization turned off. As in Section 4.3.6 the comparison is made upstream of the R.L. Sutton WWTP outfall in order to avoid the concentrations added by this plant.

Volatilization was most significant for TCEP though it did not account for much loss and resulted in the TCEP concentration in the base case being only 3% less than that in the case without volatilization. Volatilization was not significant for TBP or TBEP and reduced TBP by 1% of the case without volatilization and did not reduce TBEP at all.

Volatilization rates in rivers are affected by water velocity and channel depth and therefore it is expected that the rate of volatilization for TCEP is affected by the river flow. Figure 4-18 shows TCEP volatilization rates and flows in the modeled reach at the beginning of the third day of the simulation.
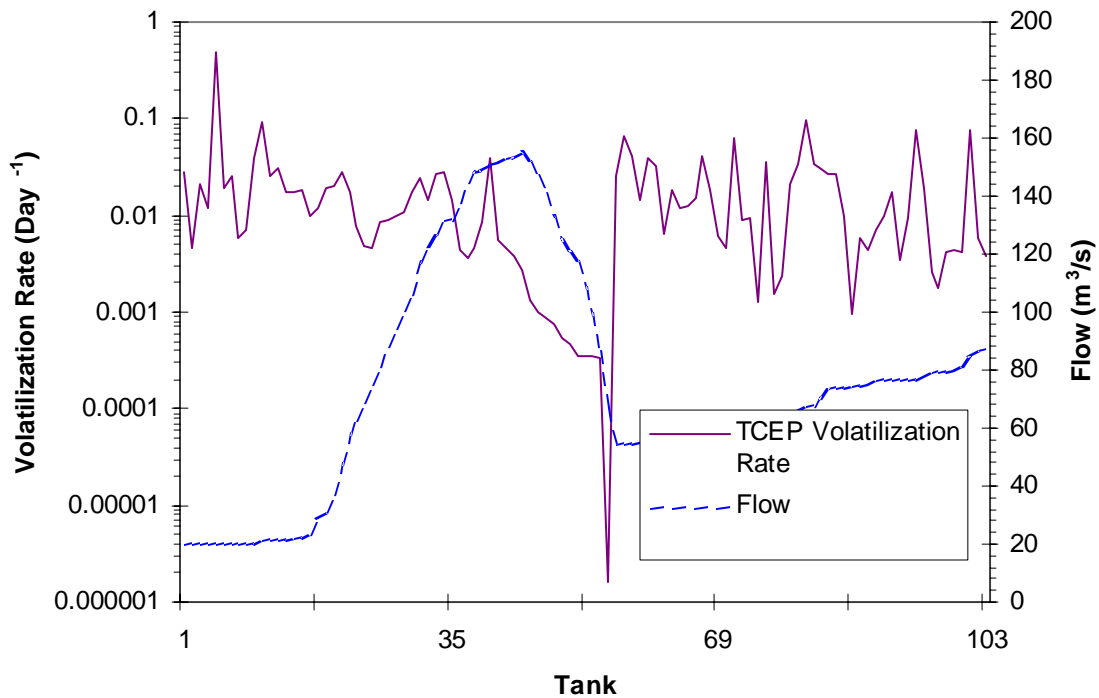
Figure 4-18 Profile of TCEP Volatilization Rate and Flow at Beginning of Third Day

Figure 4-19 shows the volatilization rates and flows six hours after the snapshot in Figure 4-18. A few tanks show marked change in volatilization rate, tank 5 and tank 11 showing the most sensitivity to flow. These are tanks in which the velocity changes dramatically with flow. These tanks are at the upstream end where concentrations are low so the rapid volatilization in these tanks does not serve to affect the downstream concentration of TCEP dramatically. Volatilization is most significant for TCEP during low flow periods, however this significance is tempered by the fact that the river reaches where it is most effective carry low concentrations.
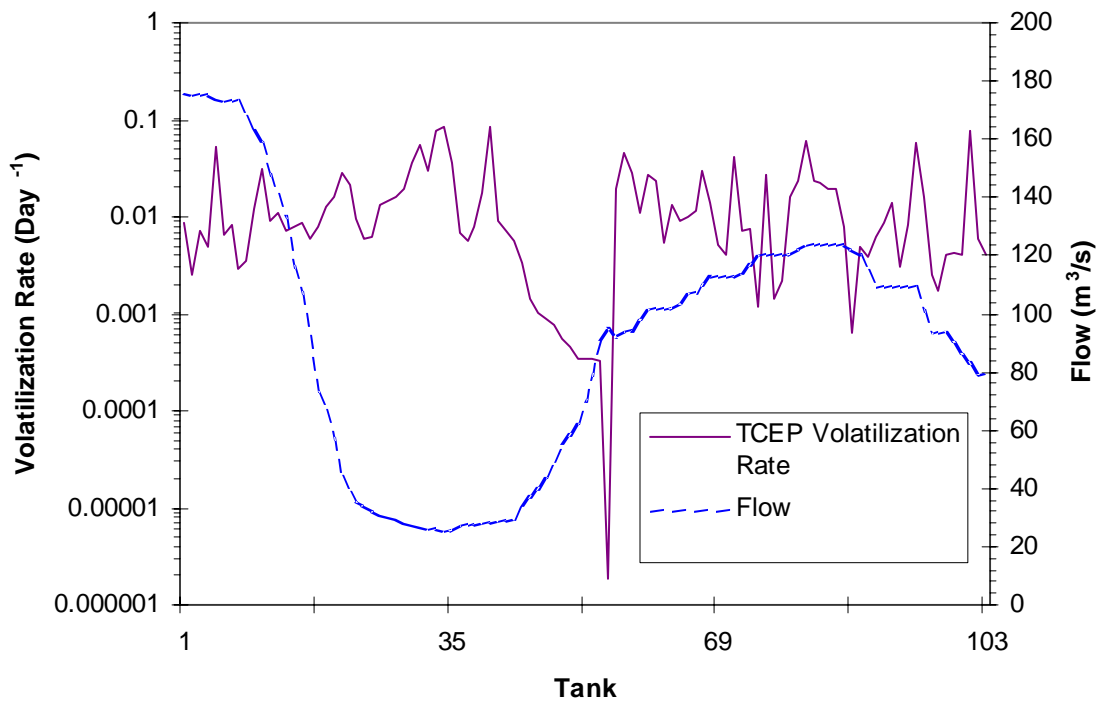
Figure 4-19 Profile of TCEP Volatilization Rate and Flow Six Hours into the Third Day

4.4   Oxidation Model Results

As in the evaluation of the other processes we compared the base case model results with a simulation that did not include oxidation by free radicals. As in the previous analysis we first investigate the concentration at tank 100. TBEP is the most susceptible to oxidation by free radicals and has an average concentration 5% less at tank 100 than the model with oxidation turned off. The concentration of TBP is less affected and has an average concentration in tank 100 2% less than the model without oxidation. TCEP was barely affected by free radical oxidation and was only reduced by 0.5%

Since the model held the concentration of free radicals constant throughout the model (Section 4.1.4), the oxidation reaction reduces to a first-order decay. Biodegradation is also modeled as first-order decay and therefore the two reactions will have similar pattern with the exception of the magnitude of the sink. The reader is referred to Section 4.3 for discussion on how oxidation will vary spatially and temporally in the model.

4.5   Comparison to Field Studies

The base case model results were compared to the results of two field studies that sampled for in-stream concentrations of TBP, TBEP, and TCEP. Andrews (2004) took samples at three locations in the modeled reach and Lin (2004) took samples of untreated water drawn from the Chattahoochee at the Atlanta Water Works drinking water treatment plant. The simulated period was chosen so as to cover the days when these samples were taken. Table 4-8 lists the average modeled concentration for the day that the sample was taken along with the observed data. The locations of the sample sites are the same as those taken for turbidity (Figure 4-20) plus the Atlanta Water Works DWTP (Figure 4-2)
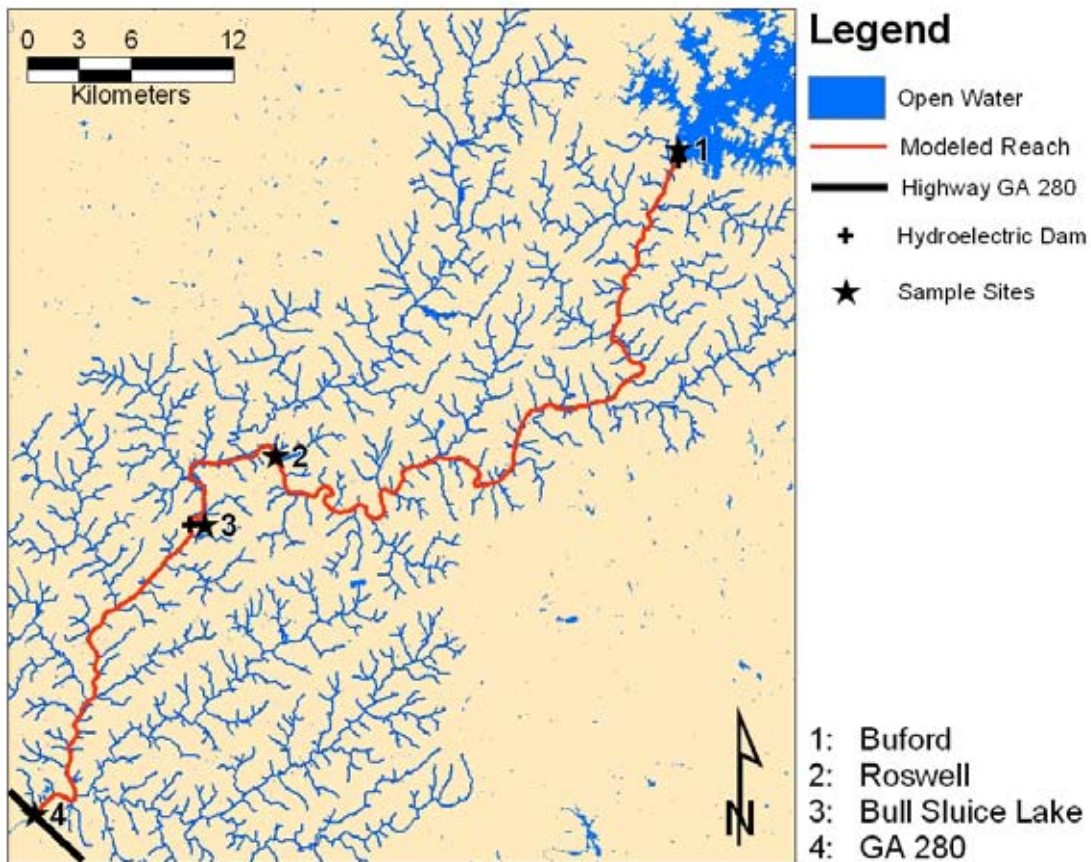

Figure 4-20 Location of Sample Sites Used in Comparison

Table 4-4-8 Sample Sites & Corresponding Model Tank
(Andrews, 2004 and Lin, 2004)

Tank	TBP		TBEP		TCEP	
	Modeled (µg/L)	Observed (µg/L)	Modeled (µg/L)	Observed (µg/L)	Modeled (µg/L)	Observed (µg/L)
Roswell	0.005	0.010	0.131	0.173	0.012	0.067
Bull Sluice Lake	0.014	0.010	0.132	0.307	0.016	0.024
Atlanta Water Works	0.024	0.027	0.148	0.119	0.020	0.020
GA 280	0.030	0.034	0.147	0.442	0.024	0.132

Inspection of Table 4-8 shows good agreement between the model and observations made by Lin (2004) at the Atlanta Water Works sample site (Tanks 99). As has been discussed in Section 4.3.1 the concentrations in this region do not fluctuate with flow but represent the well-mixed concentrations leaving Morgan Falls Dam, and the agreement with observation here supports the analysis. In most other cases the model results are within a factor of two of the observations. Still discrepancies exist.

The observations of TCEP at the Highway GA 280 crossing and to a lesser extent TBEP are significantly greater than the model predictions. This can be explained by observing that the sample site is only 1.6 kilometers downstream from the R.M. Clayton WWTP outfall and 1.9 kilometers downstream of the R.L. Sutton outfall. Phosphate esters released in the outfall will be concentrated on the outfall side of the river and it will take some time for the lateral mixing processes to spread the phosphate esters uniformly across the channel.

4.6   Conclusions

The model predictions were reasonably close to observations of phosphate ester concentrations made during the modeled period. These results show that predictions of phosphate ester concentration distributions in the Chattahoochee River are feasible through a numerical modeling approach. Furthermore the results show that the diurnal flow pattern imposed by the operation of the hydroelectric dams affects the concentration distribution in time and space. Any future attempt to model water quality in this reach of the Chattahoochee River must account for the time varying river flow.

The predictions of the model allow the phosphate esters to be rated on a scale of resistance to the natural attenuation processes. TCEP is the most resistant followed by TBP. TBEP is the most susceptible to degradation. TBEP was predicted to be most susceptible to biodegradation and loss due to sorption to settling particles. TBEP concentrations in the base case scenario were an average of 11% lower than the model run without biodegradation. However, even after increasing the biodegradation rate for TBEP by a factor of 2 concentrations remained reasonably close to the base case concentration. This indicates that travel times between the WWTP outfalls above Morgan Falls Dam and downstream DWTP intakes are insufficient for biodegradation to substantially reduce TBEP concentrations.

Loss due to sorption to settling solids may also be a significant mechanism for removing TBEP from the water column under certain conditions. Gaps in data forced the approximation of many of the parameters in the suspended solids model and the magnitude of predicted TBEP loss due to sorption to settling solids proved to be highly sensitive to variations in organic carbon content and average particle size. Observations of the suspended solids characteristics in the Chattahoochee River are necessary to further evaluate the magnitude of this sink. It must also be kept in mind that TBEP sorbed to settling particles deposits on the riverbed where concentrations build up over time and may be re-released to the water column.

The above conclusions suggest that from the standpoint of keeping Chattahoochee River water concentrations low, TBEP is the preferred phosphate ester to use when practicable. Further studies must be conducted to evaluate the potential for TBEP buildup in the riverbed.

The discussion of the results explains the pattern of concentration downstream of Bull Sluice Lake and upstream of the R.L. Sutton and R.M. Clayton WWTPs. Two municipal drinking water treatment plants servicing the greater Atlanta area draw raw drinking water from the Chattahoochee River in this reach. Results indicate that the model predictions reasonably agree with observations made at the most downstream of these DWTPs. The Atlanta Water Works DWTP. The patterns suggest that a pulse of

relatively high phosphate ester concentration travels through this reach on the second day of the week and that concentrations in the drinking water may be higher during this time.

5 Drinking Water Treatment Plant Processes

Mr. Lin focused on drinking water treatment processes, and whether or not these processes were effective in removing the phosphate triesters. Specifically, he took samples after major processes at the Chattahoochee Water Treatment Plant (CWTP) in Atlanta, GA. Description of the sampling sites in the CWTP, materials and methods used, and findings are discussed in this chapter.

5.1 Description of Sampling Sites in the CWTP

5.1.1 Intake
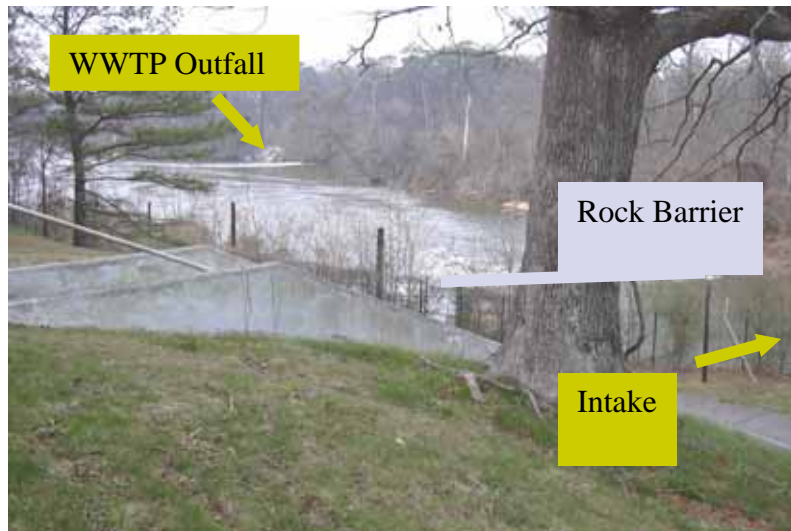
Figure 5-1 Location of WWTP outfall compared to the location of the intake. A rock barrier prevents wastewater effluent from entering the intake.

The intake water of the CWTP comes from the Chattahoochee River. The major sources of the phosphate triesters are four major WWTPs that discharge their effluent upstream of the CWTP: Crooked Creek Water Pollution Control Plant (WPCP), Johns Creek WPCP, the City of Cummings WPCP, and the Big Creek WPCP. The R.M. Clayton WPCP, which is the main wastewater treatment facility for the Atlanta area, has its outfall located approximately half a mile past the intake. To prevent this effluent from contaminating the intake, a rock formation was added between the two sites (Figure 5-1).

5.1.2   Addition of Aluminum Sulfate and Sodium Hypochlorite

The raw water travels via pipeline approximately 1000 feet from the intake to a pre-treatment chemical addition area, where solutions of aluminum sulfate (alum) and sodium hypochlorite are added.

Aluminum sulfate promotes the coagulation of colloidal particles into flocs. In drinking water treatment plants, this mainly happens through three different mechanisms: charge neutralization through adsorption of oppositely charged ions, inter-particle bridging, and precipitate enmeshment. Inter-particle bridging is where the coagulant forms a polymer chain with two or more particles. Enmeshment is the trapping of particles when the colloidal floc forms or when the floc is settling.

Aluminum sulfate, when in the aqueous phase, dissociates into the aluminum and sulfate ions. Depending on the pH of the water, the aluminum ion will undergo hydrolysis, thus adding hydroxyl ions (Figure 5-2). At pH 6-8, which are the usual pH values in the CWTP, the solubility of aluminum is quite low and aluminum will thus precipitate out. This precipitate will also include the potential flocs.
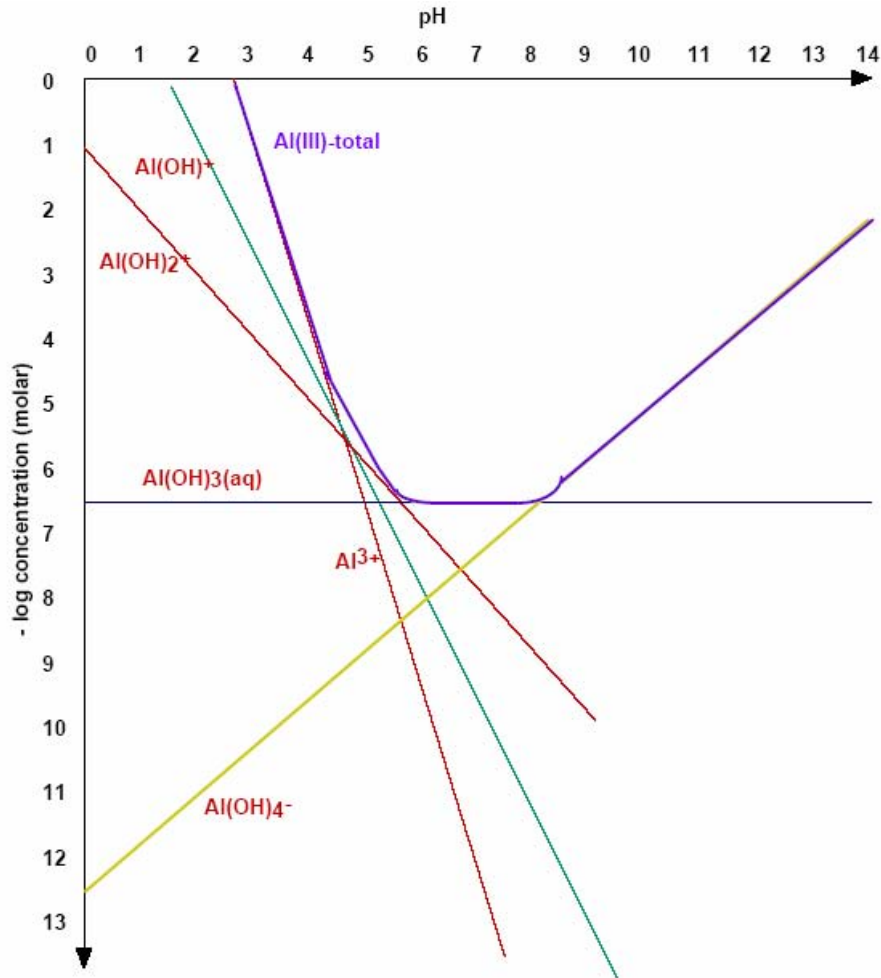
Figure 5-2 Diagram of solubility of different aluminum hydroxides exist at different pH values. For pH 6-8, the Al(OH)$_3$ solubility is the highest. Source: Danish University of Pharmaceutical Sciences (2003).

Coagulation is an important step to lower the turbidity in water. For an initial turbidity of 10 NTU, the final turbidity after using coagulation, flocculation, and filtration is 0.2 NTU, while the final turbidity after using only filtration is 5 NTU. (ASCE/AWWA, 1990 and Nazaroff and Alvarez-Cohen, 2001). This applies to the CWTP as well, where the average turbidity of raw water is about 15 NTU.

Sodium hypochlorite (NaOCl) is used to disinfect the water. Disinfection this early in the treatment sequence is not uncommon, as a typical drinking water treatment plant will have a pre-treatment chlorine addition (to keep a chlorine residual within the treatment plant) along with a post-treatment chlorine addition (to keep a chlorine residual within

the distribution system). Sodium hypochlorite, when added to water, dissociates into a single positive-charge sodium ion and a single negative-charge hypochlorite ion. This hypochlorite ion becomes hypochlorous acid (HOCl) as long as a certain pH is maintained below about 7 (Figure 5-3). Hypochlorous acid reacts with bacteria to kill the bacteria. Hypochlorous acid also reacts with different chemicals. For example, hypochlorous acid can react with hydrogen sulfide (which is toxic, and also has a bad smell), converting it to less toxic products. But, hypochlorous acid also reacts with natural organic substances to produce trihalomethanes, a undesirable product (Nazaroff and Alvarez-Cohen, 2001).
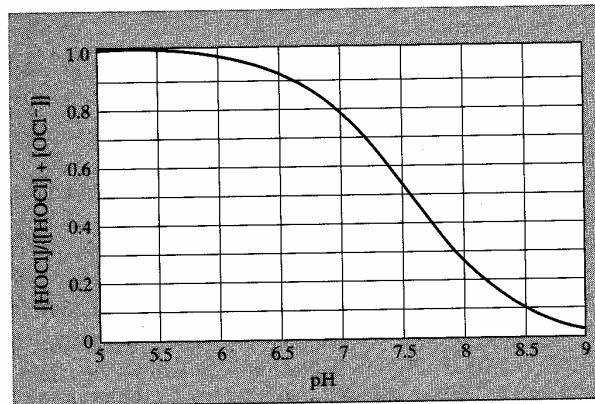
Figure 5-3 Curve of pH versus fraction of hypochlorous acid concentration over the free chlorine concentration. Source: Nazaroff and Alvarez-Cohen (2001).

Because the hypochlorite ion is basic, the addition of sodium hypochlorite increases the pH in the water. But, at the CWTP, the pH is affected more by the addition of alum. For instance, the intake water's pH is usually between 6.8 and 7. After the addition of alum (typically at a dose of 10 mg/L for a turbidity of 15 NTU) and sodium hypochlorite (typically at a dose of 3-4 mg/L), the pH is usually between 6.2 and 6.5. In addition, a high fraction of hypochlorous acid is maintained in the sedimentation basin, which usually has an effluent pH of 6.6.

In addition to pH, one must also examine the disinfection kinetics within the treatment plant. Watson's law proposes that $C * t_c = \mathbf{b}$, where C is the free chlorine concentration, t_c is the contact time, and b is a constant (Nazaroff and Alvarez-Cohen, 2001). Values of $\mathbf{b}$ have been tabulated for specific amounts of bacteria kill. For example, the free chlorine

concentration at the CWTP is always at least 0.5 mg/L in the sedimentation basins. Using this number, and assuming a pH of 7 and a 4-hour residence time in the basin, the value of **b** is 120 min-mg/L. Because there is a 4-log kill of bacteria when **b** is equal to 20 min-mg/L at pH 7, this implies that there is a 24-log kill in the sedimentation basin with **b** equal to 120. Thus, bacteria are sufficiently killed in the treatment plant even before the post-chlorine addition.

5.1.3   Flocculation/Sedimentation

After the addition of alum and sodium hypochlorite, the water goes through a flocculation and sedimentation phase. Flocculation is the thorough mixing of the water to promote the collision of colloidal particles, as discussed in the previous section. The mixing in this stage is slow enough, though, such that the flocs do not break apart.

Sedimentation is the quiescent flow of the water for a long time. This allows larger-diameter particles (e.g., particles formed from flocculation) to settle to the bottom of the tank. To find out what size particles will settle out in the sedimentation process, the flow rate into the plant, the surface area of the basin, and the height of the basin are needed. During mid-January 2004, the average flow rate was around 35 MGD, the numbers of basins in service was 4 (out of 6), and each sedimentation basin is 188 feet long, 88 feet wide, and 14 feet deep. Given the volume of a single sedimentation basin, the residence time in the basin is approximately 4 hours. With a depth of approximately 5 meters, most particles 30 μm in diameter or larger will settle and be collected by the sludge collectors at the bottom of the basin.

5.1.4   Filtration

After the sedimentation phase, the effluent goes through a filtration phase. Filtration is required under federal regulations in any DWTP where the intake comes from surface water. The purpose of filtration is to remove smaller particles that sedimentation could not take care of. Each of the 13 filters at the CWTP uses a dual-media filter, where the

top layer is anthracite coal, and the next layer is sand. A bottom gravel layer does not contribute to the filtering due to its large pore size, but is there to help keep the denser particles near the bottom (Figure 5-4). The sand is comprised to two types, with 1" of larger-diameter torpedo sand above 12" of finer sand.

Figure 5-4 Scale model of the dual-media filter used at the CWTP.

Dual-media filters are preferred to a single-media sand filter because there is less maintenance required. For instance, during backwashing of sand filters (done to remove buildup of particles), heavier sand would tend to settle toward the bottom. Thus, the finer and less dense particles migrate towards the top of the filter, making for a very effective filter up top, but a very ineffective filter everywhere else. The result is less effective filtration and higher head loss. But, by using a dual-media filter, the denser, finer particles stay near the bottom during backwashing, while the less dense and coarser particles stay near the top. This keeps the filter effective for long periods of time.

At the CWTP, a filter is backwashed when one of three parameters is exceeded: head loss, turbidity, or time. If the head loss is above 6 feet, the filter is backwashed. If the effluent turbidity is above 0.30 NTU, the filter is backwashed. Lastly, if the time since the last backwash exceeds 72 or 120 hours (depending on the filter size), the filter is backwashed.

5.1.5 Post-Chemical Addition

After filtration, there is a post-chemical addition phase, where fluoride, phosphoric acid, lime, and more sodium hypochlorite are added. Fluoride is added to promote stronger teeth when the water is consumed. Phosphoric acid is added to prevent corrosion in the piping distribution system. These two chemicals are added according to required effluent concentrations.

Lime promotes precipitation of some specific metals, such as calcium and magnesium, in the solid forms such as calcium carbonate ($CaCO_3$). These solids are collected in the clearwell, located in between the post-treatment addition and the piping distribution system. The approximate clearwell residence time at the CWTP is around 40 minutes, which is sufficient time for these solids to precipitate and settle to the bottom collectors. Lime also has a second purpose of increasing the pH from a filter pH of approximately 6.6 to a final value of 7.0 to 7.2. The pH value controls the addition of lime, as pH control is more important than removing the metals. In fact, the hardness of the water, which is a measure of the positive multi-charged ions, such as the calcium and magnesium ion, is already quite soft before entering the plant, as the hardness is 12 mg/L, while a 20 mg/L hardness in tap water is considered soft.

Lastly, more sodium hypochlorite is added to achieve a 1.1-1.3 mg/L residual during the fall and early spring, a 1.7-1.9 mg/L residual during the summer and early fall, and a 1.4-1.6 mg/L residual at all other times. These numbers were picked to maintain a required 0.2 mg/L residual in the farthest part of the distribution system. Because the pH is between 7.0 and 7.2, there is still a sufficient amount of hypochlorous acid to continue the disinfection process in the piping distribution system.

5.2   Materials and Methods

All field sampling was conducted at the CWTP in Atlanta, GA on January 14, 2004. A total of ten 3.8-liter samples were collected after major treatment steps in the CWTP. Then, the samples were reduced to 400 mL extracts of chloroform through liquid-liquid extraction. Subsequent reductions to 50-200 μL resulted in the final extract volume.

The JEOL GCmate semi-high resolution gas chromatograph/mass spectrometer was used for the analysis. After obtaining total ion current (TIC) chromatograms from JEOL's Shrader data acquisition and data reduction software, peaks were obtained for the three organophosphate triesters and an injection standard. Using these peak values, the mass of the organophosphate triesters was found by:

$$M_{organophosphatetriester} = \left(\frac{Peak_{organophosphatetriester}}{Peak_{inj.std}} \right) \cdot M_{inj.std} \cdot \left(\frac{R_{injstd}}{R_{organophosphatetriester}} \right)$$

Equation 5-1 Finding the mass of the organophosphate triesters in the GC/MS vial.

Where Peak is the peak value, M is the mass in the sample vial (units of pg), and R is the counts per unit mass of chemical (1/pg). Dividing this mass by the sample size (3.8-liters) resulted in the concentrations.

See Lin (2004) for details concerning fieldwork and labwork procedure, observations, errors, and for formation of Equation 5-1.

5.3 Results and Discussion

There were three major observations from the values presented in the tables and figures below: after the pre-treatment chemical addition step, the concentrations of the organophosphate triesters decreased significantly compared to the intake concentrations; the concentrations of TCEP increased significantly after filtration and at the final effluent; and, there was no measurable removal of the chemicals after the sedimentation phase.

5.3.1 Measured Concentrations of the Organophosphate Triesters

Table 5-1 Concentrations of the Samples (Units: ng/L)

Sample Name	TBP	TCEP	TBEP
Raw #1	24	5	118
Raw #2	29	34	120
Chemical Addition #1	BR	BR	BR
Chemical Addition #2	7	11	18
Sedimentation #1	18	17	13
Sedimentation #2	5	10	21
Filter #1	17	43	ND
Filter #2	6	211	38
Final #1	16	8	10
Final #2	8	651	23

Note: BR = bad run, ND = no detection (< 1 ng/L for this study. See Lin (2004) for determination of no detection limit). Chemical Addition #1 dried up multiple times during the Cambridge laboratory work, resulting in invalid concentrations.

The concentration values were averaged. Error bars indicated the range of concentration values measured for each site. No error bars were indicated for sites and chemicals for which there was one value (i.e. either there was a bad run or no detection for the other value).
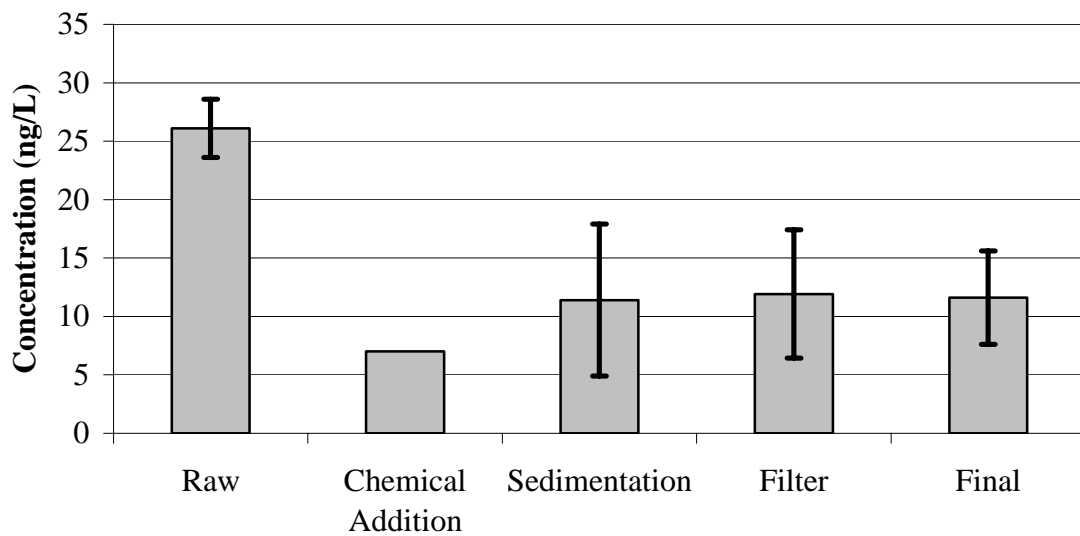
Figure 5-5 Average concentration of TBP measured in this study. Error bars indicated range of values measured.
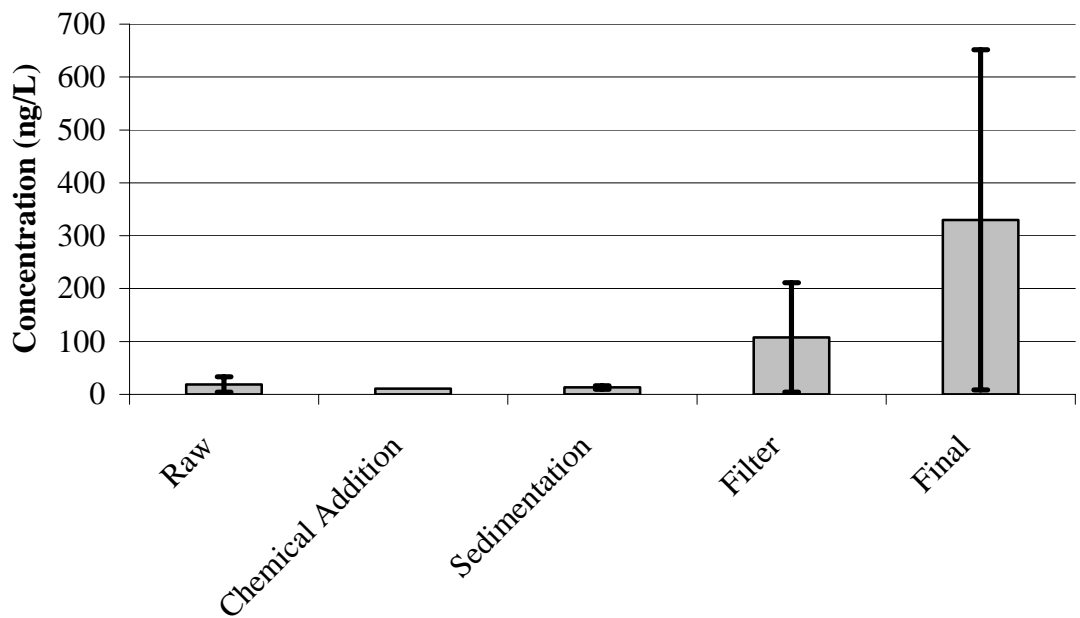

Figure 5-6 Average concentration of TCEP measured in this study.
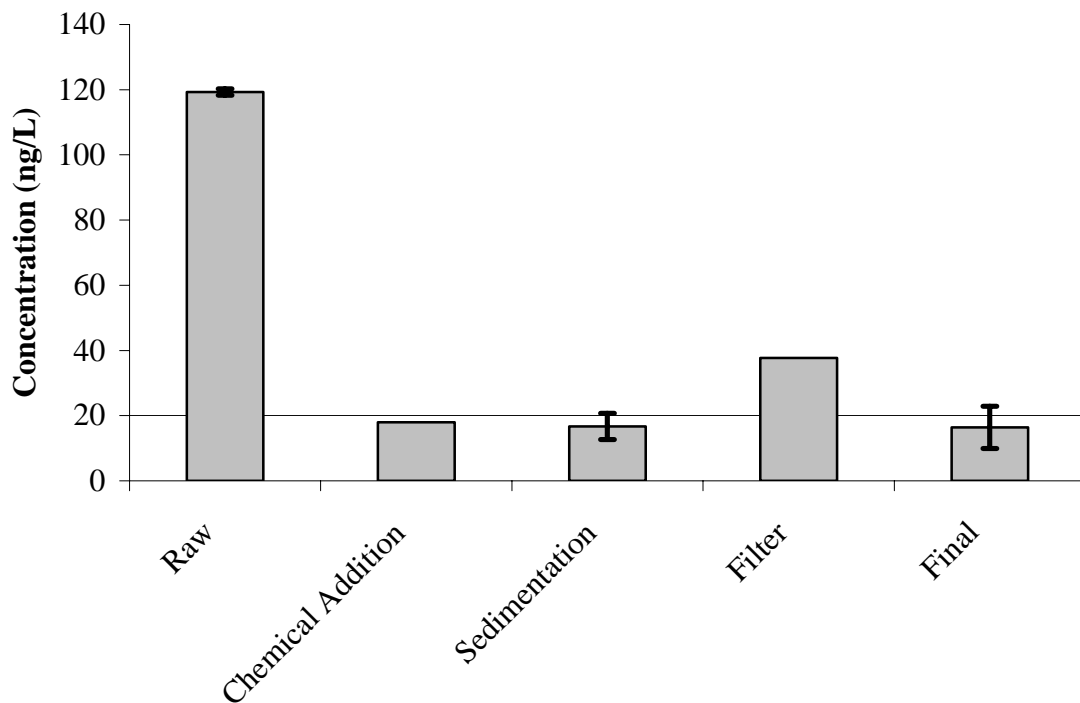
Figure 5-7 Average concentration of TBEP measured in this study.

5.3.2 Comparison to Other Findings

Now that the concentrations had been found, Mr. Lin explored how well his numbers compared to other findings.

5.3.2.1 Analysis of Data from Frick et al. (2001) and Henderson et al. (2001)

In Frick and Zaugg (2003), the percentage of detections, the number of samples, the reporting limit, and the maximum concentrations detected were the only parameters listed. But, a little more information can be extracted by looking at the raw numbers from Henderson et al. (2001) and Frick et al. (2001) For example, these two studies also took samples from the CWTP. Thus, Mr. Lin directly compared these numbers to his own (Table 5-2):

Table 5-2 Comparison of Samples from Frick et al. (2001) and Henderson et al. (2001) (these are the July-September 1999 samples) compared to the January 2004 samples. Concentrations in (ug/L)

Chemical Name	Sample Date	Atlanta Intake	CWTP Finished
TBP	Jul-99	< 0.06	< 0.06
	Aug-99	< 0.06	0.093
	Sep-99	< 0.06	< 0.06
	Jan-04	0.026	0.012
TCEP	Jul-99	< 0.04	0.06
	Aug-99	0.057	0.093
	Sep-99	< 0.04	0.055
	Jan-04	0.019	0.33
TBEP	Jul-99	0.26	< 0.07
	Aug-99	< 0.07	0.3
	Sep-99	< 0.07	< 0.07
	Jan-04	0.119	0.016

Note: the values highlighted in yellow were values there were above the detection limit. The January 2004 concentrations were based on one sample from the intake and two samples from the finished water.

The values found in Frick et al. and Henderson et al. are comparable to the January 2004 samples. One interesting observation was that TCEP was detected in all finished water samples, and was also detected in the Final #2 sample. Therefore, the heightened concentrations may be due to plastics contributed from the plant. But, the numbers are close to the detection limit, and no error bars are available for the USGS data. Further research should look at taking more samples, to gather more points. In addition, these further samples should look at different times of the year to examine different loadings into the CWTP.

The finished samples in Frick et al. and Henderson et al. had a higher percentage of detections than the raw water. But, this is based on three different treatment plants, one of which is the CWTP. Mr. Lin does not know what the other two treatment plants, the Cobb DWTP and Roswell DWTP, have in their major treatment processes to make any conclusive judgments. But, if more information about the plants is found, then some conclusions about the CWTP could be deduced. For example, if the other two plants have

no plastic components, but still have detections of the phosphate triesters, then plastic contact may not be as important in the CWTP.

5.3.2.2 Comparison with Frick and Zaugg (2003), Stackelberg and Lippincott (undated), and Kolpin et al. (2002)

Section 2 discussed the detection percentages of the phosphate triesters in other USGS surveys. Because the sampling sites vary in so many different ways, making any specific judgments would be quite difficult. For example, Stackelberg and Lippincott only sampled sites within New Jersey, which may have much different loadings than in the Atlanta area. But, one good conclusion from the USGS data was that the values found from the January 2004 samples were within the range of concentrations found in the USGS studies.

5.3.2.3 Comparison with Haffey (2004)

Haffey (2004) developed a computer model to follow the transport and transformations of TBP, TCEP, and TBEP in the Chattahoochee River. Haffey used values from Frick et al. (2001) and Henderson et al. (2001) to estimate the loadings coming from major WWTPs. In conclusion, his estimated values compared favorably with the average concentration measured by Mr. Lin (Table 5-3)

Table 5-3 Comparison of Mr. Lin's intake concentrations compared to modeled values from Haffey (2004). Note that Haffey's numbers were average concentrations for the modeled day. Units: ng/L.

	Lin	Haffey (2004)
TBP	26	24
TCEP	19	20
TBEP	119	148

5.3.3 Discussion of Trends after Pre-Treatment Chemical Addition

The concentrations of the phosphate triesters drop off significantly after the pre-treatment chemical addition. There was 73% removal of TBP, 42% removal of TCEP, and 85% removal of TBEP after the pre-treatment chemical addition stage.

5.3.3.1 Errors in Values Due to Over-Drying of the Samples

In the case of full drying, there may have been some concern for high concentrations in the air of the vial. Using TBP, because it has the highest vapor pressure of the three organophosphate triesters studied, the density of TBP in air can be calculated with the following equation:

$$\rho_{TBP,air} = \rho_{air} \frac{MW_{TBP}}{MW_{air}} \frac{VP_{TBP}}{VP_{air}}$$

Equation 5-2 Calculating the concentration of TBP in the air when the vial fully dried.

Where ρ is the density (g/L), MW is the molecular weight (g/mol), and VP is the vapor pressure (mm Hg). All values other than the vapor pressure of TBP are a constant value. One can approximate the vapor pressure of TBP in the vial to be about 1% of its normal vapor pressure (Lin, 2004). Therefore, the approximate equilibrium density of TBP in the air was 0.5 µg/L. In a 15-mL vial, the most TBP that can be in this volume was 8 ng. Therefore, the full drying of the samples should not be of concern for TBP, as 2% of the mass at most was lost. For TCEP and TBEP, the vapor pressures of the pure liquid were much lower than TBP. Full drying occurred in the 15 mL vial for Chemical Addition #1 and #2, and Sedimentation #1 and #2.

5.3.3.2 Interactions of Phosphate Triesters with Aluminum Sulfate

To figure out what pathways may cause phosphate triesters to directly or indirectly interact with aluminum sulfate, Mr. Lin first referred to the methods of coagulation: charge neutralization through adsorption of oppositely charged ions, inter-particle bridging, and precipitate enmeshment. Because the aluminum was mainly $Al(OH)_3$ (s)

(Figure 5-2), and because the phosphate triesters themselves were neutrally charged in water, charge neutralization should not be a significant interaction. Inter-particle bridging may result if the phosphate triesters were sorbed to the colloidal particles. To find out how effective this phenomenon may have been, one can compute what percent of the chemical will sorb onto the organic carbon. The average total organic carbon (TOC) during January 2004 at the CWTP intake was 1.6 mg/L (Kopanski, 2004, personal conversation). One assumption was made: all the TOC precipitated out of the water due to the aluminum sulfate addition. Starting with the definition of the organic carbon partition coefficient (Karickhoff et al., 1979, and Chiou et al., 1979):

$$K_{oc} = \frac{C_{oc}}{C_{water}}$$

Equation 5-3 Definition of the organic carbon partition coefficient.

Where C_{water} is the concentration of the chemical in the water (mg chemical/L water), and C_{oc} is the concentration in the organic carbon (mg chemical/kg organic carbon), the concentration of chemical in the organic carbon can be found. Therefore, if there was 1.6 x 10^{-6} kg organic carbon per liter of intake water:

$$C_{sorbed} = C_{oc} \cdot TOC$$

$$C_{sorbed} = C_{water} \cdot K_{oc} \cdot TOC$$

Equation 5-4 Calculating the concentration sorbed on the TOC.

Where C_{sorbed} is the concentration of chemical sorbed per liter of intake water. Now, using TBEP's K_{oc} value of 24000 L/kg, and using a concentration of 1 mg/L of TBEP:

$$C_{sorbed} = 1\frac{mg}{L} \cdot 24000\frac{L}{kg} \cdot 1.6 \cdot 10^{-6}\frac{kg}{L}$$

$$C_{sorbed} \approx 0.04\frac{mg}{L}$$

Equation 5-5 The concentration of TBP sorbed was approximately 4% of what was in the water.

Thus, the most that can be adsorbed for TBEP was about 4% of the concentration in the water. TBP and TCEP will have even lower percentages because of their much lower K_{oc} values (1900 and 300 L/kg, respectively).

Last, the organophosphate triesters may be trapped in the flocs through precipitate enmeshment. Assuming an aluminum sulfate concentration of 10 mg/L in the water after addition, one may also assume that all 1.6 mg/L of TOC precipitates with the aluminum sulfate. But, if both aluminum sulfate and TOC precipitate (a total of 11.6 mg/L), this was still only about 1% of the total water mass. Therefore, the interactions due to precipitate enmeshment were small, if negligible.

Aluminum oxides are also known to catalyze the hydrolysis of *p*-nitrophenyl phosphate (PNPP) (Baldwin et al., 1995). But, the chemical structure of PNPP differs greatly from the phosphate triesters studied in this thesis, as PPNP is a monoester. That leaves the phosphate moiety available for acid/base reactions and ionic interactions with oxides. From Schwarzenbach et al. (2003), hydrolysis of the phosphate triesters happens under neutral and basic pH conditions. But, the fastest reacting of the phosphate triesters listed, triphenyl phosphate, has a half-life of 320 days at pH 7, which is a comparable pH to the CWTP. This half-life is significantly longer than the 10-minute residence time from the intake to after the pre-treatment chemical addition.

5.3.3.3   Interactions of Phosphate Triesters with Sodium Hypochlorite

Sodium hypochlorite may interact with the phosphate triesters through the subsequent hypochlorite ion produced when sodium hypochlorite is initially added to the water. There may be a nucleophilic substitution of the phosphate triester, where the hypochlorite ion attacks the phosphorus atom. Yet, this process is similar to the hydrolysis discussion in the previous section, where hydrolysis is deemed negligible to the removal of the organophosphate triesters.

Oxidation of the sodium hypochlorite with the phosphate triesters was another potential interaction. The hypochlorous ion and the hypochlorous acid generated from the sodium hypochlorite, along with a hydroxyl ion, may attack the hydrogen atoms on the phosphate triesters, leaving a hydroxyl group. To find the potential rate of removal, assume the

reaction occurred in first order with the hypochlorous acid (or hypochlorite ion), and first order with the organophosphate triester. The concentration of hypochlorous acid was approximately 10^{-4} M, and the concentration of TBP was the fraction of the TOC, which is approximately 10^{-4} M. In addition, the half-life for a second order reaction where the concentrations are similar is (Purdue University, undated):

$$t_{1/2} = \frac{1}{k \cdot 10^{-4} M}$$

Equation 5-6 Calculation of half-life for a second-order reaction, where the initial concentration in 10^{-4} M.

Where $t_{1/2}$ is the half life (second), k is the rate constant (M^{-1}/second), and the 10^{-4} M concentration is from the two concentrations noted above. Harrison et al. (1976) indicate that the rate constant for pyrene with hypochlorous acid is 34.4 M^{-1}/second at 20 °C and a pH above 6.6. For a pyrene concentration of 10^{-4} M, this would indicate a half time of approximately 300 seconds. Even though the phosphate triesters do not have similar composition to pyrene, all are organic compounds, with hydrogen atoms that are available for attack. Mr. Lin cannot confirm how fast the reaction may take place, but a bench-scale experiment involving the phosphate triesters and sodium hypochlorite at similar pH values and concentrations at the CWTP would suffice to find out if there were any interactions.

Therefore, the reasons for removal and for the different amounts of removal for each chemical were inconclusive. To better quantify the results, a suggestion for further research would be to simulate the CWTP's pre-treatment chemical addition by adding aluminum sulfate and sodium hypochlorite at similar conditions, and determine whether there was significant removal after 10 minutes (i.e. the residence time from the intake to after the pre-treatment chemical addition).

5.3.4 Discussion of TCEP Concentrations of Filter #2 and Final #2

The TCEP concentrations of Filter #2 and Final #2 were significantly larger than other values found. The concentrations were one to two orders of magnitude above the Raw,

Chemical Addition, and Sedimentation samples. There were a few reasons why this may happen. There may have been some laboratory errors. Or, there may have been phosphate triester contamination in the treatment plant. Alternatively, these two samples may have been collected at a period of high phosphate concentration. One may also hypothesize that there was some formation of the phosphate triesters through reaction during the filtration and post-treatment chemical addition phase.

5.3.4.1 Laboratory Issues

First, problems may occur in the laboratory work. Looking at the runs completed on March 5, 2004, Filter #2, Final #2, and Roswell 2-24 all had very high peak sizes compared to other peak sizes that day for TCEP (Table 5-4) This trend was also abnormal compared to other days' runs, where there were no large spikes in any specific chemical. Therefore, laboratory issues may be a source of error.

Table 5-4 Peak sizes for the March 5th, 2004 runs. Even though the samples have much larger numbers than the standards, the TCEP values highlighted are much larger than the other two phosphates studied.

			10:58	12:16	18:11	16:18
Date	Time	Sample Name	TBP (99.3)	TCEP (63.2)	TBEP (57.3)	Inj Std (130)
5-Mar	3:13	500 std	952	508	435	11190
5-Mar	3:43	2500 std	5319	3954	1415	12518
5-Mar	4:13	1000 std	1804	1159	653	12071
5-Mar	4:43	Filter #2	2659	**56935**	5654	135115
5-Mar	5:14	Final #2	2177	**119214**	2328	91733
5-Mar	5:44	1000 std	2971	2981	1055	29503
5-Mar	6:13	Roswell 2-0	443	3563	6217	76694
5-Mar	6:43	Roswell 2-5	2006	2749	12561	171698
5-Mar	7:13	Roswell 2-24	4337	**75433**	10859	143456
5-Mar	7:43	1000 std	8533	6264	2967	64315
5-Mar	8:13	Spike #3	43778	27838	71997	723040
5-Mar	8:43	1000 std	6291	5669	1648	51761

One hypothesis for the abnormal numbers was that a peak might have formed even though none of the compound existed. When calculating the concentrations, the assumption that the peak size was zero at zero concentration was done due to runs completed beforehand (Lin, 2004). But, if this was not true, there may be measured

concentrations when none actually existed. To find out whether this was true, Mr. Lin examined the three standard runs at the beginning of the day of March 5. From section 4, the standards generally formed a linear isotherm and had an approximately zero intercept when counts versus standard concentration was plotted. But, on that day, there might have been a large positive y-axis intercept (Figure 5-8). When the concentration was extrapolated to zero, there was still a peak measured.

But, this was not the case for the standards run on March 5, as there were negative intercepts for two of the three chemicals. The third one had a small intercept, and thus could not account for the large peak size.
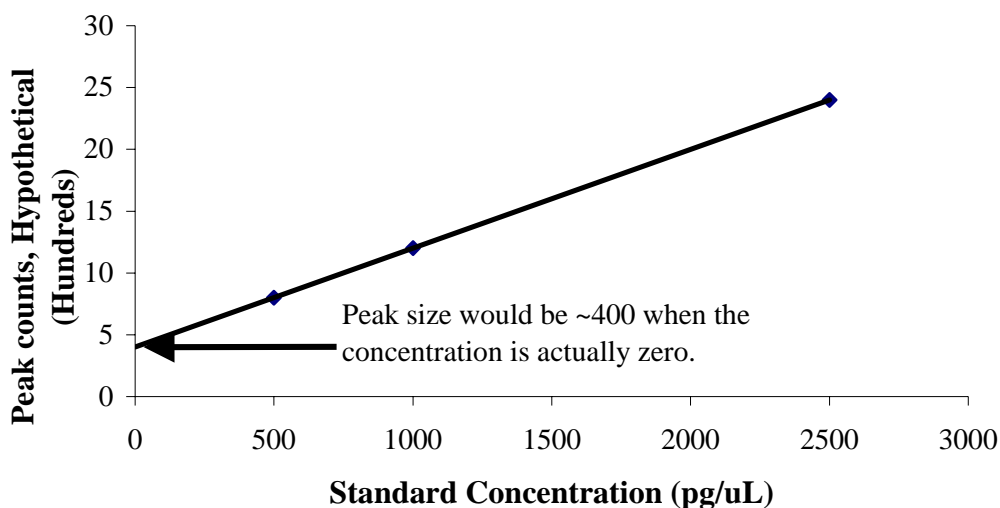
Figure 5-8 Graph of hypothetical situation where a peak may be measured when the concentration of the phosphate triesters was actually zero.

Another hypothesis was that the peaks measured are not from the organophosphates. To check this, one must look at the confirmation ion that was also measured during the GC/MS runs. The findings were that the peaks measured did, in fact, come from the organophosphates, unless some other compounds that elute at the same time as the organophosphates and fragment with the same base peak ion and confirmation ion.

There were other ways in which phosphate triester may be added. During much of the field and lab work, aluminum foil was used to prevent exposure to plastics. But, the aluminum foil itself may have phosphate triesters, as they are also used as lubricants! Because the aluminum foil was never washed before using, there could be significant amounts of phosphate triester being added into the samples. But, for this study, every sample had a significant exposure to aluminum foil, and the Final #2 and Filter #2 samples were not exposed significantly more than the other samples. This idea also was relevant to plastic cap exposure and exposure due to the rubber septum used in the GC/MS vial

Therefore, there was no concrete explanation for these large numbers. But, from what work had been done, these numbers may actually be that large. Further samples need to be taken at those sites and more runs need to be set up on those samples to make better conclusions. In addition, to check the interactions of the injection standard with the gas chromatographer versus the interactions of the phosphate triesters with the gas chromatographer, one should conduct standard additions of the phosphate triesters.

5.3.4.2 Drinking Water Treatment Plant Issues

Second, Mr. Lin examined the possibility the TCEP may have been contributed from the plant itself. One main concern during the whole sampling process was exposure to any plastic material because the phosphate triesters in the plastics may leach into the water (i.e. they are used as plasticizers in resins and PVC piping). For example, in our sampling procedures, all plastic caps were lined with aluminum foil before capping the bottles, jars, or vials to prevent plastic exposure. But, what kind of exposure to plastics existed in the CWTP?

According to Mr. Lin's findings, there does not seem to be any exposure to plastics in the filtration stage. The filter bottoms were made of steel and concrete, with no plastic materials involved. The only exposure to plastics during the post-treatment chemical addition came from the plastic day tanks in which the phosphoric acid and fluoride were

held (i.e. the lime and sodium hypochlorite were dispensed directly from the holding tanks). But, the supervisor at the CWTP, Tom Kopanski (2004), indicated that the day tanks need to be replaced, especially the fluoride tanks. Thus, the day tanks may have deteriorated such that plastic material would get into the liquid fluoride. Thus, there was a chance that leaching of phosphate triesters into the water may be occurring.

In addition, the day tanks must contribute a significant amount of TCEP into the water to account for the increase. Assuming a 100 ng/L increase in TCEP concentration, and assuming 40 MGD $\sim= 160 \times 10^6$ L/day, there would need to be 16 g/day of TCEP, or approximately 5 kg/year of TCEP contributing to the final effluent. Further research should look into the composition of the plastic day tanks, and the concentrations of phosphate triesters in each of the day tanks.

Another contribution may come from the anthracite coal in the filter. Anthracite coal is a type of granulated activated carbon (GAC), where GAC has been found to remove TBP and TBEP (Paune et al., 1998). But, the filters at the CWTP may have had different conditions than the ones presented in Paune et al. First, Mr. Lin cannot confirm how long the anthracite coal had been in the filter since the last (re)activation. Second, he also cannot confirm how long the filter had been used since the last backwashing. Last, he cannot find information on how effective the removal of phosphate triesters were when exposed to the anthracite coal for only a small period of time (e.g., if the total residence time was 20 seconds in the filter, the exposure to coal was at most 20 seconds). Further research must determine the effectiveness of removing or <u>adding</u> the chemicals with those three considerations in mind.

5.3.4.3   Timing of Samples Issues

Mr. Lin explored the possibility of variations in concentrations due to the time of sample. Filter #2 was collected five minutes after Filter #1, and Final #2 was collected five minutes after Final #1. Due to such a large change in concentration, the chances of detecting such different compositions in such a short time difference does not seem

possible. Therefore, one can be quite sure that time variances could not have been the main problem for these samples. But, to confirm this, more samples should be taken to study the time variance effects.

5.3.4.4 Reactions that May Form the Phosphate Triesters within the Filtration and Post-Treatment Chemical Addition Stage

Forming the phosphate triesters through reaction during the filter and post-treatment chemical addition was not feasible. To form an ester, an alcohol reacts with a carboxylic acid, producing an ester along with a water molecule. If formation were to occur, there would have to be no presence of water to drive the reaction. Instead, water was amply present. Therefore, the formation reaction should not occur in water.

In conclusion, the plant may be contributing to the addition of TCEP, either due to the day tanks or from other exposures, such as the anthracite coal. Laboratory issues, issues with timing of the samples, and issues concerning reactions were small or negligible.

5.3.5 Discussion of Other Samples

After sedimentation, the concentration values indicate there is no measurable removal or addition for TBEP and TCEP. But, TBP has an increase in concentration. This may occur due to flocs breaking up in the coagulation stage, resulting in the sorbed TBP going back into the water. Yet, this result is inconclusive without exactly knowing what goes on in the pre-treatment chemical addition phase. Further research must either take more samples at the CWTP after flocculation and sedimentation, or try to simulate the plant conditions of those two processes through bench-scale experiments.

TBP does not exhibit any significant removal or addition after filtration and post-treatment chemical addition. This should be the case if there is no plant exposure (either through the anthracite coal or plastics in the day tanks), no reaction in the filter, and no time variability.

TBEP does have a small increase after filtration. Thus, all filtration discussion for TCEP in section 4.4 also applies to TBEP. TBEP does not exhibit any significant removal or addition after post-treatment chemical addition.

6 The UV/H2O2 Advanced Oxidation Process in UV disinfection units: removal of selected phosphate esters by hydroxyl radical

As we have seen the phosphate esters are very persistent in the water environment and do not degrade significantly in Chattahoochee river. In addition it has been proven that they are able to survive the usual drinking water treatment stages without substantial removal.

Currently there are no immediate concerns regarding the removal of OCWs during drinking water treatment. There are more urgent needs to be addressed like persistent micro-organisms such as cryptosporidium and toxic metals as arsenic. This of course does not mean that OWCs can be neglected. Their chronic effects on human health have not been assessed and fears exist that they might prove harmful even at these very low concentrations. OWCs are anthropogenic compounds which do not occur naturally at the environment and certainly their presence in drinking water is not desirable.

Advanced Oxidation Processes (AOPs) were identified as the most promising processes for the removal of the phosphate esters at DWTPs. Advanced oxidation processes are based on generating reactive radicals, mainly hydroxyl radical, which oxidize the target organic pollutants. Alternative treatment processes are granular activated carbon (GAC) filtration or membrane micro-filtration. These processes have a significant cost and especially GAC efficiency is reduced to only hydrophobic compounds.

Currently the AOPs proposed in the literature are UV/H2O2, O3/UV, O3/UV/H2O2 and UV/TiO2 systems. All of the above systems generate hydroxyl radicals as the main oxidant. From these systems, UV/H2O2 was selected for the current work.

The hydrogen peroxide ultraviolet light system was selected because its reaction mechanism is well researched and understood. In addition the UV disinfection reactors are designed to mimic plug flow reactors enabling an accurate and simple model of the progress of the chemical process. Finally ultraviolet disinfection is expected to become more popular in the near future since it has been proven to inactivate cryptosporidium,

which is required by the Long Term 2 Enhanced Surface Water Treatment Rule (LT2ESWTR) currently in development by EPA.

Implementing the UV/H2O2 system in a UV disinfection unit would just require a rapid mixing tank prior to the UV reactor for the mixing of hydrogen peroxide. Therefore no substantial capital costs or engineering problems are involved with implementing such a system. In addition hydrogen peroxide is a relatively cheap chemical; the average price per pound in 2000 was 44 cents/lb. (http://www.manufacturing.net/pur/article/CA1543)

The aim of the current work is to assess the efficiency of the UV/H2O2 advanced oxidation process, when applied in UV disinfection units, to remove the selected phosphate esters. The main oxidizing agent in this process is hydroxyl radical. An accurate knowledge of the reaction rate constants of the phosphate esters with hydroxyl radical is essential to the model that will be developed. Since the second-order rate constants were not known (except for TBP) the first step for this work is to derive the reaction rates through experiments.

Having derived the reaction rate constants our next step is to model conceptually the advanced oxidation process. The reaction mechanism has to be considered and the UV unit must be modeled as a reactor tank. In addition the specifications of the UV reactor must be defined, which proves to be very difficult. Finally issues about the implementation of the model have to be addressed.

At this stage the model is ready to be used and the efficiency of the process can be evaluated. The chemistry of natural waters is complicated and various parameters affect the removal potential. Each of these parameters has to be considered and the effects it has on the process must be investigated.

6.1 Experiments

When designing experiments to estimate the rate constant of a chemical compound with hydroxyl radical, two major decisions must be made: how to generate hydroxyl radical, and how to conduct the experiments so that the rate constants can be derived from them. For a compact review of mechanisms for generating hydroxyl radical and methods for deriving reaction rates the reader is referred to Buxton et al (1988).

In the present work, hydroxyl radicals were generated using the Fenton reaction and the rate constants were obtained through a competition method.

The Fenton reaction was chosen because of its simplicity. The reaction mechanism consists of the oxidation of ferrous iron to ferric iron by hydrogen peroxide with products hydroxide ions and hydroxyl radicals.

Equation 6-1

$$Fe^{+2} + H_2O_2 \rightarrow OH\bullet + Fe^{+3} + OH^-$$
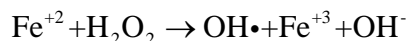
The competition method is a very widely used method to derive reaction rate constants when direct measurement of the reaction progress is difficult or impossible. The method is based on knowing the reaction rate constant of a chemical compound with hydroxyl radical that will act as the reference compound. If the chemical compound whose reaction rate constant with hydroxyl radical we wish to measure does not react with the reference compound, and neither compounds react with any other species present during the experiment, these two compounds will be competing for the hydroxyl radicals present in the solution. Therefore the reactions through which the reference compound R and the other compound A are lost in the experimental solution are:

Equation 6-2

$$R + OH\bullet \xrightarrow{k_R} \text{Products R}$$

$$A + OH\bullet \xrightarrow{k_A} \text{Products A}$$
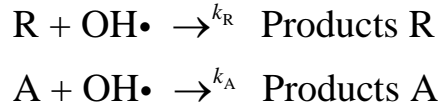
For each of the two chemical compounds, we can write the differential equation governing its concentration.

Equation 6-3

$$\frac{d[R]}{dt} = -k_R \cdot [R] \cdot [OH\bullet]$$

$$\frac{d[A]}{dt} = -k_A \cdot [A] \cdot [OH\bullet]$$

Where [R], [A] and [OH•] are the molar concentrations (moles/liter) of compound R, compound A and hydroxyl radical respectively. Using simple algebraic manipulations a relationship between the two reaction rates can be established.

Equation 6-4

$$k_A = k_R \cdot \left(\ln[\frac{[A]_{t-1}}{[A]_t}] / \ln[\frac{[R]_{t-1}}{[R]_t}] \right)$$

Therefore, the ratio of the rate constants is a function of how much of each compound was consumed during the reaction.

The competition method can be applied to any given time advancement of the reaction. In this work, we consider the initial conditions (prior to generating hydroxyl radicals) and the final conditions, when the reaction has come to a completion. This method has the significant advantage that it does not require monitoring the progress of the reaction and taking samples while the reaction is proceeding. To obtain the rate constant k_A, the only measurements needed are the initial and the final concentrations of the two chemical compounds. The equation for deriving the rate constant is then:

Equation 6-5

$$k_{\mathrm{A}} = k_{\mathrm{R}} \cdot \left(\ln[\frac{[A]_0}{[A]_\infty}] / \ln[\frac{[R]_0}{[R]_\infty}] \right)$$

This method can also be used with more than two chemical compounds present simultaneously in the experimental solution.

For a detailed discussion of the experimental procedure, materials used and analytical procedures used in the experiments the reader is referred to Machairas (2004).

6.1.1   Experimentally derived reaction rate constants

The analysis of the experimental results proved to be very difficult since there was systematic inconsistency in the GC/MS results. Numerous statistical analyses were used to derive the rate constants and try and increase the accuracy of the results.

Table 6-1 Reaction Rate Constants (for a specific statistical analysis)

Experiment	kTCEP [$M^{-1}s^{-1}$]	kTBEP [$M^{-1}s^{-1}$]
2.1	2.6E+09	1.0E+10
2.2	1.7E+09	1.1E+10
2.3	2.2E+09	1.0E+10
2.4	1.6E+09	1.1E+10
Regression	~1.5E+09	~1.0E+10
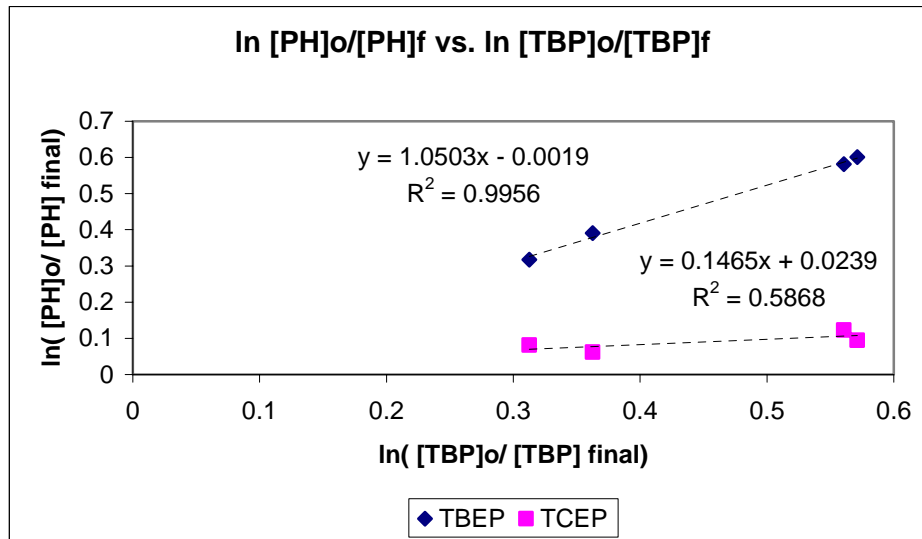
Figure 6-1   **Reaction rate constants and regression lines**

The previous figure and table show only some of the results. From all of the analyses performed it was concluded that the reaction rate constants of TCEP and TBEP with hydroxyl radical proposed from the experimental values are:

$k\text{TCEP} = 2 \cdot 10^9$ $M^{-1}s^{-1}$ with a 90% confidence interval of approximately $1 \cdot 10^9$ $M^{-1}s^{-1}$

and

$k\text{TBEP} = 2 \cdot 10^{10}$ $M^{-1}s^{-1}$ with a 90% confidence interval of approximately $1 \cdot 10^{10}$ $M^{-1}s^{-1}$

Due to the uncertainty that the experiments had, a detailed discussion of the reaction rates from a theoretical point of view follows

6.2 A theoretical approach for the reaction rate constants of the phosphate esters with hydroxyl radical

From the analysis of the experimental results and the methods used to derive the reaction rate constants it is obvious that there is some intrinsic uncertainty to the results. Because the precise knowledge of the reaction rate constants of TCEP and TBEP with hydroxyl radical is essential for the rest of this work, a theoretical approach will be used to evaluate the plausibility of the experimentally derived constants. The theoretical approach consists of applying the encounter theory to the phosphate esters in question and taking into account the possible effects that their structure might have on the reaction rate constants with hydroxyl radical.

6.2.1 Determining upper limits for the reaction rates of the phosphate esters with hydroxyl radical

For very fast chemical reactions like ones in which hydroxyl radical is a reactant, an upper limit for the reaction rate constants can be set by the encounter theory. The encounter theory states that the rates of these reactions are limited by the molecular collision frequency. An upper limit on molecular collision frequency is set by molecular diffusion and can be described by the Smoluchowski – Debye theory.

From Stumm and Morgan (1996), the equation for diffusion-controlled rate constant $(M^{-1}s^{-1})$ is

Equation 6-6

$$k_E = \frac{4\pi N}{1000}(D_A + D_B)(r_A + r_B)f$$

where N is Avogadro's number, D is the diffusion coefficient $(cm^2 s^{-1})$, r the solute species radius (cm) and f a factor that accounts for long range forces (electrostatic effects).

Equation 6-6 will be used to calculate the diffusion-controlled rate constants for the phosphate esters reactions with hydroxyl radical. The required values of molecular diffusivity and solute species radii will be estimated with the method presented by

Schwarzenbach, Gschwend and Imboden (2003). Also it has to be noted that f is equal to 1 since hydroxyl is a neutral species.

Solute Species molecular diffusivities and radii

For hydroxyl radical $(OH\bullet)$ Buxton et al. (1988) give the following values for molecular radius and diffusion coefficient:

$$r_{OH\bullet} = 2.2\cdot 10^{-8}\,cm \text{ and } D_{OH\bullet} = 2.3\cdot 10^{-5}\,cm^2 s^{-1}$$

For the phosphate esters the molecular radius can be estimated from their molecular weight and their liquid density, assuming that the molecules are spherical.

Equation 6-7

$$r = \left[\frac{3\dfrac{MW}{\rho_L}}{4\pi N} \right]^{1/3}$$

The molecular diffusion coefficients can be estimated from their molar mass from the following relationship given by Schwarzenbach, Gschwend and Imboden (2003):

Equation 6-8

$$D_w = \frac{2.4\cdot 10^{-4}}{MW^{0.71}} \; (cm^2 s^{-1})$$

Using the previous equations and the physical data for the phosphate esters, the following radii, molecular diffusion coefficients and rate constant can be estimated:

Table 6-2 Phosphate Esters Molecular radii, diffusion coefficients and reaction rates

	Molecular radius (cm)	Molecular diffusion ($cm^2 s^{-1}$)	Rate ($M^{-1}s^{-1}$)
TBP	$4.8\cdot 10^{-8}$	$5.1\cdot 10^{-6}$	$1.5\cdot 10^{10}$
TCEP	$4.3\cdot 10^{-8}$	$4.9\cdot 10^{-6}$	$1.4\cdot 10^{10}$
TBEP	$5.4\cdot 10^{-8}$	$3.8\cdot 10^{-6}$	$1.5\cdot 10^{10}$

6.2.2 Effects of Structure of the Phosphate Esters on their Reaction Rate

The three phosphate esters in question have similar physical characteristics but their small differences might have a substantial effect on their reaction rates with hydroxyl radical.
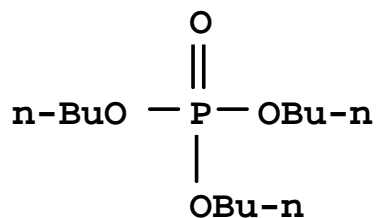
$$n\text{-BuO} - \overset{\overset{\displaystyle O}{\|}}{\underset{\underset{\displaystyle OBu\text{-}n}{|}}{P}} - OBu\text{-}n$$

Figure 6-2   Structure of TBP, Molecular formula $C_{12}H_{27}O_4P$

$$ClCH_2 - CH_2 - O - \overset{\overset{\displaystyle O}{\|}}{\underset{\underset{\displaystyle O - CH_2 - CH_2\,Cl}{|}}{P}} - O - CH_2 - CH_2\,Cl$$
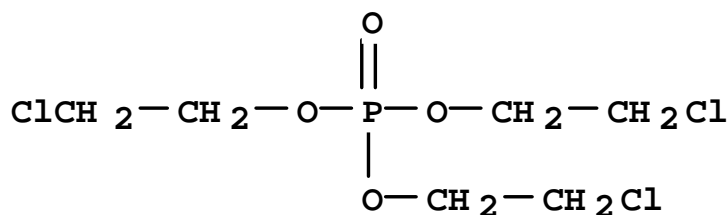
Figure 6-3   Structure of TCEP, Molecular formula $C_6H_{12}Cl_3O_4P$

$$n\text{-BuO} - CH_2 - CH_2 - O - \overset{\overset{\displaystyle O}{\|}}{\underset{\underset{\displaystyle O - CH_2 - CH_2 - OBu\text{-}n}{|}}{P}} - O - CH_2 - CH_2 - OBu\text{-}n$$
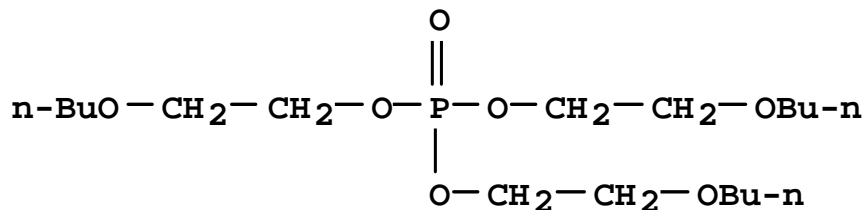
Figure 6-4   Structure of TBEP, Molecular formula $C_{18}H_{39}O_7P$

Hydroxyl radical is known to react mainly via three different mechanisms with organic compounds in aqueous solutions (Masschelein, 2002). These mechanisms are:

- Hydrogen atom abstraction
- Electrophilic addition to carbon bonds
- Electron transfer reactions

Of these mechanisms, the first two are generally considered the most important.

Since TBP, TBEP and TCEP all have completely saturated carbon bonds, the main mechanism of reaction with hydroxyl radical is hydrogen abstraction.

Effect of size

It can be argued that when a molecule has more hydrogen atoms readily available for abstraction, it will react faster with hydroxyl radical. This can be attributed to the fact that more collisions in such a molecule will be successful than in a molecule with fewer available hydrogen atoms. From Table 6-3 we can observe that the reaction rate of hydroxyl radical with selected alkanes decreases with decreasing number of available hydrogen atoms.

Based on this observation it is expected that the reaction rate constants of the organo-phosphates will follow the pattern:

$$k_{TBEP} > k_{TBP} > k_{TCEP}$$

**Table 6-3**   **Reaction Rates of various compounds from Notre Dame Radiation Laboratory**

Compound		Reaction Rate (M-1s-1)
Pentane	CH3-CH2-CH2-CH2-CH3	$5.4 \cdot 10^9$
Butane	CH3-CH2-CH2-CH3	$2.9 \cdot 10^9$
Propane	CH3-CH2-CH3	$2.3 \cdot 10^9$
Ethane	CH3-CH3	$1.4 \cdot 10^9$
Methane	CH4	$1.2 \cdot 10^8$
Ethanol	CH3-CH2-OH	$1.9 \cdot 10^9$
2-Chloroethanol	Cl-CH2-CH2-OH	$9.5 \cdot 10^8$

Effect of the Chlorine atoms in TCEP

The presence of the three chlorine atoms at the end of the carbon chains in TCEP is expected to affect the reaction rate of TCEP with hydroxyl radical.

Chlorine atoms are highly electronegative, making hydrogen abstraction less feasible. In addition, according to the suggested reaction mechanisms a number of collisions will result in electron transfer reactions:

Equation 6-9

$$OH \bullet + RX \rightarrow OH^- + RX^{+\bullet}$$
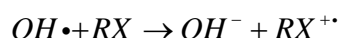
$RX^{+\bullet}$ is some form of radical but it is probable that it does not initiate other reactions than the back reaction with hydroxyl radical. Therefore this mechanism might not lead to successful collisions.

These effects of chlorine atoms have been studied in more depth in the gas phase, where structure-reactivity models have been proposed for estimating the reaction rate constants of organic compounds with hydroxyl radicals. Schwarzenbach, Gschwend and Imboden (2003) present a model in which the substitution of a chlorine atom (group substituent – CH_2Cl) results in a decrease of the reaction rate for hydrogen abstraction by a factor of 0.36. In TCEP three such groups are present. Therefore the above model, which cannot be readily extended for aqueous solutions, predicts a significant decrease of the reaction rate.

In Table 6-3 data are presented for the reaction rates of Ethanol and 2-Chloroethanol that show this decrease. The decrease is a factor of 0.5.

Conclusion

Based on all the previous arguments and assuming that the effects are additive (they might even be multiplicative), a reasonable expectation would be that the reaction rate constants of the organo-phosphate will follow the pattern $k_{TBEP} > k_{TBP} >> k_{TCEP}$.

It is not expected that TBEP and TBP react at significantly different rates, but for TCEP a slower reaction rate of an order of magnitude would seem reasonable.

6.2.3 Discussion on reaction rate constants and closure

It is evident that in general the experimentally derived reaction rate constants agree well with the theoretical predictions. Taking into account all of the previous analyses, the following rate constants are proposed for the reactions of TCEP and TBEP with hydroxyl radical:

Equation 6-10

$$k\text{TCEP} = 2 \cdot 10^{9} \ \text{M}^{-1}\text{s}^{-1}$$

and

Equation 6-11

$$k\text{TBEP} = 2 \cdot 10^{10} \ \text{M}^{-1}\text{s}^{-1}$$

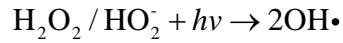## 6.3 The H_2O_2/UV oxidation process

The elementary reactions of H_2O_2 photolysis

From investigations of hydrogen peroxide photolysis it is indicated that radical chain reactions occur in a hydrogen peroxide solution under UV light irradiation. According to the mechanism of the H_2O_2/UV oxidation process presented by Crittenden et al. (1999) the following reactions take place.
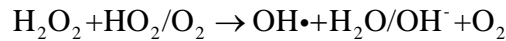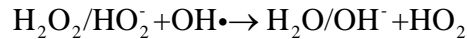
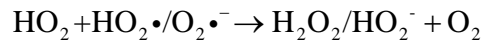Initiation: (primary photolysis of H_2O_2 or HO_2^-)

Equation 6-12

$$H_2O_2 / HO_2^- + hv \rightarrow 2OH\bullet$$

Propagation:

Equation 6-13

$$H_2O_2/HO_2^- + OH\bullet \rightarrow H_2O/OH^- + HO_2$$

$$H_2O_2 + HO_2/O_2 \rightarrow OH\bullet + H_2O/OH^- + O_2$$

Termination:

Equation 6-14

$$OH\bullet + OH\bullet \rightarrow H_2O_2$$

$$HO + HO_2\bullet/O_2\bullet^- \rightarrow H_2O/OH^- + O_2$$

$$HO_2 + HO_2\bullet/O_2\bullet^- \rightarrow H_2O_2/HO_2^- + O_2$$
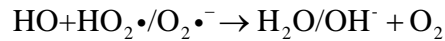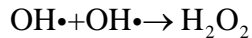
Although the primary quantum (Φp) of the hydrogen peroxide photolysis reaction (4.1) is at 254 nm 0.5, due to reaction (4.5) the overall quantum yield (Φ_T) of hydrogen peroxide in the above reaction mechanism is 1.

Other species of significance

There is a great variety of naturally occurring species in unpurified water that act as hydroxyl radical scavengers to reduce the oxidation efficiency of any AOP. The most important inorganic hydroxyl radical scavengers in natural waters are the carbonate and bicarbonate ions. Carbonate and bicarbonate ions (CO_3^{2-}/HCO_3^-) react with hydroxyl radicals to produce carbonate radicals ($CO_3^-\bullet/HCO_3\bullet$) which are equally active. The carbonate radicals react with hydrogen peroxide to form superoxide radicals ($HO_2\bullet$). It is important to note that the carbonate ion is a much more active hydroxyl radical scavenger than bicarbonate ion (the reaction rate for bicarbonate ion is two orders of magnitude larger than for the carbonate ion). Therefore the solution pH affects the hydroxyl radical concentration.

Kinetic Rates

Based on the above mechanism for the H_2O_2/UV AOP the kinetic rate expressions can be written for the species of interest which are: H_2O_2/HO_2^- , $OH\bullet$, $HO_2\bullet/O_2^-\bullet$, $CO_3^-\bullet$, CO_3^{2-}/HCO_3^- & R where R is the target organic compound.

Equation 6-15

$$r_{H_2O_2/HO_2^-} = r_{UV,H_2O_2}(-k_1[H_2O_2]) - k_2[H_2O_2][OH\bullet] - k_3[HO_2^-][OH\bullet]$$
$$-k_4[H_2O_2][HO_2\bullet] - k_5[H_2O_2][O_2^-\bullet] - k_8[H_2O_2][CO_3^-\bullet]$$
$$-k_9[HO_2^-][CO_3^-\bullet] + k_{10}[OH\bullet][OH\bullet]$$
$$+k_{12}[HO_2\bullet][HO_2\bullet] + k_{13}[HO_2\bullet][O_2^-\bullet]$$

Equation 6-16

$$r_{OH\bullet} = r_{UV,OH\bullet}(+2k_1[H_2O_2]) - k_2[H_2O_2][OH\bullet] - k_3[HO_2^-][OH\bullet]$$
$$+ k_4[H_2O_2][HO_2\bullet] + k_5[H_2O_2][O_2^-\bullet]$$
$$- k_6[OH\bullet][CO_3^{2-}] - k_7[OH\bullet][HCO_3^-]$$
$$- k_{10}[OH\bullet][OH\bullet] - k_{11}[OH\bullet][HO_2\bullet]$$
$$- k_{14}[OH\bullet][O_2^-\bullet] - k_{15}[OH\bullet][CO_3^{2-}\bullet]$$
$$- k_{TBP}[OH\bullet][TBP] - k_{TCEP}[OH\bullet][TCEP] - k_{TBEP}[OH\bullet][TBEP]$$

Equation 6-17

$$r_{HO_2\bullet/O_2^-\bullet} = k_2[H_2O_2][OH\bullet] + k_3[HO_2^-][OH\bullet] - k_4[HO_2\bullet][H_2O_2]$$
$$- k_5[O_2^-\bullet][H_2O_2] + k_8[H_2O_2][CO_3^-\bullet] + k_9[CO_3^-\bullet][HO_2^-]$$
$$- k_{11}[HO_2\bullet][OH\bullet] - k_{12}[HO_2\bullet][HO_2\bullet] - k_{13}[HO_2\bullet][O_2^-\bullet]$$
$$- k_{14}[O_2^-\bullet][OH\bullet] - k_{16}[O_2^-\bullet][CO_3^-\bullet]$$

Equation 6-18

$$r_{CO_3^-\bullet} = k_6[OH\bullet][CO_3^{2-}] + k_7[OH\bullet][HCO_3^-]$$
$$- k_8[CO_3^-\bullet][H_2O_2] - k_9[CO_3^-\bullet][HO_2^-]$$
$$- k_{15}[CO_3^-\bullet][OH\bullet] - k_{16}[CO_3^-\bullet][O_2^-\bullet]$$
$$- k_{17}[CO_3^-\bullet][CO_3^-\bullet]$$

Equation 6-19

$$r_{CO_3^{2-}/HCO_3^-} = -k_6[CO_3^{2-}][OH\bullet] - k_7[HCO_3^-][OH\bullet]$$
$$+ k_8[CO_3^-\bullet][H_2O_2] + k_9[CO_3^-\bullet][HO_2^-]$$
$$+ k_{17}[CO_3^-\bullet][O_2^-\bullet]$$

For the oxidation of the target phosphate esters (TBP, TCEP and TBEP) in the current model it has been assumed that they only react with hydroxyl radical. It is possible that the phosphate esters react with the other radicals that are created and that they have

various oxidation steps prior to being completely mineralized. All these steps will be neglected since there is no knowledge of the exact products.

Therefore the reaction rates for the phosphate esters are:

Equation 6-20

$$r_{TBP} = -k_{TBP}[OH\bullet][TBP]$$
$$r_{TCEP} = -k_{TCEP}[OH\bullet][TCEP]$$
$$r_{TBEP} = -k_{TBEP}[OH\bullet][TBEP]$$

For the relevant reaction rates the reader is referred to Machairas (2004)

6.3.1 Conceptual Model of the ultraviolet disinfection unit

The disinfection process that is considered for implementing an Advanced Oxidation Process for the removal of the phosphate esters from drinking water is Ultraviolet disinfection.

Ultraviolet disinfection units usually consist of flow through reactors with an exposure to almost homogeneous light intensities for a small period of time (less than one minute in most designs). These reactors are designed to achieve the least dispersive behavior trying to mimic a plug flow reactor. Therefore for the purposes of this work they can be modeled as one.

Flow

Parcel modeled as batch reactor

Constant Irradiation
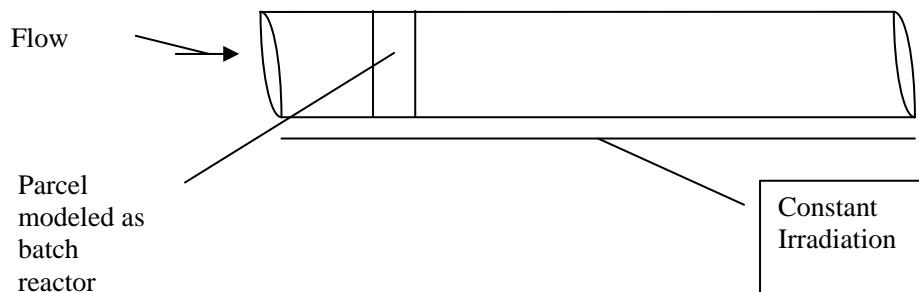
Schematic view

The steady state equation for conservation of mass in a plug flow reactor is

Equation 6-21

$$U \frac{dC}{dx} = \sum \text{sources-} \sum \text{sinks}$$

Assuming a moving coordinate system, $x = Ut$ and using the chain rule of differentiation the equation transforms to

Equation 6-22

$$\frac{dC}{dt} = \sum \text{sources} - \sum \text{sinks}$$

The equation now corresponds to the time domain and not the spatial domain and essentially tracks a parcel of water that enters the reactor.

The parcel of water entering this reactor is advected while experiencing homogeneous ultraviolet irradiation. Equation 6-21 implies that the degradation of pollutant for this parcel of water can be modeled as a batch reactor process since due to absence of dispersion it does not mix with the surrounding water. For this parcel the reaction time is equal to the hydraulic residence time $\tau = \frac{L}{V}$. The governing equation derived from mass conservation is Equation 6-22, where sources and sinks refer to the various chemical reactions taking place in the parcel.

6.3.2 Characteristics of our Ideal UV reactor

The first documented large-scale application of UV disinfection systems for drinking water is in Marseille, France from 1906-1909 (Masschelein 2002). Since then the application of UV light for disinfection and other treatments of water, wastewater and industrial effluents has grown significantly. As a consequence, specialized companies have appeared that offer compact off-the-shelf solutions to various engineering needs. These companies have accumulated substantial knowledge of the various design factors

and have been involved in extensive research. As a result they offer proprietary technology and they are involved in the design procedure of every UV installation, offering expert consulting services.

The exact characteristics of all of these UV disinfection units are not publicly available and even if they were, there are so many competing designs that one cannot be chosen without considering other attributes, such as the economic cost or the proximity of the manufacturer. Berson-UV, Wedeco and Trojan Technologies are only a few of the leading manufacturers of UV units. For the goals of the present work, it has been decided to use an "ideal" reactor.

The first consideration about a UV disinfection unit is the germicidal efficiency it has. Because this is a matter of public health, government agencies around the world have developed regulations specifying the minimum UV irradiation dose that each UV disinfection unit must provide. Here we will follow the Austrian regulations, which require a UV irradiation dose of 400 J/m^2.

It has to be noted that in everything that follows we are only considering light with a wavelength of 254 nm.

Following the description of a UV reactor as a plug flow reactor, we will assume the simplest design, a cylindrical reactor with a length of 2 m and a diameter of 1 m with one lamp in the center. In addition we will assume that the hydraulic residence time in the reactor is 20 sec. This leads to a mean velocity for water of 0.1 m/sec and a flow rate of 283 m^3/hour.

The light intensity inside the reactor is not homogeneous. As the light travels away from the source it is attenuated. This happens due to two mechanisms, dissipation and absorption. Dissipation is the effect of the increasing area in which the energy is projected away from the source, and the effect can be calculated as follows:

Equation 6-23

$$I = \frac{S}{2\pi d^2}$$

where S is the power of the light source (Watts) and d the distance from the source (cm) and I the intensity (Watts/cm^2).

Absorption is described by Beer's law which relates the attenuation to the absorptive properties of the medium that light travels through.

Equation 6-24

$$I = Io \cdot e^{-A \cdot d}$$

where A is the absorbance of the solution (cm^{-1}) and d the length of the absorbing media (cm).

Combining both attenuation processes we can derive an expression describing the intensity at any point away from a single source.

Equation 6-25

$$I = \frac{S}{2\pi d^2} \cdot e^{-A \cdot d}$$

where the intensity is given as power per unit area (Watts/cm^2).

The lamp in the UV reactor is a line source that can be approximated as a series of point sources. This method is called point source summation and the reader is referred to the EPA's Design Manual for Municipal Wastewater Disinfection for a complete description. The Figure 6-5 shows the basis of the method.

The equation governing the light intensity at any given point in the reactor is:

Equation 6-26

$$I(r,z_o) = \sum_{n=1}^{n=N} \frac{S/N}{4\pi(r^2 + z_n^2)} \cdot e^{-A \cdot \sqrt{r^2 + z_n^2}}$$

with $z_n = z_o - L(n/N)$

where N is the number of point sources that the UV lamp is approximated by, L the length of the UV lamp, r and zo are the radial distance and the z coordinate respectively of the point for which we are calculating the intensity from the UV lamp. zn is a relative distance defined in Figure 6-5.
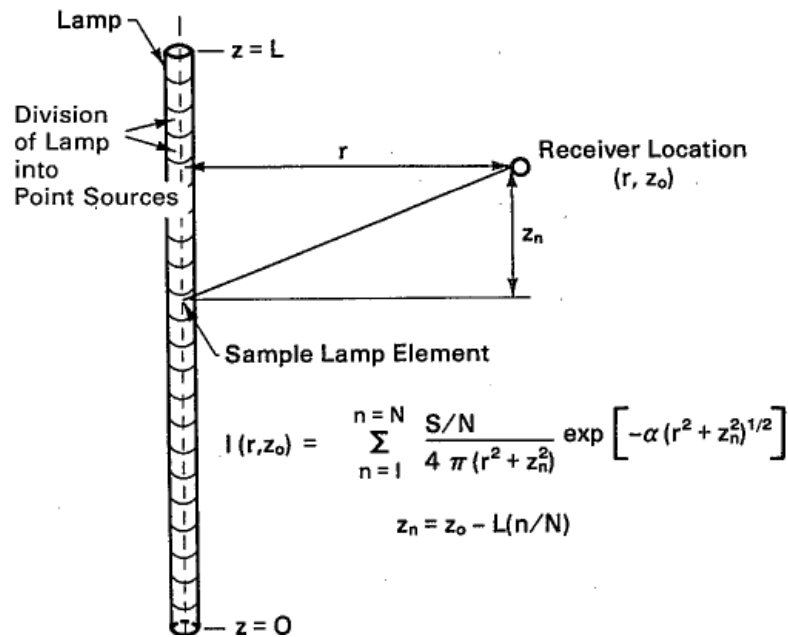
Figure 6-5 Point Source Summation from Design Manual: Municipal Wastewater Disinfection

The required intensity can be evaluated based on the assumption of plug flow. In a plug flow reactor flow lines are straight. We must design the reactor with a sufficiently high intensity to satisfy the exposure dose requirement even for the flow line of minimum intensity.

In a reactor with one UV lamp in the center, the minimum intensity flow lines are the ones in the perimeter of the circle (r = 50 cm). Using the point source summation technique we can calculate the required power of the lamp to realize the exposure dose for these flow lines. The absorbance of the solution needs to be defined first. Following suggestions of Masschelein, (2002) we will assume an absorbance of 0.02 cm^{-1}. (for detailed discussion the reader is referred to Machairas (2004), chapter 4.3)

The dose of UV radiation for any particle traveling along a flow line can be defined as $D=\bar{I}\times t^{*}$ where t* is the residence time in the reactor and $\bar{I}$ the average light intensity along the flow line. The average light intensity along the flow line can be calculated using the point source summation method: the intensity is calculated for a number of points in the flow line zo, and the average is found by summing the calculated intensities and dividing by the number of calculation points. Since we are trying to find the necessary power of the lamp we use the point source summation assuming a power source of 1 Watt. To realize the necessary exposure dose the source needs to emit the following power:

Equation 6-27

$$S=\frac{D(J/cm^{2})}{f(\text{geometry,absorbance})\ (cm^{2})\cdot t^{*}(sec)}\quad (J/sec=Watts)$$

where D is the exposure dose and f the result of the calculation of the average light intensity along the flow line of minimum intensity for a light source of power 1 Watt.

For the characteristics of our reactor (geometric factors and properties of the solution) the required power of the lamp is S ~ 459 Watt.

 The units must be converted to einsteins since this is the unit associated with the quantum yield of the compounds. One einstein (ein) is the energy equivalent of 1 mole of photons at a specified wavelength. For the wavelength of 254 nm the energy of 1 einstein

is $\text{E=Ne} \cdot h \cdot \dfrac{c}{\lambda} = 6 \cdot 10^{23} \cdot 6.63 \cdot 10^{-34} \cdot \dfrac{3 \cdot 10^8}{254 \cdot 10^{-9}} J \approx 469842.5 J$. Therefore the necessary

power of the lamp in einsteins per second is: $S \approx 9.77 \cdot 10^{-4}$ ein/sec .

Our ideal UV reactor has been fully defined based on the necessary UV dose. The chosen characteristics are:

Table 6-4 Ideal UV reactor's characteristics

Length	L	2 m
Diameter	D	1 m
Hydraulic residence time	t*	20 sec
Mean velocity	V	0.1 m/sec
Flow rate	Q	282.74 m^3/hour
Exposure dose	D	400 J/m^2
Power output of lamp	S	459 Watt ~ 0.000977 ein/sec

6.3.3   Photolysis rate

As we have seen when the mechanism of the AOP was developed, the overall reaction mechanism commences with the primary photolysis of hydrogen peroxide. It is obvious that this reaction is the one that governs the progress of the oxidation reaction. The rate with which the photolysis of hydrogen peroxide occurs can be derived based on the notion of quantum yield. Quantum yield is defined as:

Equation 6-28

$$\Phi_\lambda = \frac{\text{number of moles reacting}}{\text{number of einsteins absorbed}}$$

The reaction rate then is equal to the quantum yield of hydrogen peroxide multiplied by the number of einsteins absorbed by hydrogen peroxide.

Equation 6-29

$$r_{UV,H_2O_2} = -\Phi_\lambda \cdot (\text{number of einsteins absorbed by } H_2O_2) \ [\text{s-1}]$$

The number of einsteins absorbed by hydrogen peroxide can be calculated using the point source summation method and Beer's law.

The number of einsteins absorbed by hydrogen peroxide can be calculated using the point source summation method and Beer's law.

When the solution absorbs a small fraction of the energy of light, we can approximate Beer's law as a linear function of the intensity in the volume of solution that absorbs light and the properties of the solution. Since we are interested in the energy absorbed from hydrogen peroxide the expression becomes:

$$\text{Photons Absorbed per cm}^2 = 2.3 \cdot \varepsilon_{H_2O_2} (M^{-1}cm^{-1}) \cdot [H_2O_2] \cdot (M) \cdot \overline{I}(ein/cm^2) \cdot \text{pathlength (cm)}$$

For this to be true we need to apply this expression to very small volumes of the solution. The total absorbed energy from hydrogen peroxide will be the integral over the relevant volume.

The method was applied based on a numerical approach. Since the intensity of light is symmetrical regarding the angular coordinates in every cross section (at zo), the calculations are done for 1 degree and then extended to the whole cross section. If we discretize the radius r in 1 cm lengths, we can calculate the intensity at every point using the point source summation method. The average intensity (eins) for the specified grid points is (points m and m+1):

Equation 6-30

$$\overline{I}_{m,m+1} = \frac{I(r_m, z_o) + I(r_{m+1}, z_o)}{2} \cdot \text{Area}_{m,m+1}$$

where

Equation 6-31

$$_{m,m+1} = \frac{\frac{2\pi r_{m+1}}{360} + \frac{2\pi r_m}{360}}{2} \times 1 \text{ cm}$$

so the absorbed energy for a one-degree width of the cross section is:

Equation 6-32

$$_{1 \text{ degree}} = 2.3 \cdot \varepsilon_{H_2O_2} \cdot [H_2O_2] \cdot \sum_{r_m=1}^{49} \frac{I(r_m, z_o) + I(r_{m+1}, z_o)}{2} \cdot Area_{m,m+1} \cdot (1 \text{ cm}) \quad (\text{ein})$$

which can also be written as:

$$P_{1 \text{ degree}} = 2.3 \cdot \varepsilon_{H_2O_2} \cdot [H_2O_2] \cdot f(A)$$

$$f(A) = \sum_{r_m=1}^{49} \frac{I(r_m, z_o) + I(r_{m+1}, z_o)}{2} \cdot Area_{m,m+1} \cdot (1 \text{ cm}) \quad (\text{ein}) \qquad (4.28)$$

Since the intensity is a function of the total absorbance of the solution and the absorbed energy per unit volume of the cross section is:

Equation 6-33

$$PVolume_{1 \text{ degree}} = \frac{P_{1 \text{ degree}} \ (\text{ein})}{\frac{(\pi \cdot 50^2 (\text{cm}^2) - \pi \cdot 1^2 (\text{cm}^2))}{360} \times 1 \text{ cm}} \quad (\text{ein/cm}^3)$$

or

Equation 6-34

$$PVolume_{1 \text{ degree}} = \frac{2.3 \cdot \varepsilon_{H_2O_2} \cdot [H_2O_2] \cdot f(A)}{\frac{(\pi \cdot 50^2 (\text{cm}^2) - \pi \cdot 1^2 (\text{cm}^2))}{360} \times 1 \text{ cm}} \quad (\text{ein/cm}^3)$$

and the average absorbed energy from hydrogen peroxide per volume in the reactor is:

Equation 6-35

$$PVolume_{Reactor} = \frac{\sum_{z=1}^{z=200} PVolume_{1 \text{ degree}}{}^z}{200} \quad (\text{ein/cm}^3)$$

which can also be written as

- 112 -

Equation 6-36

$$\text{PVolume}_{\text{Reactor}} = [H_2O_2] \cdot \frac{2.3 \cdot \varepsilon_{H_2O_2}}{\dfrac{(\pi \cdot 50^2 - \pi \cdot 1^2)}{360}} \cdot \frac{\sum\limits_{z=1}^{z=200} f(A)}{200} \quad (\text{ein/cm}^3)$$

Since the intensity is a function of the absorbance of the solution and the absorbance is affected by the concentration of hydrogen peroxide, we can repeat the calculation steps and derive an expression for the average absorbed energy from hydrogen peroxide per volume in the reactor as a function of the hydrogen peroxide concentration. For this calculation, we assume a constant background absorbance of 0.02. The total absorbance of the solution is then given by
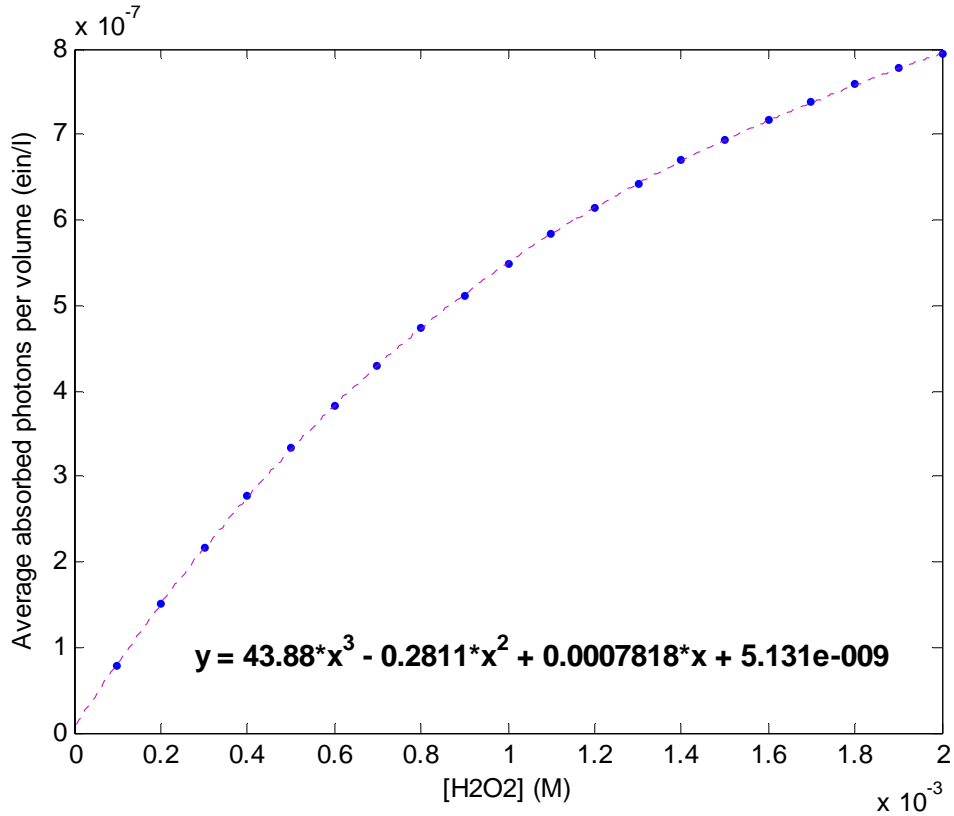
Equation 6-37

$$A = \left[[H_2O_2] \cdot \varepsilon_{H_2O_2} + [HO_2^-] \cdot \varepsilon_{HO_2^-} + \text{background absorbance} \right] \ (\text{cm}^{-1})$$

For the range of pH encountered in natural waters the concentration of hydroperoxide ion is insignificant compared to the concentration of hydrogen peroxide ($pKa = 11.6$). Therefore the absorbance from the hydroperoxide ion can be neglected for this range of pH.

In what follows, the absorbed number of photons is given in einsteins per liter. The conversion from ein/cm^3 to ein/liter is straightforward ($1000 \text{ cm}^3 = 1$ liter).

This procedure was done in Matlab and the results are:

The figure shows a plot with y-axis labeled "Average absorbed photons per volume (ein/l)" ranging from 0 to 8 ×10⁻⁷, and x-axis labeled "[H2O2] (M)" ranging from 0 to 2 ×10⁻³. The fitted curve equation shown is:

y = 43.88*x^3 - 0.2811*x^2 + 0.0007818*x + 5.131e-009

Figure 6-6   **Average absorbed ein/liter per volume from hydrogen peroxide for a water with a background absorbance of water of 0.02 cm-1**

From a curve fit of the above results, the average absorbed energy from hydrogen peroxide per volume in the reactor is given by the following expression:

Equation 6-38

$$\text{Absorbed}_{H_2O_2} = 43.88 \cdot [H_2O_2]^3 \text{-} 0.2811 \cdot [H_2O_2]^2 + 7.818 \cdot 10^{-4} \cdot [H_2O_2] + 5.131 \cdot 10^{-9}$$

$$\text{(ein/liter)}$$

We can also use the expression (number) which is a more general formulation and plot

$$\frac{2.3 \cdot \varepsilon_{H_2O_2}}{(\pi \cdot 50^2 - \pi \cdot 1^2)} \frac{\sum_{z=1}^{z=200} f(A)}{200}$$ versus the total absorbance of the solution. This way for the

given geometry of the reactor knowing the background absorbance and the hydrogen

peroxide concentration we can calculate the absorbed energy from hydrogen peroxide per cross section.
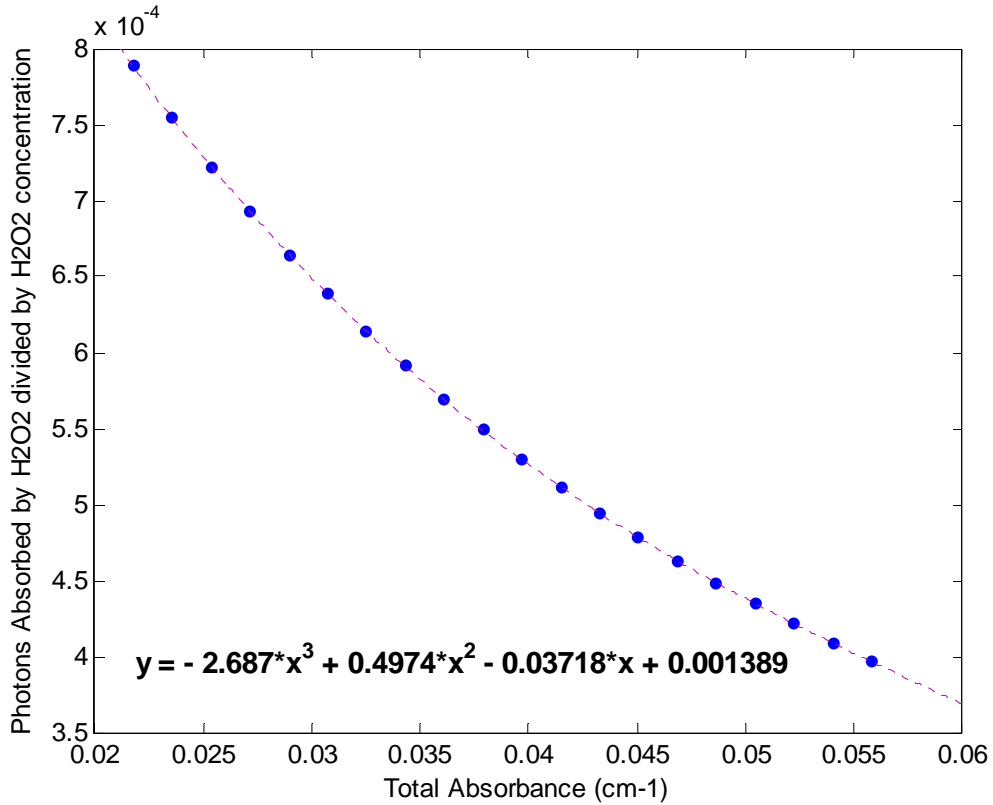
Figure 6-7   Average absorbed ein/liter per cross section from hydrogen peroxide divide by hydrogen peroxide concentration for a given range of total absorbance

With this formulation, we can compute the average absorbed photons by hydrogen peroxide in this reactor for any given total absorbance of the solution and hydrogen peroxide concentration.

Equation 6-39

$$\text{Absorbed}_{H_2O_2} = [H_2O_2] \cdot (-2.687 \cdot A^3 + 0.4974 \cdot A^2 - 0.03718 \cdot A + 0.001389)$$

$$(\text{ein/liter})$$

For further details regarding the implementation of the model and the Matlab code developed the reader is referred to Machairas (2004).

6.4 Results of the model

The goal of this work is to explore the ability of the UV/H2O2 system to remove the phosphate esters from drinking water. It is clear that if such a process is necessary in the future, special design of the UV reactors will be used. In the current work, it has been assumed when developing the "ideal" UV reactor that design characteristics similar to the ones in water disinfection will be used. This poses a severe limitation since UV disinfection generally requires much lower exposure dosages than the oxidation of micro-pollutants through hydroxyl radical.

In the example runs of the model to follow, some of the properties of the solution will always be kept within a narrow range. This is because we are interested in applying such a treatment process to natural waters that are destined to reach distribution networks. The chemistry of good quality freshwater generally tends to be pretty consistent concerning the two major parameters that influence the performance of the UV/H2O2 process, pH and the total carbonate species.

The typical pH of natural waters is in the range of 6 to 9 and the typical concentration of total carbonate species (C_T) is in the range of 10^{-4} to $5*10^{-3}$ M

The third important parameter of the performance of the UV/H2O2 process is the initial concentration of added hydrogen peroxide. As it will be shown later, increasing the hydrogen peroxide dose up to a point improves dramatically the removal of the phosphate esters. Because hydrogen peroxide is a mild pollutant in water we are interested in the final concentration of hydrogen peroxide at the outflow of the UV reactor. In this work we will adopt as the desired outflow concentration of hydrogen peroxide the maximum allowed level in Germany which is 17 mg/l. According to Masschelein (2002), this value will soon be adopted from the European Union. This concentration when translated to molar concentration becomes $5*10^{-4}$ M.

In the following pages the effect of these parameters on the efficiency of the UV/H_2O_2 will be examined. A steady state approximation of the hydroxyl radical concentration will be presented and finally the model will be applied to the Atlanta Water works plant.

6.4.1 Effects of pH

Holding the total inorganic carbonate concentration and the initial hydrogen peroxide dose steady and changing the pH of the solution allows us to study the effects of pH on the efficiency of the solution. In the following figure, the pseudo-first-order rate coefficients are shown as a function of the solution pH. The first order decay rate coefficients were calculated as: $k_{TBP} = -\dfrac{\ln([TBP_{final}]/[TBP_{initial}])}{t}$
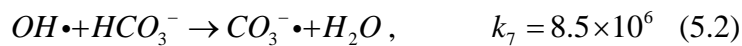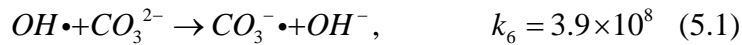
The parameters for the simulations are:

Table 6-5

Characteristics of Runs	
Lamp Power	459 W
pH	5 - 12
Hydrogen peroxide [M]	0.001
Ct [M]	0.001
Exposure time	20 sec

It is obvious that the increase in the pH of the solution decreases the pseudo-first-order rate coefficients . This is because increase in the pH affects the species that exhibit acid-base chemistry and alters their equilibrium concentrations.

The major hydroxyl radical scavengers in natural waters are the carbonate species. When the pH increases, the dissociation of bicarbonate ion to carbonate ion increases, rendering the carbonate species an even more effective scavenger.
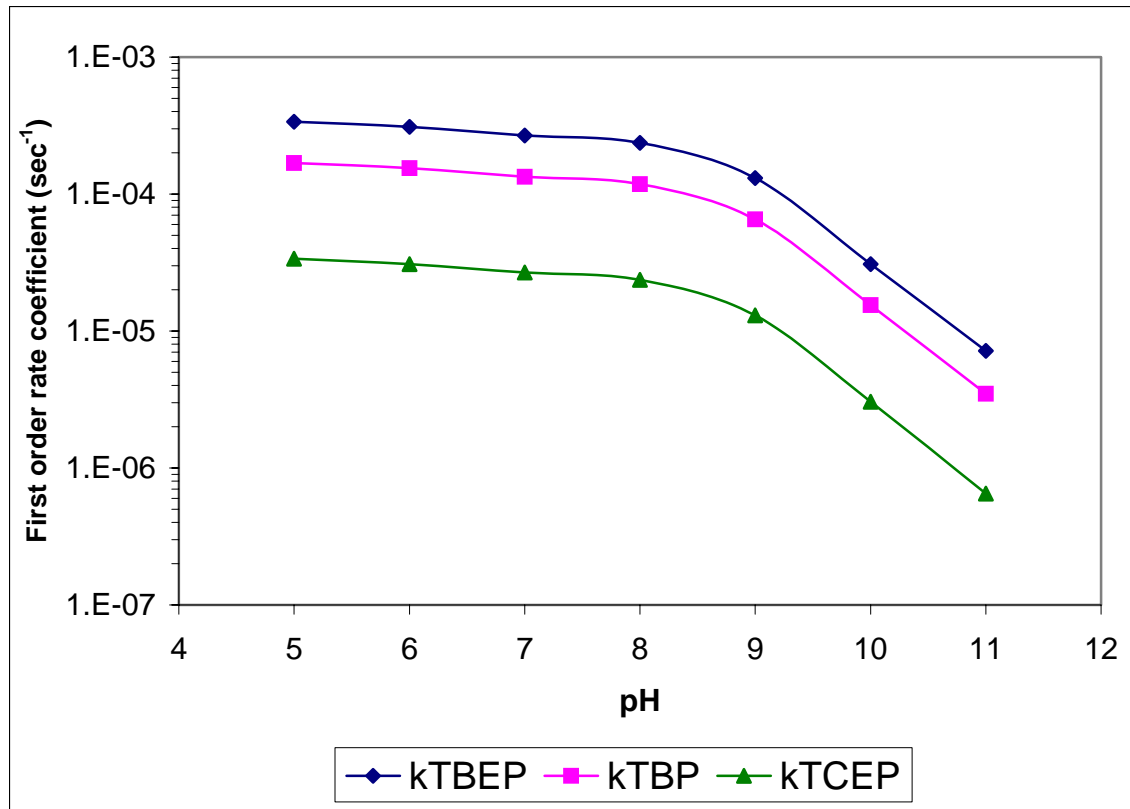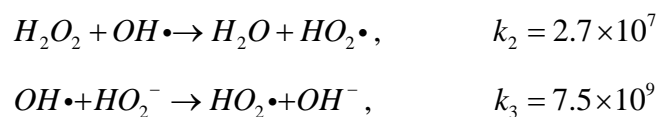
$$OH\bullet + CO_3^{2-} \rightarrow CO_3^{-}\bullet + OH^{-}, \qquad k_6 = 3.9 \times 10^8 \quad (5.1)$$

$$OH\bullet + HCO_3^{-} \rightarrow CO_3^{-}\bullet + H_2O, \qquad k_7 = 8.5 \times 10^6 \quad (5.2)$$

Figure 6-8   **First order reaction rate coefficients vs. pH. $H_2O_2=10^{-3}$ M, $C_T=10^{-3}$ M**
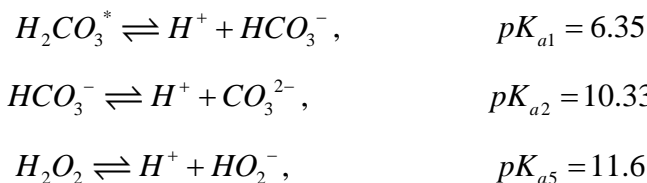
Another effect of increasing the pH is that the concentration of hydroperoxide ion increases from the dissociation of hydrogen peroxide. Again, hydroperoxide ion is a more effective hydroxyl radical scavenger and this affects the efficiency of the process.

Equation 6-40

$$H_2O_2 + OH\bullet \rightarrow H_2O + HO_2\bullet, \qquad k_2 = 2.7\times10^7$$

$$OH\bullet + HO_2^- \rightarrow HO_2\bullet + OH^-, \qquad k_3 = 7.5\times10^9$$

From Figure 6-8 it is obvious that when the pH is low, an increase does not affect the pseudo first order rates significantly. From pH 8 and above, any increase in the pH has dramatic effects in the efficiency of the process. This can be explained based on the pKa values of the carbonate species and hydrogen peroxide.

Equation 6-41

$$H_2CO_3^* \rightleftharpoons H^+ + HCO_3^-, \qquad pK_{a1} = 6.35$$

$$HCO_3^- \rightleftharpoons H^+ + CO_3^{2-}, \qquad pK_{a2} = 10.33$$

$$H_2O_2 \rightleftharpoons H^+ + HO_2^-, \qquad pK_{a5} = 11.6$$

For low pH values (<6) most of the inorganic carbonate is present as $H_2CO_3^*$ which does not take part in the reaction mechanism. For pH values above pH=8 the carbonate ion starts having a significant concentration and reduces the efficiency of the process. At really high pH values (abnormal for natural waters) most of the carbonate species are present as carbonate ion and significant percentage of hydrogen peroxide is dissociated to hydroperoxide ion, rendering the solution an excellent hydroxyl radical scavenger.

Since natural waters typically have a pH in the range of 6 to 9 it is not expected that pH t will pose a significant problem for the efficiency of the process. In any case, artificial lowering of the pH is advantageous for the process.

6.4.2   Effects of C_T

The effect of the concentration of carbonate species is easily predictable. Increasing their concentration decreases the pseudo-first-order rate coefficients because the scavenging of hydroxyl radical is increased. A series of simulations were done to show this effect.

Table 6-6

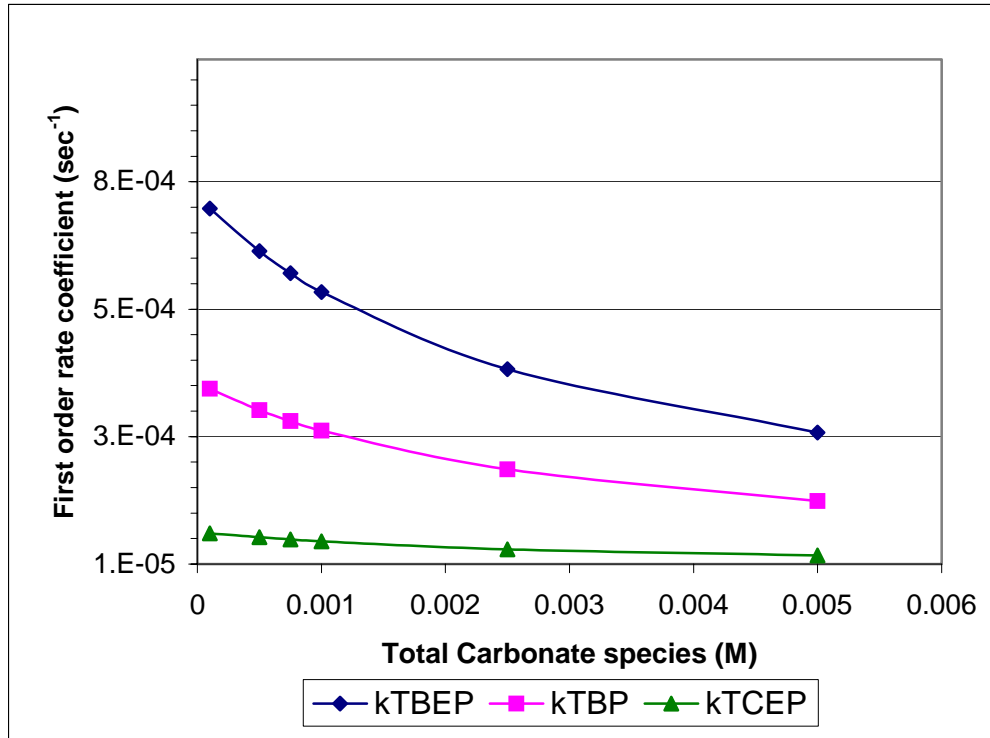| Characteristics of Runs	
Lamp Power	459 W
pH	8
Hydrogen peroxide [M]	0.001
Ct [M]	1*10^-4 - 7.5*10^-3
Exposure time	20 sec

Figure 6-9   **First order reaction rate coefficients vs. C_T. $H_2O_2 = 10^{-3}$ M, pH=8**

Decreasing the concentration of carbonate species significantly improves the efficiency of the process. Therefore pre-softening of high alkalinity waters is suggested

6.4.3   Effects of initial Hydrogen Peroxide dose

The hydrogen peroxide dose is a very important parameter for the efficiency of the treatment process and the economic desirability. In the UV/H2O2 process, the photolysis of hydrogen peroxide is the major mechanism generating hydroxyl radicals. Therefore it is logical to assume that increasing the dose of hydrogen peroxide would increase the steady-state concentration of hydroxyl radicals. This is not the case though, because hydrogen peroxide acts as a hydroxyl radical scavenger too.

Equation 6-42

$$H_2O_2/HO_2^- + OH\bullet \rightarrow H_2O/OH^- + HO_2$$
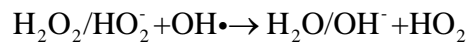
with a reaction rate constant $k_2 = 2.7 \times 10^7 \ M^{-1}s^{-1}$ for hydrogen peroxide and $k_3 = 7.5 \times 10^9$ for hydroperoxide ion.

In order to show the effect of the initial H2O2 concentration on the pseudo-first-order reaction rate constants of the phosphate esters a series of simulations were done with increasing the hydrogen peroxide dose. The input parameters were:

Table 6-7

Characteristics of Runs	
Lamp Power	459 W
pH	7
Hydrogen peroxide [M]	5*10^-5 - 10^-2
Ct [M]	0.001
Exposure time	20 sec
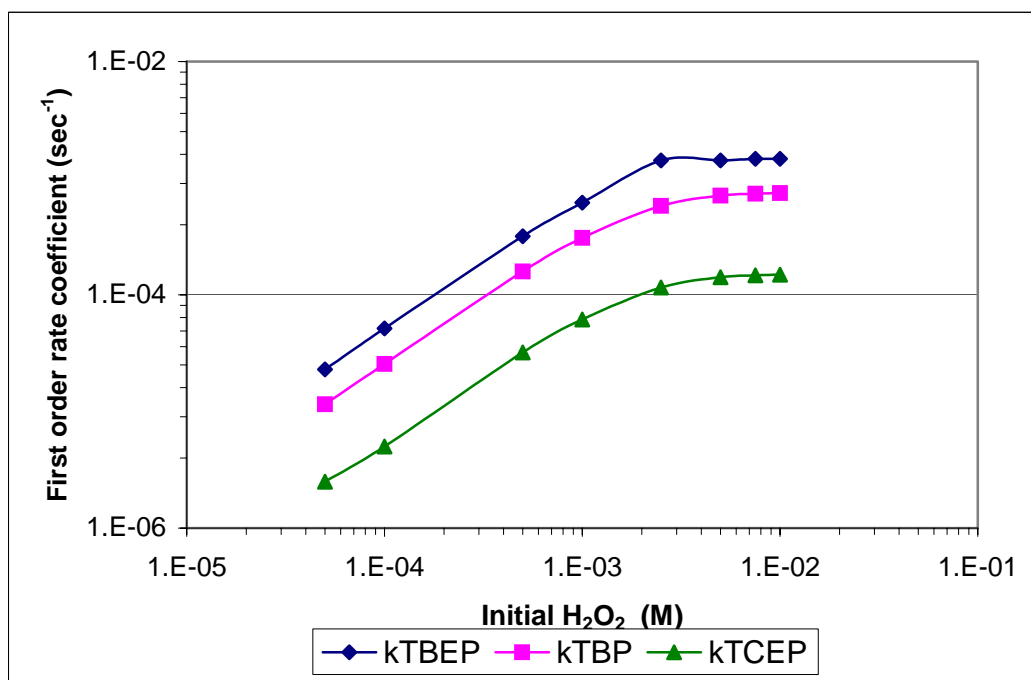
Figure 6-10   **First order reaction rate coefficients vs. H_2O_2. = $C_T = 10^{-3}$ M, pH=7**

From Figure 6-10, it is obvious that at low initial hydrogen peroxide concentrations, increasing the dose significantly increases the degradation rate of the phosphate esters. At higher concentrations (>0.005 M), the effect of increasing the dose is negligible.

6.4.4 Effects of Lamp power

The effect of the lamp power is expected to be straightforward. Since the major mechanism for generation of hydroxyl radical is photolysis of hydrogen peroxide, increasing the power of the UV lamp should increase the generation rate of hydroxyl radical and thus the oxidation of the phosphate esters. For the following simulations, an increased light power was assumed (by a factor of 5, 10 and 50). Since the absorbed photons per volume are proportional to the lamp power, the original expression for the average absorbed energy from hydrogen peroxide per volume in the reactor can be used multiplied by the relevant factor

The following simulations were done:

Table 6-8

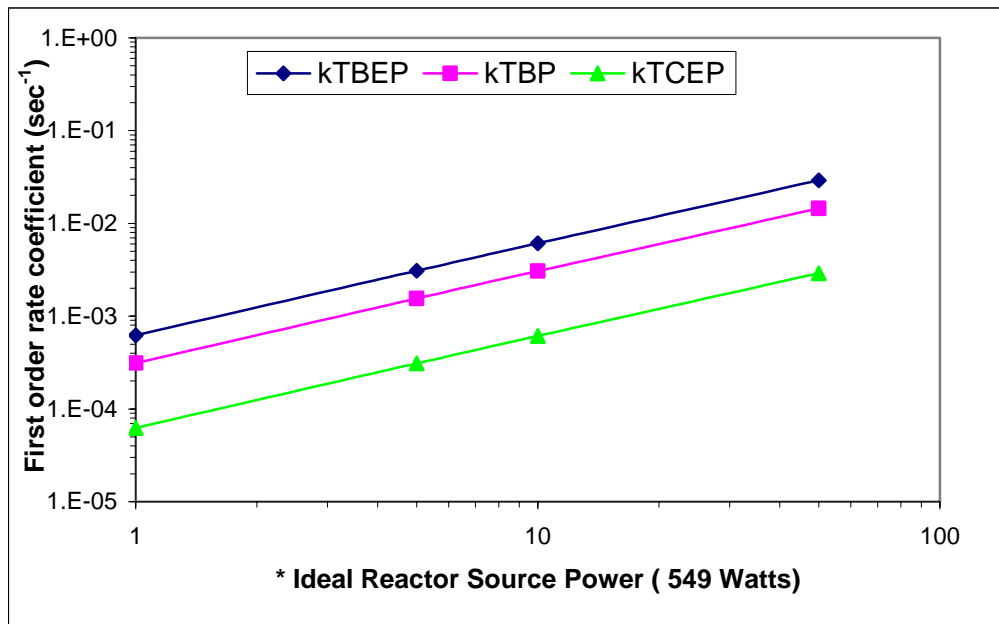| Characteristics of Runs	
Lamp power	1,5,10,50* 459 W
pH	8
Hydrogen peroxide [M]	0.005
Ct [M]	0.0005
Exposure time	20 sec

Figure 6-11 First order reaction rate coefficients vs. lamp power. $H_2O_2=10^{-3}$ M, pH=8, $C_T=5*10^{-4}$ M

6.4.5 Steady state considerations and quick and dirty calculations

When the micro-pollutants exist in very small concentrations and the pH of the solution does not change significantly, the hydroxyl radical concentration reaches a steady state. For the preliminary design steps, a steady-state assumption can be used to provide the basic required characteristics of the UV reactor and the recipe of the solution.

Assuming a steady-state concentration of hydroxyl radical and a known initial concentration of a micro-pollutant, we can predict the latter's removal rate in the UV reactor. For example for TBP we would have:

Equation 6-43

$$\frac{dTBP}{dt} = -k_{TBP} \cdot [OH\bullet]_{SS} \cdot [TBP]$$

$$[TBP]_{final} = [TBP]_o \cdot e^{-k_{TBP} \cdot [OH\bullet]_{SS} \cdot t}$$

so constant [OH•] leads directly to a pseudo first order rate coefficient.

It is evident that formulating an expression for pseudo-steady-state concentration of hydroxyl radical is very helpful. The first step is to assume that the rate of change of hydroxyl radical is zero, and by an order of magnitude analysis to neglect some of the terms. For details, Machairas (2004)

These approximations lead to the following expression for the steady state concentration of hydroxyl radicals:

Equation 6-44

$$[OH\bullet]_{SS} = \frac{2 \cdot r_{UV,OH\bullet} [H_2O_2]}{k_2[H_2O_2] + k_3[HO_2^-] + k_6[CO_3^{2-}] + k_7[HCO_3^-]}$$

For a given recipe of the solution (pH, C_T and initial H2O2 dose) the expression can be evaluated. A series of simulations were conducted to estimate the error introduced by using the previous expression to evaluate the steady-state concentration of hydroxyl radical.

Table 6-9   Pseudo steady state assumption, Results

	pH	Ct	H2O2o	Predicted	Simulated		Error
1	6	0.0001	0.0005	2.4E-14	2.4E-14		0.11%
2	6	0.0005	0.0005	2.2E-14	2.2E-14		0.09%
3	6	0.001	0.0005	2.0E-14	2.0E-14		0.06%
4	7	0.0001	0.0005	2.3E-14	2.3E-14		0.25%
5	7	0.0005	0.0005	1.9E-14	1.9E-14		0.19%
6	7	0.001	0.0005	1.6E-14	1.6E-14		0.13%
7	8	0.0001	0.0005	2.1E-14	2.1E-14		0.27%
8	8	0.0005	0.0005	1.7E-14	1.7E-14		0.19%
9	8	0.001	0.0005	1.3E-14	1.3E-14		0.13%
10	9	0.0001	0.0005	1.3E-14	1.3E-14		0.35%
11	9	0.0005	0.0005	9.4E-15	9.4E-15		0.29%
12	9	0.001	0.0005	7.0E-15	6.9E-15		0.25%

From Table 6-9 we can see that the steady-state assumption gives very accurate results. Of course such a simplifying approach needs to be used with caution, but for preliminary design calculations it could give useful insight. Machairas (2004) examines cases where such an approximation is not valid and will yield unreasonable results.

6.4.6   Atlanta Water Works

Lin (2004) conducted a study on the fate of flame-retardants in the Atlanta Water Works drinking water treatment plant in Atlanta, Georgia and reports values for the phosphate esters concentration after the filtration step.

Table 6-10   From Lin (2004)

Pollutant	ug/l	[M]
TBP	0.019	7.0E-11
TBEP	0.444	1.6E-09
TCEP	0.158	4.0E-10

In addition, Lin reports values for the pH at the various treatments stages. After filtration the pH is 6.6. Unfortunately the C_T is not reported for the sampled water but pre-softening treatment of the water is done.

Using the values from Table 6-10 the reported value for pH and reasonable values for C_T, we will estimate the potential removal that the UV/H2O2 process could accomplish.

It has been assumed that since pre-softening of the water is used the total carbonate species can be as low as 10^{-4} M.

From Table 6-11 it is obvious that when the "ideal" reactor is used that has been designed based only on disinfection requirements there is very small removal of the phosphate esters.

In Table 6-12 the same simulations are presented but this time the UV light source power in the reactor is increased by a factor of 10 and a factor of 50.

Table 6-11   **Base case removal**

Lamp power	459 W
Ct	10^-4
pH	6.6

	Initial	Final	Removal	1st order
H2O2	5.0E-04			
TBP	7.0E-11	7.0E-11	0.5%	2.3E-04
TCEP	4.0E-10	4.0E-10	0.1%	4.6E-05
TBEP	1.6E-09	1.6E-09	0.9%	4.7E-04

When the intensity is increased by a factor of 50 the removal efficiency of the treatment process becomes significant. TBEP is removed at a ~36% level and TBP at level of ~20%. TCEP is removed at a lower level, ~5%, due to the slower reaction rate constant.

Table 6-12   **Increase in the UV lamp power**

Lamp power	10* 459W
Ct	10^-4
pH	6.6

	Initial	Final	Removal	1st order
H2O2	5.0E-04			
TBP	7.0E-11	6.7E-11	4.5%	2.3E-03
TCEP	4.0E-10	4.0E-10	0.9%	4.6E-04
TBEP	1.6E-09	1.5E-09	8.8%	4.6E-03

Lamp power	50* 459W
Ct	10^-4
pH	6.6

	Initial	Final	Removal	1st order
H2O2	5.0E-04			
TBP	7.0E-11	5.6E-11	20.1%	1.1E-02
TCEP	4.0E-10	3.8E-10	4.4%	2.2E-03
TBEP	1.6E-09	1.0E-09	36.2%	2.2E-02

In Table 6-13 it has been assumed that there are three identical reactors in line. The UV lamp power is now 10 times the one used in the ideal reactor.

Table 6-13   **Three reactors in line**

Lamp power	10* 459 W
Ct	10^-4
pH	6.6

	Initial	Final	Removal	1st order
H2O2	5.0E-04			
TBP	7.0E-11	6.1E-11	12.9%	6.9E-03
TCEP	4.0E-10	3.9E-10	2.7%	1.4E-03
TBEP	1.6E-09	1.2E-09	24.1%	1.4E-02

The removal efficiency now reaches ~25% for TBEP, ~13% for TBP and ~3% for TCEP.

It is important to note that in the previous cases the dose of hydrogen peroxide complies with the limit of 17 mg/l mentioned before.

As a final scenario, we will consider the removal efficiency of 3 identical reactors in line with a UV lamp power 10 times the one used in the ideal reactor and a hydrogen peroxide dose of 10^{-3} M. This scenario is meant to resemble a design specifically targeted for the oxidation of micro-pollutants. The reason why here it was chosen to increase the hydrogen peroxide dose instead of increasing the UV lamp power is that it is less costly to increase the hydrogen peroxide dose and treat the water for the excess hydrogen peroxide than to increase the power of the UV lamp.

Table 6-14   Three reactors in line, Initial hydrogen peroxide 10^{-3} M

Lamp power	10* 459 W
Ct	10^-4
pH	6.6

	Initial	Final	Removal	1st order
H2O2	1.0E-03			
TBP	7.0E-11	5.6E-11	20.2%	1.1E-02
TCEP	4.0E-10	3.8E-10	4.4%	2.3E-03
TBEP	1.6E-09	1.0E-09	36.3%	2.3E-02

The removal efficiency now reaches ~36% for TBEP, ~20% for TBP and ~5% for TCEP. The magnitude of the removal is equal to the scenario of one reactor with 50 times the lamp power of the ideal reactor and a dose of hydrogen peroxide of $5*10^{-4}$ M. The removal in these two scenarios is significant and such a treatment process would offer a valid solution for the Atlanta Water Works plant if the removal of the phosphate esters from drinking water became a necessity.

6.5 Conclusions

In this work the issue of removing phosphate esters from drinking water has been examined. From the various treatment processes available, the oxidation of phosphate esters through hydroxyl radical generated by the UV/H2O2 process was selected.

The results of the advanced oxidation process when it is applied in a UV unit specifically designed for disinfection purposes are not very encouraging. The potential removal of the phosphate esters under the UV intensity conditions specified by disinfection guidelines is very low.

It is obvious that the UV/H2O2 advanced oxidation process has significant potential for removal of the phosphate esters if the UV intensity in the reactor is increased. Further increase in the efficiency of the AOP process can be made by adding higher hydrogen peroxide doses (order of 1 to 5 mM). Such a design scheme is clearly focused in the advanced oxidation process rather than disinfection. The higher hydrogen peroxide doses will allow lower UV intensities in the reactor for the same removal but will require additional treatment stages for the removal of hydrogen peroxide from water. In any case, based on the required removal efficiency for the reactor the exact choice of the UV lamps power and the initial hydrogen peroxide dose is an optimization issue.

Even though UV/H2O2 advanced oxidation process is the most researched AOP, various issues require further study.

The reaction rates of the phosphate esters with hydroxyl radical need to be more accurately defined. From the experience gained by the experiments performed for this work it seems that very accurate determination of the reaction rates will require substantial research effort.

In the model developed here, since the products of the oxidation of the phosphate esters are not known, the oxidized mass of the phosphates is not accounted for. One simplifying approach is to assume that the phosphate esters are completely mineralized to carbon dioxide and phosphoric acid. We feel that such an approach is over

simplifying and will yield worse results than just ignoring the products. Stefan, Hoy and Bolton (1996) present a kinetic model for the degradation of acetone in an UV/H2O2 process where the products are known. Their analysis is excellent and the results from their kinetic model agree very well with the observed experimental data. Therefore, what is suggested is when designing such a treatment process targeting at specified organic chemicals, detailed experiments to be performed to establish the reaction mechanism concerning the products.

The model developed for this work considers the various other radicals emerging in the solution ($HO_2\bullet/O_2\bullet^-$, $CO_3^{2-}\bullet$) as non reactive. This assumption has also been done by Stefan, Hoy and Bolton (1996), Glaze, Lay and Kang (1995) and Crittenden et al. (1999). Even though these radicals are not expected to be as reactive as hydroxyl radical, it is clear that they react with organic chemicals at some extent. Therefore research must be done to at least identify the general pattern of their reactions and to establish some relevant reaction rates.

Finally, the chain reaction mechanism needs further investigation. The $HO_2\bullet/O_2\bullet^-$ radicals that emerge probably are associated with the existence of some metal catalysts in the solution. Their emergence complicates significantly the reaction mechanism it has to be very clear under which conditions they are created and how they react.

All the issues stated above are well beyond the scope of this work. Because advanced oxidation processes is expected to find significant applications in the near future research in the previous issues will prove very valuable for the environmental engineering science.

7   Bibliography

Adams, C., Y. Wang. K. Loftin, and M. Meyer. 2000. Removal of Antibiotics from Surface and Distilled Water in Conventional Water Treatment Processes. *Journal of Environmental Engineering* 3: 253-260.

Ambrose, Robert B. Jr., Tim A. Wool, and James L. Martin. *The Water Quality Analysis Simulation Program, WASP5.* Athens, GA: Environmental Research Laboratory U.S. Environmental Protection Agency, 1993.

Andrews, Matthew. "Natural Attenuation of Organophosphates in River Systems: Case Study Chattahoochee River". (Master of Engineering Thesis, Massachusetts Institute of Technology, 2004)

ArcGIS Version 8.1, Computer Program. Redlands, CA, ESRI, 2003.

ASCE/AWWA. *Water Treatment Plant Design.* 2nd edition. McGraw-Hill, New York, Chapters 5, 10, and 15, 1990.

ATSDR. *ATSDR – ToxFAQs™: Polychlorinated Biphenyls (PCBs).* [updated February 2001, cited May 9, 2004]. Available from http://www.atsdr.cdc.gov/tfacts17.html

Baldwin, D. S., J. K. Beattie, L. M. Coleman, and D. R. Jones. 1995. Phosphate Ester Hydrolysis Facilitated by Mineral Phases. *Environmental Science Technology* 29: 1706-1709.

Berk, Kenneth N., Patrick Carey. *Data Analysis with Microsoft Excel.* Austrailia: Duxbury Thomson Learning, 2000.

Brown, S.L., F.Y. Chan, J.L. Jones, D.H. Liu, and K.E. McCaleb. Research Program on Hazard Priority Ranking of Manufactured Chemicals (Chemicals 61-79). Performed by the Stanford Research Institute. NTIS PB 263-164. Sponsored by the National Science Foundation, April 1975.

Brunner, Gary W. *HEC-RAS River Analysis System User Manual Version 3.1.* Davis CA: U.S. Army Corps of Engineers Hydrologic Engineering Center, 2002.

Buxton G.V., Greenstock C.L., Helman P.W., Ross A.B. 1988. Critical Review of Rate Constants for Reaction of Hydrated Electrons, Hydrogen Atoms and Hydroxyl Radicals ($^{\cdot}OH / ^{\cdot}O^{-}$) in Aqueous Solution. *J. Phys. Chem. Ref. Data* 17**:**513-886

California Office of Environmental Health Hazard Assessment. *Proposition 65 – Administrative Listing*. Website leading to chemicals listed under Proposition 65 rules. [updated May 7, 2004, cited May 7, 2004]. Available from http://www.oehha.ca.gov/prop65/prop65_list/Newlist.html

Chastain, Eddie. "Inquiry for discharge rates". E-mail to Samuel Haffey, 23 Feb 2004.

Chemical Sources International, Inc. *Chemical Sources International*. [cited May 1, 2004]. Available from http://db.chemsources.com/cgi-bin/foxweb.exe/validate_user@csi/login?

Chiou, C.T., L.J. Peters, and V.H. Freed. 1979. A Physical Concept of Soil-Water Equilibria for Nonionic Organic Compounds. *Science* 206(16): 831-832.

City of Atlanta. *Atlanta Water Quality Report 2002 WSID 1210001*. [cited May 1, 2004]. Available from http://apps.atlantaga.gov/citydir/water/WQR2002.pdf

City of Atlanta. *Atlanta Water Quality Report 2003 WSID 1210001*. [cited May 1, 2004]. Available from http://apps.atlantaga.gov/citydir/water/WQR2003.pdf

Crittenden J.C., Hu S., Hand D.W., Green S.A. 1999. A Kinetic Model for H2O2/UV Process in a Completely Mixed Batch Reactor. *Wat. Res. 33*

Danish University of Pharmaceutical Sciences. *7. Precipitation and Dissolution*. [updated April 28, 2003, cited May 7, 2004]. Available from http://www.dfh.dk/~fi/A317/noter/kap7%20prec%20wpc[1].pdf

Daughton, Christian. *Pharmaceuticals and Personal Care Products – Overarching Issues and Overview, EPA*. [updated March 15, 2004; cited April 11, 2004]. Available from http://www.epa.gov/esd/chemistry/pharma/book-summary.htm

Drugstore Cowboys, Inc. "Flame Retardant chemicals in the Chattahoochee River." Master of Engineering Proposal, December 2003.

Environmental Defense. *About the Chemicals*. [updated 2003, cited May 1, 2004]. Available from http://www.scorecard.org/chemical-profiles/index.tcl

Environmental Protection Agency, U.S. (EPA). *Water Discharge Permits*. http://www.epa.gov/enviro/html/pcs/pcs_query_java.html (24 Nov 2003)

European Community. *Poseidon Project*. [updated April 13, 2003; cited April 11, 2004]. Available from http://www.eu-poseidon.com/

European Union. *ENVIRPHARMA – Pharmaceuticals in the Environment*. [updated October 24, 2003; cited April 11, 2004]. Available from http://www.envirpharma.org/

Fischer, Hugo B., E. John List, Robert C.Y. Koh, Jorg Imberger, and Norman H. Brooks. *Mixing in Inland and Coastal Waters*. San Diego: Academic Press, 1979.

Frick E.A., and S.D. Zaugg. 2003. Organic Wastewater Contaminants in the Upper
Chattahoochee River Basin, Georgia, 1999—2002. Proceedings of the 2003
Georgia Water Resources Conference, held April 23-24, 2003, at the University
of Georgia. Kathryn J. Hatcher, editor, Institute of Ecology, The University of
Georgia, Athens, GA. [cited April 28, 2004]. Available from
http://georgia.usgs.gov/pubs/other/gwrc2003/pdf/Frick_wastewater-
GWRC2003.pdf

Frick, E.A., A.K. Henderson, D.M. Moll, E.T. Furlong, and M.T. Meyer. 2001. Presence
of Pharmaceuticals in Wastewater Effluent and Drinking Water, Metropolitan
Atlanta, Georgia, July—September 1999. Proceedings of the 2001 Georgia Water
Resources Conference, K.J. Hatcher, editor, Carl Vinson Institute of Government,
The University of Georgia, Athens, GA, p. 282. [cited April 28, 2004]. Available
from http://ga.water.usgs.gov/nawqa/Pharm_final.pdf

Frick, Elizabeth A., Daniel J. Hippe, Gary R. Buell, Carol A. Couch, Evelyn H. Hopkins,
David J. Wangsness, and Jerry W. Garrett. 1998. Water Quality in the
Apalachicola-Chattahoochee-Flint River Basin, Georgia, Alabama, and Florida,
1992-1995. U.S. Geological Survey Circular 1164.

Fries, Elke, and Wihelm Puttmann. 2003. Monitoring of the three phosphate triesters
TBP, TCEP, and TBEP in river water and ground water (Oder, Germany).
Journal of Environmental Monitoring 5: 346-352.

Fries, Elke, and Wilhelm Puttmann. 2001. "Occurance of phosphate triesters in surface
water and ground water in Germany." *Journal of Environmental Monitoring* 5:
621-626.

Georgia Department of Natural Resources (GNR) Environmental Protection Division.
Chattahoochee River Basin Management Plan 1997. Atlanta, GA: Georgia:
Department of Natural Resources, 1997.

Glaze W.H, Lay Y.Kang J.W. 1995. Advanced Oxidation Processes: A Kinetic Model for
the Oxidation of 1,2-Dibromo-3-chloropropane in Water by the Combination of
Hydrogen Peroxide and UV Radiation, *Ind. Eng. Chem. Res. 34*

Gschwend, Philip. Personal discussions with Joseph Lin, Matthew Andrews, Samuel
Haffey, Alexandros Machairas, and Peter Shanahan. October 2003 – May 2004.

Haffey, Samuel. "Numerical Model of Phosphate Esters in the Chattahoochee River".
(Master of Engineering thesis, Massachusetts Institute of Technology, 2004)

Harburn, James. "discharge rates Sutton & South Cobb". E-mail to Samuel Haffey, 3 Mar
2004.

Harrison, M.H., R. Perry, and R.A. Wellings. 1976. Chemical Kinetics of Chlorination of Some Polynuclear Aromatic Hydrocarbons Under Conditions of Water Treatment Processes. *Environmental Science & Technology* 10(12): 1156-1160.

Hemond, H. F., and E. J. Fechner-Levy. *Chemical Fate and Transport in the Environment*. 2nd edition. San Diego: Academic Press, 2000.

Henderson, A.K., D.M. Moll, E.A. Frick, and S.D. Zaugg. 2001. Presence of Wastewater Tracers and Endocrine Disrupting Chemicals in Treated Wastewater Effluent and in Municipal Drinking Water, Metropolitan Atlanta, 1999 (abstract). From proceedings of the 2nd International conference on pharmaceuticals and endocrine disrupting chemicals in water, 110. [cited April 28, 2004]. Available from http://ga.water.usgs.gov/nawqa/henderson.pdf

Hutzinger, O. 2000. Drugs in the Environment. *Chemosphere*, 40(7): 691-793.

Karickhoff, S.W., D.S. Brown, and T.A. Scott. 1979. Sorption of Hydrophobic Pollutants on Natural Sediments. *Water Research* 13:241-248.

Kawagoshi, Yasunori, Sachiko Nakamura, and Isao Fukunaga. 2002. Degradation of organophosphoric esters in leachate from a sea-based solid waste disposal site. *Chemosphere* 38: 219-225.

Kolpin, Dana W., E. T. Furlong, M. T. Meyer, E. M. Thurman, S. D. Zaugg, L. B. Barber, and H. T. Buxton. 2002. Pharmaceuticals, Hormones, and Other Organic Wastewater Contaminants in U.S. Streams, 1999-2000: A National Reconnaissance. *Environmental Science Technology* 36: 1202-1211.

Kopanski, Tom. Personal e-mail correspondence and personal discussions with Joseph Lin. January 2004 – May 2004.

Lin, Joseph C. "Determining the Removal Effectiveness of Flame Retardants from Drinking Water Treatment Processes". (Master of Engineering Thesis Massachusetts Institute of Technology, 2004)

MacFarlane, John. Personal discussions with Joseph Lin and Matthew Andrews. December 2003 – May 2004.

Machairas, Alexandros. "The UV/H2O2 Advanced Oxidation Process in UV Disinfection Units: Removal of Selected Phosphate Esters by Hydroxyl Radical". (Master of Engineering thesis, Massachusetts Institute of Technology, 2004)

Masschelein W.J. *Ultra Violet light in Water and Wastewater Sanitation*. Lewis Publishers, 2002.

National Institute of Standards and Technology (NIST). *NIST Chemistry WebBook*. NIST Standard Reference Database Number 69 – March, 2003 Release. Look up CAS registry numbers 78-51-3, 115-96-8, and 126-73-8. [updated March, 2003, cited May 7, 2004]. Available from http://webbook.nist.gov/chemistry.

National Institutes of Health (NIH). *Household Products Database*. Look up CAS registry number 78-51-3. [updated May 12, 2003, cited May 7, 2004]. Available from http://householdproducts.nlm.nih.gov/ingredients.htm

National Library of Medicine. *HSDB Search*. [database updated March 4, 2004; cited April 11, 2004]. Available from http://toxnet.nlm.nih.gov/cgi-bin/sis/htmlgen?HSDB.

Nazaroff, William, and Lisa Alvarez-Cohen. *Environmental Engineering Science*. New York: John Wiley & Sons, Inc., 2001.

Notre Dame Radiation Laboratory, Radiation Chemistry Data Center, [cited November 20, 2004]. Available from http://www.rad.nd.edu/rcdc/.

Paune, F., J. Caixach, I. Espadaler, J. Om, and J. Rivera. 1998. Assessment on the Removal of Organic Chemicals from Raw and Drinking Water at a Llobregat River Water Works Plant Using GAC. *Water Research* 32(11): 3313-3324.

Purdue University. *Half Lives*. [cited May 10, 2004]. Available from: http://www.chem.purdue.edu/gchelp/howtosolveit/Kinetics/Halflife.html

Rhodium. *Solubility and Drying Agents*. [updated 2004, cited May 4, 2004]. Available from http://www.rhodium.ws/chemistry/equipment/dryingagents.html.

Risk Assessment Information System. *Toxicity and Chemical—Specific Factors – Nonradionuclides*. [updated January 2004, cited May 1, 2004]. Available from http://risk.lsd.ornl.gov/cgi-bin/tox/TOX_select?select=nrad

Schwarzenbach, R. P., P. M. Gschwend, and D. M. Imboden. *Environmental Organic Chemistry*. 2nd edition. Hoboken: John Wiley & Sons, Inc., 2003.

Stackelberg, P., and R.L. Lippincott, undated. Pharmaceuticals and Other Wastewater Organics in New Jersey's Streams and Drinking-Water Supplies. [cited April 28, 2004]. Available from http://www.state.nj.us/dep/dsr/presentations/drinkingwater/stackelbergpresentation.pdf.

Stamey, Timothy C.(USGS). "Re: [RE] http://ga.wayterdata.usgs.gov/nwis/current/". E-mail to Samuel Haffey. 7 Mar 2004.

Stefan M.I, Hoy A.R, Bolton J.R. 1996. Kinetics and Mechanism of the Degradation and Mineralization of Aceton in Dilute Aqueous Solution Sensitized by the UV Photolysis of Hydrogen Peroxide, *Env. Sci. Tech. 30*

Stumm W., Morgan J.J. *Aquatic Chemistry*, 3rd edition, Wiley-Interscience, New York, 1996.

Syracuse Research Corporation. *Environmental Science – DATALOG.* [database updated January 26, 2004; cited April 11, 2004]. Available from http://www.syrres.com/esc/datalog.htm

Thomas, Russell A.P., and L.E. Macaskie. 1998. The effect of growth conditions on the biodegradation of tributyl phosphate and potential for the remediation of acid mine drainage waters by a naturally-occurring mixed microbial culture. *Applied Microbiology Biotechnology* 49: 202-209.

U.S. Geological Survey (USGS). Real-Time Data for Georgia. [cited May 8, 2004]. Available from http://waterdata.usgs.gov/ga/nwis/rt

United States EPA. *EPA/OPPT/Inventory Update Rule/2002 TSCA Inventory Update Rule*. Production of High Production Volume chemicals in the United States. [updated March 4, 2004, cited May 1, 2004]. Available from http://www.epa.gov/oppt/iur/iur02/index.htm

US EPA. *Gas Chromatography*. [updated January 2003, cited May 4, 2004]. Available from http://fate.clu-in.org/gc.asp?techtypeid=44

US EPA. *Mass Spectrometry*. [updated January 2003, cited May 4, 2004]. Available from http://fate.clu-in.org/mspec.asp?techtypeid=47

US EPA. *Origins and Fate of PPCPs in the Environment*. [updated January 2004, cited May 7, 2004]. Available from http://epa.gov/nerlesd1/chemistry/pharma/images/drawing.pdf

USGS Water Resources of the United States. *Real-Time Data for Georgia*. [cited February 1, 2004]. Available from: http://waterdata.usgs.gov/ga/nwis/rt

World Health Organization. *IPCS INCHEM – Environmental Health Criteria Monographs.* Environmental Health Criteria for flame retardants (EHC 192, 1997), flame retardants (EHC 209, 1998), flame retardants (EHC 218, 2000), and tributyl phosphate (EHC 112, 1991). [cited April 28, 2004]. Available from http://www.inchem.org/pages/ehc.html